# IN VIVO FAST SCAN CYCLIC VOLTAMMETRY REVEALS THAT RESTRICTED DIFFUSION MAINTAINS DISCRETE DOPAMINE DOMAINS IN THE DORSAL STRIATUM

by

Ian Mitchell Taylor

B.S. Chemistry, Westminster College, 2008

Submitted to the Graduate Faculty of the

Kenneth P. Dietrich School of Arts and Sciences in partial fulfillment

Of the requirement for the degree of

Doctor of Philosophy

University of Pittsburgh

2014

UNIVERSITY OF PITTSBURGH

DIETRICH SCHOOL OF ARTS AND SCIENCES

This dissertation was presented

by

Ian Mitchell Taylor

It was defended on

April 3, 2014

and approved by

Renã A.S. Robinson, Assistant Professor, Department of Chemistry

W. Seth Horne, Assistant Professor, Department of Chemistry

Gonzalo E. Torres, Associate Professor, Department of Neurobiology

Dissertation Director: Adrian C. Michael, Professor, Department of Chemistry

Copyright © by Ian Mitchell Taylor
2014

Adrian C. Michael, PhD

IN VIVO FAST SCAN CYCLIC VOLTAMMETRY REVEALS THAT RESTRICTED DIFFUSION MAINTAINS DISCRETE DOPAMINE DOMAINS IN THE DORSAL STRIATUM

Ian Mitchell Taylor, PhD

University of Pittsburgh, 2014

Dopamine is an important neurotransmitter involved in a variety of physiological functionality such as motor control, cognition, sexual arousal and reward. Furthermore, dysfunction in the dopaminergic system can lead a number of devastating neurological disorders including Parkinson's disease, schizophrenia, Alzheimer's, and substance abuse. Therefore, understanding the real-time mechanisms of dopamine signaling is of utmost importance.

Real-time analysis of *in vivo* dopamine poses an interesting analytical challenge. Dopamine is released into the extracellular space deep below the cortical surface in nanomolar to micromolar concentrations on a sub-second timeframe. Because of these conditions, effective dopamine quantification requires a small selective detector that exhibits high temporal resolution and a low limit of detection. Fast scan cyclic voltammetry at carbon fiber microelectrodes has proven to be ideal for this task. The work detailed in this dissertation pairs *in vivo* voltammetry with electrical stimulation of dopaminergic axonal projections to controllably study dopamine kinetics.

Previously our laboratory discovered the existence of two discrete dopamine domains in the rat dorsal striatum that exhibit unique dopamine kinetic responses to electrical stimulation. This dissertation is built on the foundation of that work. First, we discovered that the effect of a competitive inhibitor of the dopamine transporter is domain dependent. The kinetics of these domain dependent effects allowed us to predict that dopamine signaling in the extracellular space is subjected to restricted

diffusion. We continued on to show that restricted diffusion prevents cross-talk between domains, thus maintaining a strict physical segregation between domains. Further work resulted in the discovery of five discrete dopamine domains. These domains exhibit differing extents of regulation, resulting in unique kinetic responses to electrical stimulation. Finally, we discovered the existence of long-term dopamine signaling. Following electrically stimulated dopamine release, free dopamine in the extracellular space is not completely cleared as previously believed. Instead, the free dopamine establishes a new steady state elevated baseline concentration. These discoveries provide new insight into the complex mechanisms that regulate dopamine signaling, and have the potential to explain the multiple functionalities of the dopaminergic system.

**TABLE OF CONTENTS**

## LIST OF EQUATIONS

**LIST OF TABLES**

**LIST OF FIGURES**

## PREFACE

I must begin this document by thanking everyone who has helped me become the person and the scientist that I am today. First and foremost, I would like to thank Adrian Michael. I cannot imagine a better graduate mentor. He pushed me when I needed the encouragement, he let me run free when I was inspired, he caught me when I foundered and most importantly he let me fall when I needed to fall. He always knew exactly what to say to keep me going and to make me be a better scientist. I have a deep respect and admiration for Adrian, and feel honored to call myself his student.

Next, I would like to thank Renã Robinson for her help and support both as my original proposal mentor and as someone that I very much appreciate and respect in the department. I would also like to thank Seth Horne, Gonzalo Torres, Stephen Weber and Shigeru Amemiya for serving as committee members throughout my years at the University of Pittsburgh. I am also appreciative of the Department of Chemistry support staff in the main office as well as in the electronic and machine shops.

Many thanks to the current Michael Lab members: Andrea Jaquins-Gerstl, Katy Nesbitt, Seth Walters, Erika Varner, and honorary member, Kat Salerno for all of your help in the lab and for keeping spirits up. Thank you to the past Michael Lab members: Keith Moquin and Yuexiang Wang for giving of your time and expertise. Most of all, I must thank Zhan Shu. Zhan and I have been together since day one. We were the perfect pair. I couldn't imagine doing all of this without my buddy. Thanks Zhan.

Last but not least, I must thank my family. I am where I am because of my parents. They have been setting me up for success since I was a child. They made it a priority to ensure that I became a well rounded individual. These experiences have made me a better scientist and a better person. Thank you to my brothers and their families. Thank you to my in-laws for welcoming me into their family and for the constant encouragement. Finally, thank you Julie. You are absolutely everything to me. You have always supported me from the beginning, even when I didn't deserve it. You have always kept me grounded and told me what I needed to hear. I couldn't have done this without you. This is for you.

# 1.0: INTRODUCTION

## 1.1: HISTORY AND ANATOMY OF DOPAMINE TRANSMISSION

Dopamine (DA) is a catecholamine neurotransmitter responsible for maintaining many vital life functions in species ranging from the simple fruit fly to humans. The molecule was first synthesized in 1910 by Carl Mannich and Willy Jacobsohn in Germany (Mannich and Jacobsohn, 1910) and by George Barger and Arthur James Ewins in England (Barger and Ewins, 1910). It has been studied extensively since its physiological relevance as a neurotransmitter was uncovered by Nobel Prize laureate Arvid Carlsson and coworkers in 1958 (Carlsson et al., 1958). In humans, as well as in the rat model, DA signaling occurs along nine distinct pathways (Winn, 2001) and control a wide variety of functioning such as motor control, reward, reinforcement, cognition and addiction (Horn et al., 1979). This dissertation focuses on transmission along the nigrostriatal dopamine pathway, which maintains reward, addiction, and motor functioning (Horn et al., 1979). In the nigrostriatal pathway the cell bodies originate within the substantia nigra portion of the midbrain, axons follow the ventrally located medial forebrain bundle and the terminals and signaling varicosities are located throughout the dorsal striatum (Horn et al., 1979, Winn, 2001). Dysfunction of DA signaling has been found to be responsible for numerous disorders such as Parkinson disease, Schizophrenia, Alzheimer's disease, ADHD and substance abuse (Phillips et al., 2003, Pappata et al., 2008, Salahpour et al., 2008, de la Fuente-Fernandez et al., 2011, Kim et al., 2011) All disorders that require treatment with drugs that alter DA signaling such as L-3,4-dihydroxyphenylalanine (L-DOPA), methylphenidate (Ritalin) and haloperidol (Haldol) (Gottwald and Aminoff, 2011, Schlochtermeier et al., 2011, Valenti et al., 2011).

DA is released at the 300 nm long by 15 nm wide synaptic junction (Garris et al., 1994) between DAergic neuron terminals and neighboring γ-aminobutyric acid (GABA) cells (Smith and Bolam, 1990). In the striatum, these synaptic junctions are located at a density of 0.05/$\mu m^3$ or one every 3.5 μm (Doucet et al., 1986, Rice and Cragg, 2008). Inside the DAergic neuron, DA is synthesized first by the conversion of L-tyrosine to L-DOPA by tyrosine hydroxylase, and then from L-DOPA into DA by DOPA decarboxylase (Elsworth and Roth, 1997). Once synthesized, DA is packaged into 50 nm diameter (Greengard et al., 1993) synaptic vesicles by the SLC18 family $2H^+$/DA antiporter protein, vesicular monoamine transporter 2 (VMAT-2) (Eiden et al., 2004, Guillot and Miller, 2009) and stored at concentrations of around 0.1 M (Elsworth and Roth, 1997). Maintenance of a high proton concentration within the synaptic vesicle is important in order to facilitate DA influx and to maintain the acidic environment needed to ensure that DA is not oxidized (Guillot and Miller, 2009). Loaded vesicles congregate near the synaptic junction and await release (Greengard et al., 1993). When the cell triggers release, rapid depolarization along the axonal membrane, termed an action potential, propagates from the cell body to the terminal region at a rate of approximately 50 m/sec (Wightman et al., 1988b). Once the action potential reaches the voltage mediated $Ca^{2+}$ channels located at the neuron terminal, $Ca^{2+}$ is allowed to enter the cell (Ceccarelli and Hurlbut, 1980), triggering intracellular pathways that cause DA vesicles to release their contents into the extracellular space via exocytotic vesicle fusion (del Castillo and Katz, 1956, Wightman et al., 1988b). DA floods into the synaptic junction and rapidly diffuses out into the extracellular space where it comes in contact with a number of regulatory and uptake proteins (Garris et al., 1994, Michael and Wightman, 1999).

Autoinhibitory regulation of DA release in the striatum, along with GABA signaling, occurs through DA binding to g-protein coupled receptors. These receptors, classified into D1 and D2 receptor families, consist of seven transmembrane domains and readily bind extracellular DA (Palermo-Neto, 1997, Missale et al., 1998). D2 type receptors, $IC_{50}$ for DA of 2.5 μM (Onali et al., 1985), are found on

both the pre and post synaptic membrane as well as on the DA neuron cell bodies in the substantia nigra. DA binding to D2 receptors corresponds to intracellular $G_i$ signaling and results in increased production of intracellular cyclic adenosine monophosphate (cAMP) (Onali et al., 1985, Palermo-Neto, 1997, Missale et al., 1998). D1 type receptors are found only on the post synaptic membrane and result in intracellular $G_s$ signaling upon DA activation that leads to a decreased production of cAMP (Onali et al., 1985, Missale et al., 1998). DA binding to presynaptic D2 receptors also serves as an autoinhibitory mechanism by decreasing vesicular release. This is caused by a g-protein coupled activation of outward $K^+$ channels, leading to a hyperpolarization that inhibits action potentials (Martel et al., 2011).

In addition to extracellular DA encountering D1 and D2 receptors, free DA is taken back into the cell by means of the DA transporter protein (DAT) (Benoit-Marand et al., 2000, Wu et al., 2001a, Torres, 2006, Salahpour et al., 2008). DAT is a typical SLC6 family $2Na^+/Cl^-$/DA symporter protein that consists of twelve transmembrane domains, forming a pore within (Fon et al., 1997, Torres, 2006, Torres and Amara, 2007). After uptake by DAT, DA is either repackaged into vesicles for rerelease (Guillot and Miller, 2009) or degraded by monoamine oxidase (MAO) found on the outer membrane of mitochondria (Waldmeier et al., 1976, Okada et al., 2011). In addition to uptake, DAT has been shown to be responsible for DA release. Numerous studies have shown that after treatment with amphetamine, spontaneous nonvesicular release occurs via the DAT (Sulzer et al., 1993, Giros et al., 1996, Kahlig et al., 2005). In addition, recent work by our laboratory has suggested that the local basal extracellular concentration of DA in the striatum is maintained by DAT mediated release (Borland and Michael, 2004, Moquin and Michael, 2009, Wang et al., 2010).

### 1.2: OXIDATION AND REDUCTION OF DOPAMINE

DA readily oxidizes to its dopamine o-quinone form through a two electron, two proton transfer reaction upon application of a potential that is more positive than DA's $E^\circ$ (Hawley et al., 1967, Tse et al.,

1976, Laviron, 1984, Deakin and Wightman, 1986, Michael and Borland, 2007). Subsequently, upon application of a potential more negative than DA's E˚, the dopamine o-quinone is reduced back to dopamine. This reduction also requires the transfer of two electrons and two protons. The electron transfer associated with these reactions produce a measurable current that can be quantified at the carbon fiber working electrode (Bard and Faulkner, 2001). The standard redox potential for DA was found to be 0.11 V versus the saturated calomel reference electrode (Bath et al., 2000), which converts to 0.10 V versus the Ag/AgCl reference electrode that is used in this study.

If the dopamine o-quinone is not reduced back to dopamine, it can undergo a number of cross reactions which could alter the magnitude of the detected current. Dopamine o-quinone readily serves as an oxidizing agent for ascorbic acid at physiological conditions. In this reaction, dopamine o-quinone oxidizes ascorbic acid by stripping it of its two electrons and two protons, thus reducing the dopamine o-quinone back to dopamine (Tse et al., 1976, Michael and Borland, 2007). If this reaction is allowed to occur, the amount of dopamine detected at the carbon fiber would be higher than expected due to a recycling of previously oxidized DA back to the carbon fiber. Also, an oxidation peak for ascorbic acid would be present that could skew the reading. Dopamine o-quinone can also undergo a cyclization reaction to an indole, which undergoes further oxidation to an aminochrome (Tse et al., 1976). Although this cyclization reaction is very slow under physiological conditions, the reaction is irreversible, and thus would cause an unexpected depletion of dopamine if the dopamine o-quinone is not reduced back to DA in a timely manner.

### 1.3: FAST SCAN CYCLIC VOLTAMMETRY

Due to the electrochemical nature of catecholamines, such as DA, cyclic voltammetry was first used by Ralph Adams' lab for the detection of neurotransmitters *in vitro* in 1967 (Hawley et al., 1967). Six years

later, Kissinger, Hart and Adams were the first to use cyclic voltammetry to detect a change in catecholamine concentration *in vivo* (Kissinger et al., 1973). Cyclic voltammetry is a method used to detect the presence of electroactive species in an environment without altering the chemical system (Bard and Faulkner, 2001). The method makes use of potential dependent electrochemical reactions following the form described in Equation 1.1, where Ox is the oxidized species, n$e^-$ is the number of electrons transferred, and Red is the reduced species.

**Equation 1.1** $Ox + ne^- \leftrightarrow Red$

When electrons are transferred in such a reaction, a measurable current is produced that is directly proportional the concentration of the electroactive species. This proportionality is governed by the Randles-Sevcik equation, shown in Equation 1.2 (Michael and Wightman, 1999, Bard and Faulkner, 2001).

**Equation 1.2** $$i_{peak} = (2.69 \times 10^5) n^{3/2} A D^{1/2} C^* v^{1/2}$$

In the Equation 1.2, $i_{peak}$ denotes the peak current, $2.69 \times 10^5$ is a constant, $n$ is the number of electrons being transferred, $A$ is the area of the electrode, $D$ is the diffusion coefficient for the species of interest, $C^*$ is the concentration of the species of interest and $v$ is the scan rate of the potential waveform. In a given experiment where the electrode, species of interest, and environment are unchanged, the constant, $n$, $A$, $D$, and $v$ all remain constant and can be combined together to form the calibration factor, $\alpha$. Equation 1.2 thereby reduces down to Equation 1.3, where current relates to concentration by a simple calibration of $\alpha$.

**Equation 1.3** $$i_{peak} = \alpha C^*$$

Using cyclic voltammetry, electrochemical reactions are driven by altering the potential, relative to a reference electrode, applied to the system via a controllably ramped waveform. The potential waveform begins at a designated resting potential, sweeps in a given direction until reaching a desired switching potential and then reverses to sweep in the opposite direction. This process is repeated until

the user defined waveform is complete and the potential returns to its resting baseline to await the next scan. When the waveform reaches potential values specific for the oxidation or reduction of the electroactive species, the electron transfer reaction will occur and a measurable current can be detected at the working electrode (Bard and Faulkner, 2001). The potential waveform can be applied at as high or low of a frequency as the user prefers. In this work, the waveform was applied at the relatively high frequency of 10 Hz to ensure sufficient temporal resolution necessary to detect changes in DA on the time scale of neuronal firing.

When the induced current is plotted versus the potential of the applied waveform, the image produced is referred to as a cyclic voltammogram. Because the potentials of oxidation and reduction for a given molecule remain unchanged as long as the run conditions are unaltered (Bard and Faulkner, 2001), this plot serves as a distinguishing fingerprint used to determine the source of the current. By qualitatively comparing the peak locations of a cyclic voltammogram to a database of standard compounds possibly located in the reaction matrix, a potential source match can be found. It is important to note that if there are two or more compounds possibly found in a given matrix that produce identical cyclic voltammograms, it is impossible to determine which is the source of the signal without further testing.

In typical cyclic voltammetry experiments, where waveforms are swept at the relatively slow rate of 0.1 V/sec to 1 V/sec, the oxidation and reduction peaks in the cyclic voltammogram are sharp and separated by 59 mV/n, where n is the number of electrons transferred (Bard and Faulkner, 2001). These peaks are found to broaden and migrate away from each other when reactions are more complex and when the scan rate of the potential waveform is increased (Michael and Wightman, 1999, Bath et al., 2000, Bard and Faulkner, 2001). Although the transfer of more than one electron should narrow the distance between peaks (59 mV/n), when more than one electron and proton are transferred, there is a possibility of the reaction following different electron and proton transfer pathways for the oxidation

and reduction reactions. This would result in the processes exhibiting different rates and thus shifting peak locations. Reactions consisting of a two electron and two proton transfer, such as DA, are modeled using the nine membered box scheme (Laviron, 1984, Deakin and Wightman, 1986). When the scan rates are increased to the range typical of fast scan cyclic voltammetry (FSCV) (100 V/sec – 1000 V/sec), peaks are shifted and broadened because the electron transfer kinetics between the analyte and the electrode surface are not instantaneous. By the time the current is detected at the carbon fiber, the potential waveform has swept to another value and shifted the peak (Bath et al., 2000). This increase in scan rate is a necessary feature for *in vivo* DA detection because of the aforementioned cross reactions that the oxidized dopamine o-quinone can undergo if not immediate reduced.

### 1.4: FSCV AT CARBON FIBER MICROELECTRODES

Due to findings indicating that damage associated with the implantation of large probes in brain tissue causes a loss of neuronal functioning (Borland et al., 2005, Jaquins-Gerstl and Michael, 2009), it is imperative that a small detector be used for implantation. In 1978 Francois Gonon and colleagues first used a carbon fiber microelectrode to detect DA *in vivo* (Gonon et al., 1978). These cylindrical probes are typically 7 µm in diameter and can be cut to whatever length desired. The use of these small electrodes allows for implantation with relatively little damage to the surrounding tissue (Peters et al., 2004, Jaquins-Gerstl and Michael, 2009). When the potential applied to the carbon fiber microelectrode is rapidly changed, such as is required for the *in vivo* detection of DA by FSCV, a large non-faradic current is observed. This is a result of ions from the brain fluid orienting along the electrode surface to balance the potential difference caused by the rapidly changing potential waveform (Michael and Wightman, 1999, Bath et al., 2000, Bard and Faulkner, 2001). This capacitive charge build up between the electrode surface and the surrounding fluid is referred to as the charging current and scales according to Equation 1.4 (Wipf et al., 1988, Michael and Wightman, 1999, Bath et al., 2000, Bard and Faulkner, 2001).

**Equation 1.4** $$i_{cap} = ACv$$

In Equation 1.4 $i_{cap}$ is the capacitive charging current, $A$ is the area of the electrode, $C$ is the capacitance and $v$ is the scan rate. It can be seen that both the faradaic peak current, $i_{peak}$ shown in Equation 1.2 and the capacitive charging current, $i_{cap}$ displayed in Equation 1.4, are dependent on scan rate, $v$. $i_{peak}$ is proportional to $\sqrt{v}$ , while $i_{cap}$ is related to $v$. This relationship indicates that if scan rates become too large, the charging current will far outweigh the peak current, thus putting a functional limit on the experimental scan rate used. Due to the presence of this charging current during all measurements, the detection of an electroactive species by FSCV requires a background subtraction of the current generated prior to the introduction of the analyte. This need for background subtraction therefore makes cyclic voltammetry a differential detection method and prevents the measurement of resting analyte levels.

As is typical with electrochemical detection in static environments, the oxidation of DA and subsequent reduction of dopamine o-quinone are dependent on diffusional mass transport of the reactive species to the electrode surface. As the layer of DA on the surface of the working electrode is oxidized to dopamine o-quinone, a flux of fresh DA is brought to the electrode surface to replace the newly produced dopamine o-quinone. The opposite is also observed for the reduction of dopamine o-quinone at the electrode surface. This motion is governed by Fick's Law (Bard and Faulkner, 2001) and allows for constant sampling of the extracellular environment. In addition to diffusional mass transport, DA and dopamine o-quinone also adsorb to the surface of the carbon fiber working electrode (DuVall and McCreery, 1999, Bath et al., 2000, DuVall and McCreery, 2000) through a process involving DA's positively charged amine moiety (Bath et al., 2000). DA is modeled to first adsorb to the carbon fiber surface, then undergo oxidation to dopamine o-quinone while adsorbed and then release the dopamine o-quinone into solution, with the adsorption and desorption processes viewed as first order kinetic processes (Bath et al., 2000, DuVall and McCreery, 2000). This adsorption was found to be a necessary

part of the electrochemical detection of DA by carbon fiber working electrodes. When adsorption to the carbon fiber was inhibited, the electrochemically detected DA signal disappeared (DuVall and McCreery, 1999).

### 1.5: QUANTIFICATION AND SITE SPECIFICITY OF EVOKED DA OVERFLOW

In 1988 Mark Wightman introduced the theory that the change in concentration of extracellular DA over time, termed evoked DA overflow, is a quantifiable balance between $Ca^{2+}$ dependent vesicular release and DAT mediated uptake (Wightman et al., 1988a, Michael and Wightman, 1999, Michael et al., 2005). His proposed mathematical model makes the assumptions that the concentration of DA released per pulse, $[DA]_p$, is constant and independent of stimulation frequency, that DAT mediated uptake is the only method of DA clearance and that DAT uptake is defined by Michaelis-Menton kinetics. The model for evoked overflow described in Equation 1.5 describes the change in concentration of extracellular DA ($[DA]_{ex}$) over a given time.

**Equation 1.5**

$$\frac{d[DA]_{ex}}{dt} = f * [DA]_p - \frac{V_{\max}}{\frac{K_m}{[DA]_{ex}} + 1}$$

In Equation 1.5, $f$ is the frequency of stimulation pulse, $[DA]_p$ is the concentration of DA released per pulse, $V_{max}$ is the maximum rate of DA uptake via DAT and $K_m$ is the binding constant. According to this model, when vesicular release is halted, the equation reduces down to solely DAT mediated uptake kinetics, shown in Equation 1.6.

**Equation 1.6**

$$\frac{d[DA]_{ex}}{dt} = \frac{-V_{\max}}{\frac{K_m}{[DA]_{ex}} + 1}$$

Wightman asserts that his model adequately fits many of the previously published DA evoked overflow curves found in the striatum (Wightman et al., 1988a). In future studies, locations within the striatum

that produced kinetics consistent with the predictions of the Wightman model came to be termed “hot spots” (Venton et al., 2003), while other locations, with kinetics deviating from the Wightman model, were labeled as “non-DAergic” (Venton et al., 2003) sites consisting of artifacts of diffusion and not studied (May and Wightman, 1989b, Garris et al., 1994, Peters and Michael, 2000, Venton et al., 2003).

The previously modeled “hot spot” type sites showed a rapid increase in evoked overflow upon the start of stimulated release, fast onset of D2 autoinhibition upon continued stimulation and fast clearance (Moquin and Michael, 2009, Moquin and Michael, 2011). This produced a characteristic concave down shape for the evoked overflow curve where the amount of DA evoked during the first 100 ms of stimulation is greater than that evoked during the following 100 ms of stimulation. Domains typical of this kinetic profile were deemed “fast sites”. A typical fast site is shown in Figure 1.1a. In 2009, our lab discovered that the “non-DAergic” sites that were previously discarded as an artifact of diffusion were reproducible and subject to pharmacological manipulation. These sites show slow initial evoked overflow signal, with no detectable change in DA present during the initial 200 ms of stimulation, an increase in signal upon further stimulation and slower clearance (Moquin and Michael, 2009, Moquin and Michael, 2011). The evoked overflow signal increases in a concave up manner, where the previous 100 ms of stimulation evoked less DA than that produced by the following 100 ms of stimulation. Although these domains exhibit the leading shoulder typical of a diffusional curve, the evoked response was found to clear immediately upon the end of stimulation, contrary to a diffusional mechanism. Domains typical of this kinetic profile were named “slow sites”. A typical slow site is shown in Figure 1.1b.

In addition to distinguishing between fast and slow sites, our lab proposed that the kinetic profile of DAergic neurons are under control of the local basal DA concentration of 2 μM DA (Borland and Michael, 2004, Wang et al., 2010). Fast sites are believed to exist in the presence of a lower extracellular basal concentration of DA and subsequently show immediate release under no initial D2

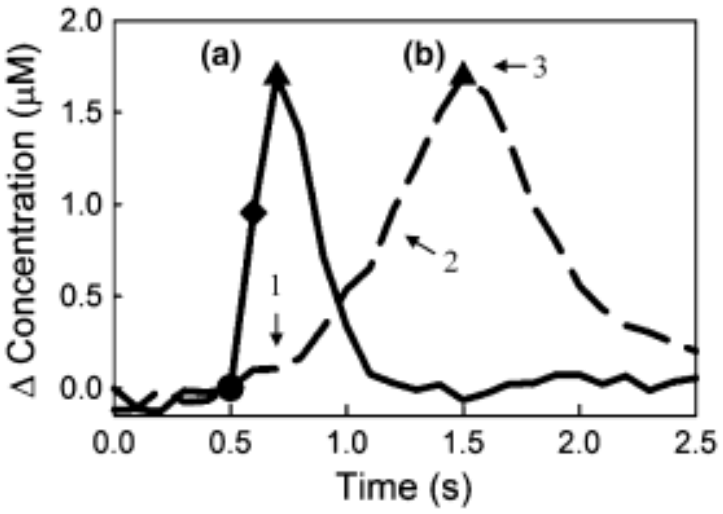


**Figure 1.1: Fast and slow domain responses.**
DA release in the dorsal striatum is heterogeneous. The response depicted in (a) is termed a "fast site" and exhibits kinetics predicted by the Wightman Model of DA transmission. Fast sites show an immediate increase in DA upon the start of stimulation (circle) and fall immediately upon the end of stimulation (triangle). Furthermore, the amount of DA released during the first 100 ms of stimulation (from the circle to the diamond) is greater than the amount of DA released during the second 100 ms of stimulation (from the diamond to the triangle), indicating an onset of autoinhibition. The response shown in (b) is that of a "slow site". Upon the start of stimulation (circle) release is slow (1), but then accelerates as stimulation continues (2) and falls immediately upon the end of stimulation (triangle) (3). Image courtesy of (Moquin and Michael, 2009).

autoinhibitory control, illustrated in Figure 1.2a. On the other hand, slow sites are modeled as existing in a high basal concentration of DA, which establishes a D2 autoinhibitory tone that inhibits release upon the start of stimulation, modeled in Figure 1.2b. This model was supported by pharmacological manipulation of the D2 autoreceptor (Moquin and Michael, 2009, Wang et al., 2010, Moquin and Michael, 2011). Treatment of a fast site with a D2 agonist, such as quinpirole, produces kinetics typical of a slow site (Figure 1.3a), whereas administration of a D2 antagonist, such as raclopride, to a slow site produces fast type kinetics (Figure 1.3b). This showed that the extent of D2 mediated autoinhibition can determine site kinetics. Furthermore, in conjunction with findings from other studies, it was shown that control over this fast and slow site specific local basal DA concentration difference is maintained by DAT mediated release (Borland and Michael, 2004, Moquin and Michael, 2009, Wang et al., 2010).

This dissertation details numerous discoveries that further the understanding of fast and slow DA kinetic domains and of DA transmission in the brain as a whole. The enclosed research discusses the domain dependent effect of the competitive DAT inhibitor, nomifensine, the important role of restricted DA diffusion in the extracellular space in maintaining fast and slow domains, the existence of four additional sub-domains of the fast domain and how highly selective and sensitive detection allows for the discovery of long term DA signaling *in vivo*. These discoveries have already become the intellectual basis of new scientific research and have the potential to uncover the unknown mechanisms underlying the multiple physiological functionalities and pathologies of the DA system.

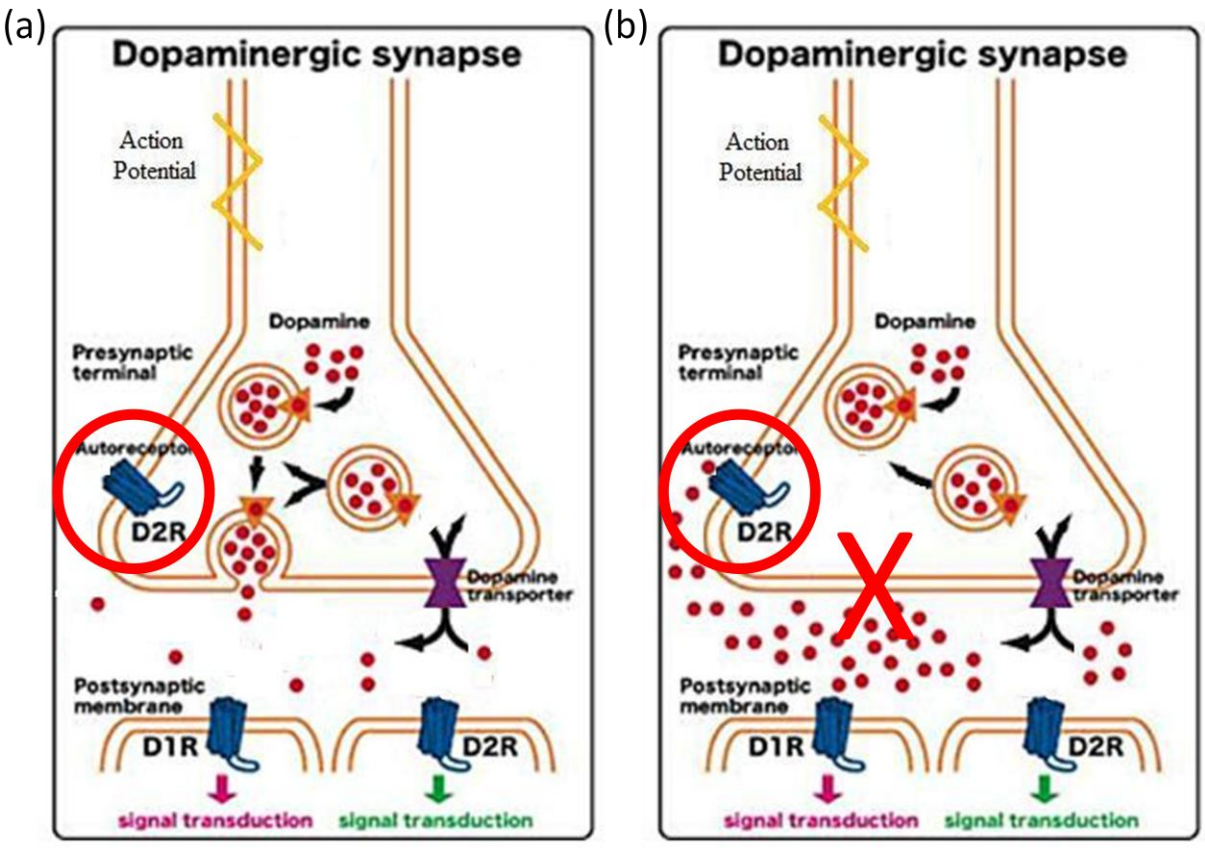


**Figure 1.2: Schematic representation of fast and slow domains.**
Domain dependent DA transmission is under the control D2 autoinhibition. (a) In fast sites, local basal extracellular DA concentrations are low enough that the D2 autoreceptor is unbound. Due to this lack of initial autoinhibition, vesicular release occurs immediately upon the presence of an action potential. (b) In slow sites, the local basal extracellular DA concentration is high enough (around 2 µM) to activate the D2 autoreceptor. Due to this autoinhibitory tone, immediate vesicular fusion does not occur upon the introduction of an action potential.

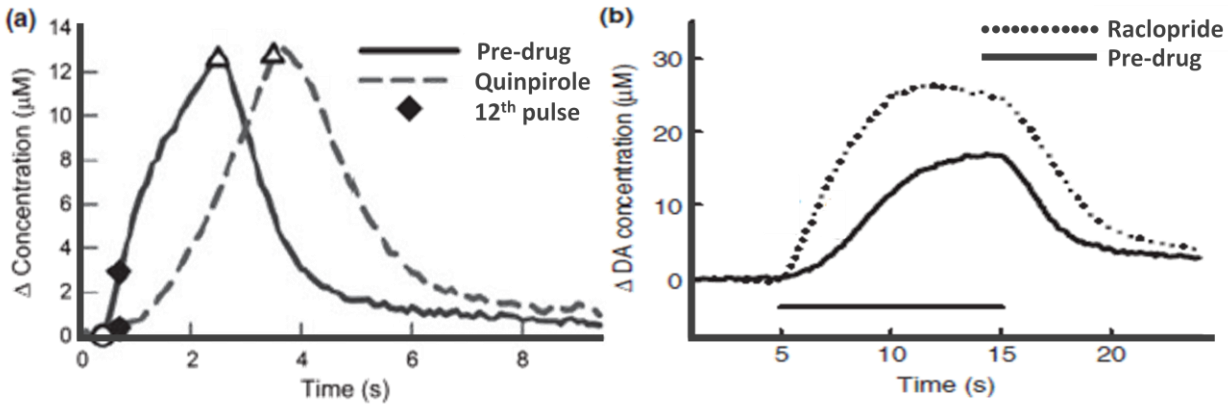


**Figure 1.3: D2 dependency of fast and slow domains.**
Domain dependent DA transmission is altered by pharmacological manipulation of D2 activity. (a) Treatment of a fast site with the D2 agonist, quinpirole, triggered the site to exhibit kinetics typical of a slow domain. (b) Treatment of a slow site with the D2 antagonist, raclopride, triggered the site to exhibit fast type kinetics. Altered images courtesy of (Wang et al., 2010).

## 2.0: DOMAIN DEPENDENT EFFECTS OF DAT INHIBITION IN THE RAT DORSAL STRIATUM

Adapted with revisions from Taylor et al. 2012. Reproduced with permission.

### 2.1: INTRODUCTION

Dopamine (DA) is a neurotransmitter that participates in multiple aspects of normal brain function (Roitman et al., 2004, Obeso et al., 2008) and a variety of brain disorders (Salahpour et al., 2008, de la Fuente-Fernandez et al., 2011, Kim et al., 2011). Consequently, drugs that act on DA have wide-ranging uses, some therapeutic (Gottwald and Aminoff, 2011, Schlochtermeier et al., 2011) and some illicit (Phillips et al., 2003, Hollander and Carelli, 2007, Ramsson et al., 2011). Understanding the actions of such drugs, including their impact on extracellular DA concentrations, is highly significant. Drugs such as cocaine, methylphenidate and nomifensine, which inhibit DA uptake (Jones et al., 1995b, Jones et al., 1998, Makos et al., 2010), are psychostimulants (Hunt et al., 1974, Nakachi et al., 1995, Garris et al., 2003) and have significant abuse potential (Spyraki and Fibiger, 1981, Phillips et al., 2003).

In the dorsal striatum of the rat, the DA terminal field exhibits domains of distinct fast and slow kinetics of DA release and clearance (Moquin and Michael, 2009, Wang et al., 2010, Moquin and Michael, 2011). We have thus far demonstrated that two drugs, raclopride and quinpirole, have domain-dependent actions on DA (Moquin and Michael, 2009, Wang et al., 2010). The activity of the DA transporter (DAT) (Gulley and Zahniser, 2003, Torres, 2006, Schmitt and Reith, 2010) appears to be domain-dependent as well, as we found the rate of extracellular DA clearance to be significantly faster in the fast compared to the slow domains (Moquin and Michael, 2011). And, DAT reversal contributes to a DA autoinhibitory tone in the slow domains (Moquin and Michael, 2009, Wang et al., 2010), which

is surprising considering that DAT reversal is thought to require amphetamine-like drugs (Sulzer et al., 1993, Sulzer et al., 1995). The objective of the present study, therefore, was to test the hypothesis that the actions of nomifensine, a competitive DAT inhibitor (Hunt et al., 1974), might also be domain-dependent.

## 2.2: MATERIALS AND METHODS

### 2.2.1: Carbon fiber electrodes

Borosilicate capillaries (0.4 mm ID, 0.6 mm OD, A-M systems Inc., Sequim, WA, USA), each containing a single carbon fiber (7-µm diameter, T650, Cytec Carbon Fibers LLC., Piedmont, SC,USA), were pulled to a fine tip using a vertical puller (Narishige, Los Angeles, CA, USA). The tip was sealed with epoxy (Spurr Epoxy, Polysciences Inc., Warrington, PA, USA), the exposed fiber was trimmed to a length of 200 µm, and a mercury drop was placed in the barrel for electrical contact to a hookup wire (Nichrome, Goodfellow, Oakdale, PA, USA).

### 2.2.2: Fast-scan cyclic voltammetry

Voltammetry was performed with an EI 400 (Ensman Instruments, Bloomington, IN) controlled by 'CV Tar Heels v4.3' software (courtesy of Dr. Michael Heien, University of Arizona, Tucson, AZ, USA). The reference electrode was Ag/AgCl. The waveform started at the rest potential (0 V vs. Ag/AgCl), ramped linearly (400 V/s) to +1.0 V, then to -0.5 V, and then to 0 V. Scans were repeated at 10 Hz. DA oxidation currents were recorded between 0.5 and 0.7 V on the initial ramp. DA was identified by inspection of background-subtracted voltammograms.

### 2.2.3: Electrode preparation and calibration

Electrodes were pretreated and calibrated in artificial cerebrospinal fluid (145 mM $Na^+$, 1.2 mM $Ca^{2+}$, 2.7 mM $K^+$, 1.0 mM $Mg^{2+}$, 152 mM $Cl^-$, and 2.0 mM phosphate, pH 7.4). The pretreatment was a triangular potential waveform (0-2 V, 200 V/s for 3 s) (Feng et al., 1987, Wang et al., 2010). Pre- and post-calibration were performed in a flow cell with freshly prepared, nitrogen-purged dopamine HCl (Sigma Aldrich, St. Louis, MO, USA) standard solutions. In vivo DA concentrations were determined by post calibration results.

### 2.2.4: Drugs

Isoflurane (Aerrane, Baxter Healthcare, Deerfield, IL, USA) was delivered by means of a calibrated gas anesthesia machine (IsoTec, Harvard Apparatus, Holliston, MA, USA). Nomifensine maleate was used as received (Sigma Aldrich, St. Louis, MO, USA) and dissolved in phosphate buffered saline (155mM $Na^+$, 155mM $Cl^-$, 100mM phosphate, pH 7.4)

### 2.2.5: Animals

All procedures involving animals (male Sprague-Dawley rats, 250-350 g, Hilltop, Scottsdale, PA, USA) were approved by the University of Pittsburgh's Institutional Animal Care and Use Committee. Rats were intubated and anesthetized with isoflurane (2.5% by volume) and placed in a stereotaxic frame with the incisor bar raised to 5 mm above the interaural line(Pellegrino et al., 1979). Internal body temperature was monitored and maintained at 37˚C by use of a heating blanket (Harvard Apparatus, Holliston, MA, USA). Holes were drilled through the skull for the reference, stimulating, and working electrodes. Electrical contact between brain tissue and a reference electrode was via a salt bridge. The stimulating electrode (bipolar stainless steel, MS303/a; Plastics One, Roanoke, VA, USA) was aimed at the medial forebrain bundle (MFB, 2.2 mm posterior to bregma, 1.6 mm lateral from bregma, and 7-8.5

mm below the cortical surface: the final vertical placement was adjusted to evoke DA release in the ipsilateral striatum) (Ewing et al., 1983, Kuhr et al., 1984, Stamford et al., 1988). The carbon fiber electrode was implanted into the dorsal striatum (2.5 mm anterior to bregma, 2.5 mm lateral from bregma and 5 mm below the cortical surface: the final vertical placement was optimized as explained in the Results Section). Confirmation of electrode placements by histology was not considered necessary in this study because the dorsal striatum is a large brain structure in the rat and easily targeted. The optically isolated stimulus waveform (Neurolog 800, Digitimer, Letchworth Garden City, U.K.) was a biphasic, constant-current, square wave (4 ms per pulse, 240 µA pulse height, and 60Hz frequency). The stimulus duration was 200 ms or 3 s (see Results section for detail on the stimulus duration).

Each rat received a series of pre-nomifensine stimuli, a single dose of nomifensine (20 mg/kg i.p) and a final post-nomifensine stimulus: the final stimulus was performed 30 min after nomifensine administration. The same electrodes, recording location, stimulating locations, stimulus parameters, etc., were used during the pre- and post-nomifensine responses. During this study, we compared pre- and post-nomifensine responses in the same group of animals to assure the effect of the drug was established at the same stimulating and recording electrodes. This approach, i.e. comparing pre- and post-drug responses is widely used (Wu et al., 2002, Venton et al., 2006, Moquin and Michael, 2009, Wang et al., 2010) and is based on a number of early voltammetric studies that established the high stability of electrically evoked DA responses (e.g. (Ewing et al., 1983, Millar et al., 1985, Michael et al., 1987a, b, Suaud-Chagny et al., 1995, Kulagina et al., 2001, Benoit-Marand et al., 2011) .

According to Davidson et al. (2000), prolonged exposure to nomifensine poisons carbon fiber electrodes. During this study, electrodes were exposed for only 30 min to a single dose of nomifensine. The poisoning effects noted by Davidson et al. were not observed during this study.

### 2.2.6: Data analysis

The initial rate of evoked DA overflow was determined from the slope of the evoked responses during the first 200 ms of each electrical stimulus. The initial linear DA clearance rate was measured from the slope of the descending phase of the response after the end of the stimulus: linear segments of this phase were defined by at least three data points with an $r^2$>0.96. Overshoot time was the length of time needed after the end of the stimulus for the evoked response to reach its maximum amplitude. The overshoot concentration was the amount by which the DA concentration continued to increase after the end of the stimulus. Statistical analyses were by t-test and two-way ANOVA with a repeated measures design (SPSS software).

### 2.2.7: Electron microscopy

Electron microscopy of carbon fiber probe tracks, including tissue processing and tracing the electrode track, was performed as previously described (Peters et al., 2004).

## 2.3: RESULTS

### 2.3.1: Domain-dependent dynamics of evoked DA release and clearance

Evoked DA responses in the rat dorsal striatum are domain-dependent (Moquin and Michael, 2009, Wang et al., 2010, Moquin and Michael, 2011). Responses in fast domains (Figure 2.1 solid line) exhibit a) a rapid onset when the stimulus starts (DA is readily detected on the first FSCV measurement 100 ms after the stimulus begins), b) short term depression (less increase in DA during the 2$^{nd}$ 100 ms of the stimulus than during the first 100 ms), c) no delay in DA clearance after the stimulus ends (no "overshoot"), and d) rapid DA clearance. Responses in slow domains (Figure 2.1 dashed line) exhibit a) a

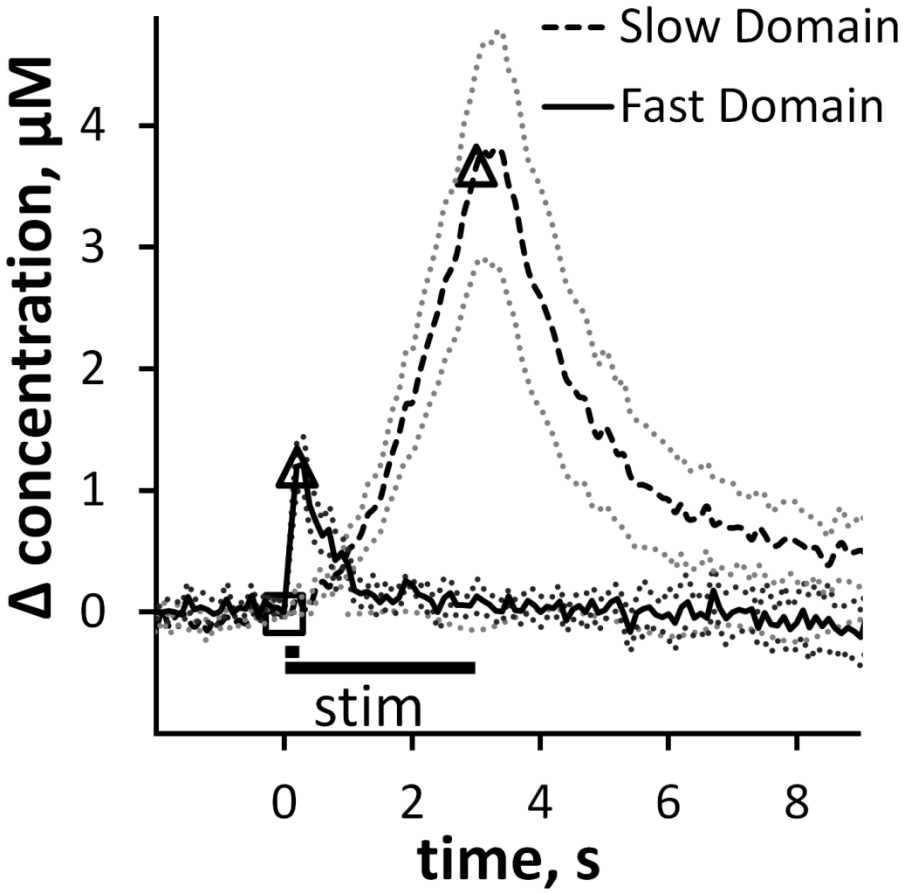


**Figure 2.1: Reproducibility of fast and slow domains.**
Fast and slow electrically evoked responses are recorded by fast scan cyclic voltammetry with carbon fiber microelectrodes in the dorsal striatum of isoflurane-anesthetized rats. In this and subsequent figures, the open symbols mark the beginning and end of the stimulus and the dotted lines show the SEM of the individual data points in each trace. These responses are the average (±SEM) of multiple individual responses (n= 6 fast and 8 slow) each recorded in a different rat with a different electrode. The fast and slow responses were obtained with identical procedures except for the stimulus duration (200 ms in the case of fast responses and 3 s in the case of slow: see text for full explanation).

slow onset when the stimulus starts (DA is non- or barely-detectable after the first 200 ms of the stimulus), b) short-term facilitation of the evoked response (the response rises more rapidly as the stimulus continues), c) a delay in clearance (overshoot) after the stimulus ends, and d) slow DA clearance.

The voltammetric responses in Figure 2.1 and subsequent figures are the average of a group of responses recorded in multiple animals. The dotted lines above and below the average responses show the SEM of each data point: individual error bars are omitted for clarity because there are so many data points (10 $s^{-1}$). The fast response in Figure 2.1 is the average (± SEM) of n=6 individual responses recorded with 6 different carbon fiber microelectrodes in 6 different rats. The slow response (Figure 2.1) is the average (± SEM) of n=8 responses recorded with 8 different carbon fiber microelectrodes in 8 different rats. So, Figure 2.1 contains data from 14 rats in total. Figure 2.1 establishes that the domain-dependent evoked responses are reproducible between subjects.

Slow domains are readily identified in all rats. However, recording from fast domains requires optimization of the placement of the voltammetric electrode (May and Wightman, 1989a, Kawagoe et al., 1992, Garris et al., 1994, Garris et al., 2003, Venton et al., 2003). Optimization involves lowering the electrode in small increments (50-100 µm) and repeating the stimulus at each new recording site. To confine this study to the dorsal striatum, the electrodes were lowered by no more than 1 mm. If a fast domain was not identified by optimization, slow responses were collected: we did not attempt multiple or deeper electrode penetrations during this study. A fast site is identified in two ways. First, evoked DA release is observed upon the very first voltammetric scan, which is performed 100 ms after the stimulus begins. Second, the response exhibits short-term inhibition, i.e. the rate of evoked overflow during the second 100 ms of the stimulus is less than during the first 100 ms. These characteristics are completely and obviously different from those associated with slow responses wherein evoked DA release is delayed and exhibits short term facilitation. In this and prior studies we have adopted the

practice of limiting the duration of the stimulus in fast domains to 200 ms. There are two reasons for this. First, beyond 200 ms the fast responses fade, i.e. the DA signal decreases even though the stimulus continues, due to the onset of autoinhibition induced by the evoked increase in extracellular DA: the fast responses, therefore, are highly transient (Moquin & Michael 2009). Second, if the stimulus continues beyond 200 ms, a slow response is observed. This implies that the dimensions of the fast domain is smaller than the length of the electrode such that the electrode is partially located in a fast domain and partially located in a slow domain (please also see Figure 2.8, below). We previously labeled this mix of fast and slow characteristics as a hybrid response (please see Moquin & Michael 2009 for additional details and examples of the hybrid response).

### 2.3.2: Domain-dependent effects of nomifensine: slow domains

Nomifensine has multiple effects on slow responses (Figure 2.2a: this figure includes the slow pre-drug response from Figure 2.1 for comparison). The post-nomifensine response (Figure 2.2a) is the average (±SEM) of the recordings in the same group of 8 rats. Nomifensine significantly ($p<0.005$) increased the initial rate of evoked overflow during the first 200 ms of the stimulus (Figure 2.2b), eliminated the tendency of the signal to rise more rapidly as the stimulus continued (Figure 2.2a: the rising phase of the post-nomifensine response is nearly linear rather than curved upwards) and significantly increased the amplitude and duration of the signal overshoot (see Figure 2.6). Nomifensine did not significantly affect the slope of the initial linear segment of the DA clearance profile (Figure 2.2c) but slowed the nonlinear segment after the DA signal fell below a DA concentration near 4 μM (see Figure 2.2a inset for a comparison of DA clearance starting at a concentration of 4 μM).

In the pre-drug condition, 200-ms stimuli evoked little-or-no detectable response in slow domains (Figure 2.3 blue). However, responses were clearly detected after nomifensine administration

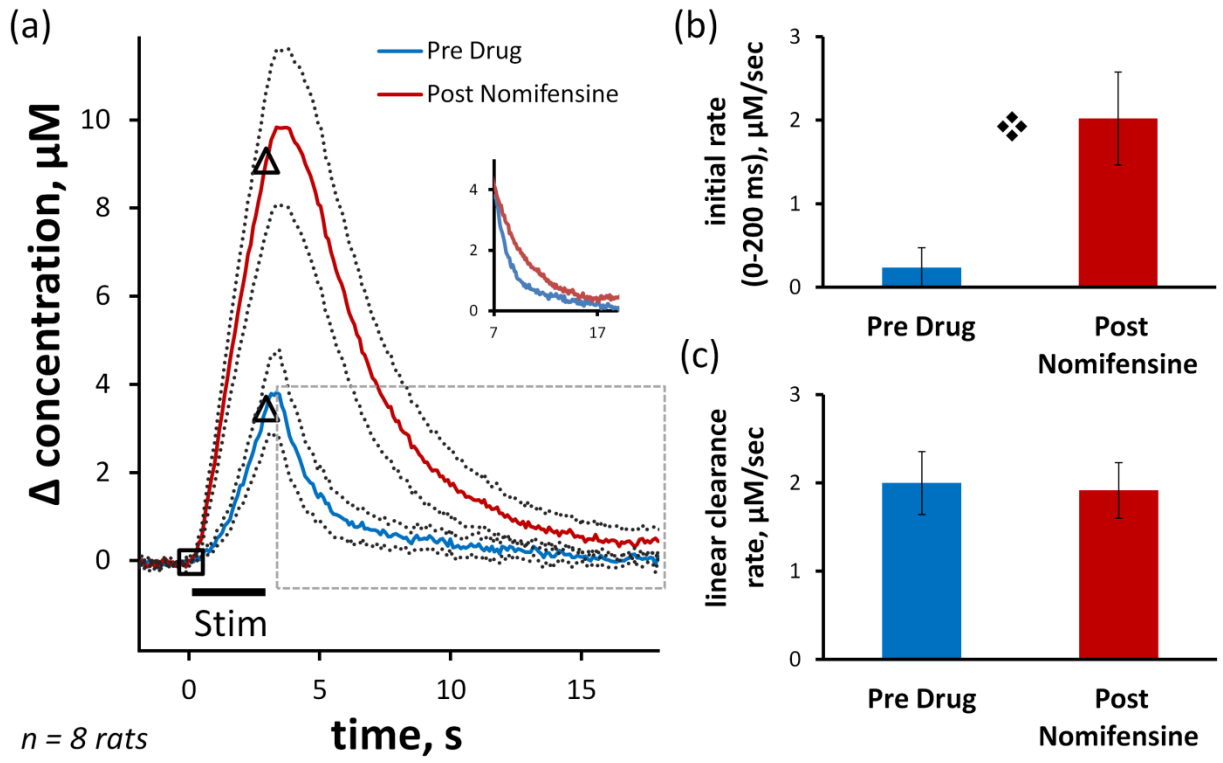


**Figure 2.2: Effect of nomifensine on the slow domain: 180 pulse stimulation.**
Nomifensine (20 mg/kg i.p.) affects evoked responses in slow domains. Figure 2.2a) Average (±SEM, n=8) of individual responses. Inset: Nomifensine slows the nonlinear segment of DA clearance below 4 µM. Figure 2.2b) Nomifensine significantly increases the rate of evoked overflow during the first 200 ms of the stimulus (❖ $p<0.005$, paired t-test). Figure 2.2c) Nomifensine has no effect on the rate of linear DA clearance during the descending phase of the response. Comparison of the clearance profiles during the final 4 µM of each response (inset) shows that nomifensine slowed the nonlinear phase of clearance in the slow domain.

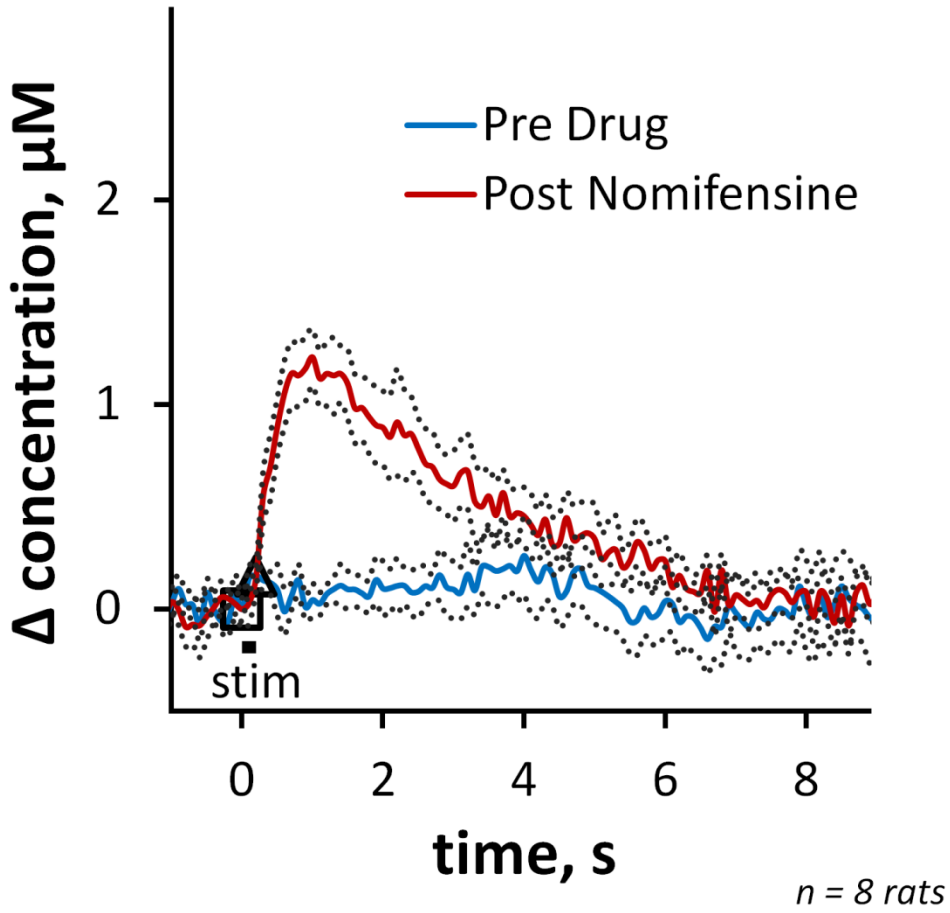


**Figure 2.3: Effect of nomifensine on the slow domain: 12 pulse stimulation.**
Pre- and post-nomifensine responses (average ±SEM, n=8) recorded in slow domains using a 200 ms stimulus duration.

(Figure 2.3 red). The onset of these responses was delayed with respect to the start of the stimulus: in 5 of 8 cases the onset of the response occurred after the end of the stimulus.

### 2.3.3: Domain-dependent effects of nomifensine: fast domains

Nomifensine has multiple effects on fast responses (Figure 2.4a: this figure includes the fast response from Figure 2.1 for comparison), however, these are distinct from the effects observed in slow domains. The post-nomifensine response is the average (± SEM) of the recordings in the same group of 6 rats. Nomifensine did not affect the initial response rate during the 200 ms stimulus (Figure 2.4a and 2.4b), dramatically increased the duration and amplitude of the stimulus overshoot (see also Figure 2.6), significantly ($p<0.0005$) decreased the slope of the initial linear segment of the clearance profile (Figure 2.4a and 2.4c) and also slowed the nonlinear segment of the DA clearance profile.

### 2.3.4: Domain-dependent effects of nomifensine: comparisons

To emphasize and clarify the domain-dependent actions of nomifensine, we report the initial response rates (0-200 ms) and linear clearance rates normalized with respect to their pre-nomifensine values (Figure 2.5). Nomifensine significantly increased the normalized initial response rate in slow but not fast domains (Figure 2.5a). According to 2-way ANOVA (details provided in the Figure 2.5 legend), the drug treatment (pre- and post-nomifensine, $p<0.002$) and interactions ($p<0.002$) are significant. Nomifensine significantly slowed the normalized rate of linear DA clearance in fast but not slow domains (Figure 2.5b): the drug treatment ($p<0.000002$) and interactions ($p<0.000005$) are significant.

Nomifensine significantly affected the duration and amplitude of the overshoot after the end of the stimulus (measured according to the guidelines in Figure 2.4a). Nomifensine significantly increased the overshoot duration ($p<0.000005$) but to a greater extent in fast domains (Figure 2.6a). Nomifensine

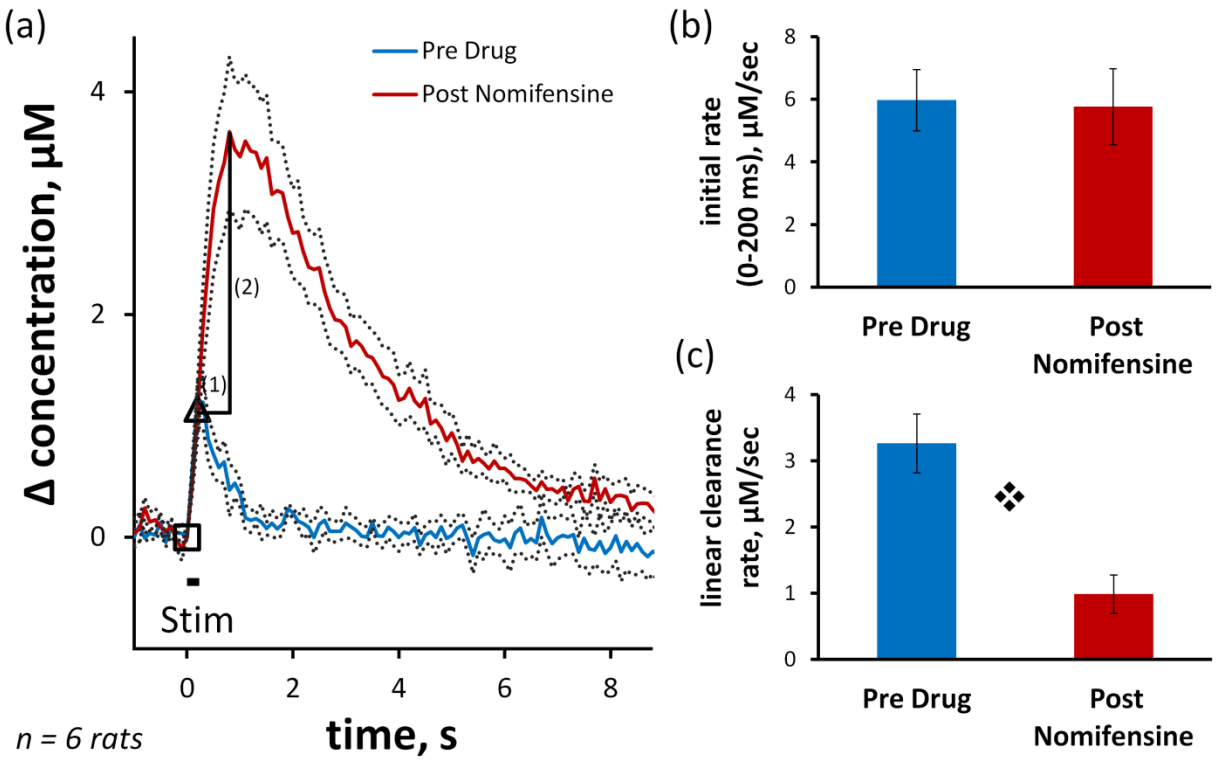


**Figure 2.4: Effect of nomifensine on the fast domain: 12 pulse stimulation.**
Nomifensine affects evoked responses in fast domains. Figure 2.4a) Average (±SEM, n=6) of individual responses. The guidelines show how the duration (1) and amplitude (2) of the overshoot are defined (see Figure 6). Figure 2.4b) Nomifensine does not affect the initial rate of evoked overflow during the first 200 ms of the stimulus. Figure 2.4c) Nomifensine significantly decreases the slope of the linear segment of DA clearance (❖ $p < 0.0005$, paired t-test).

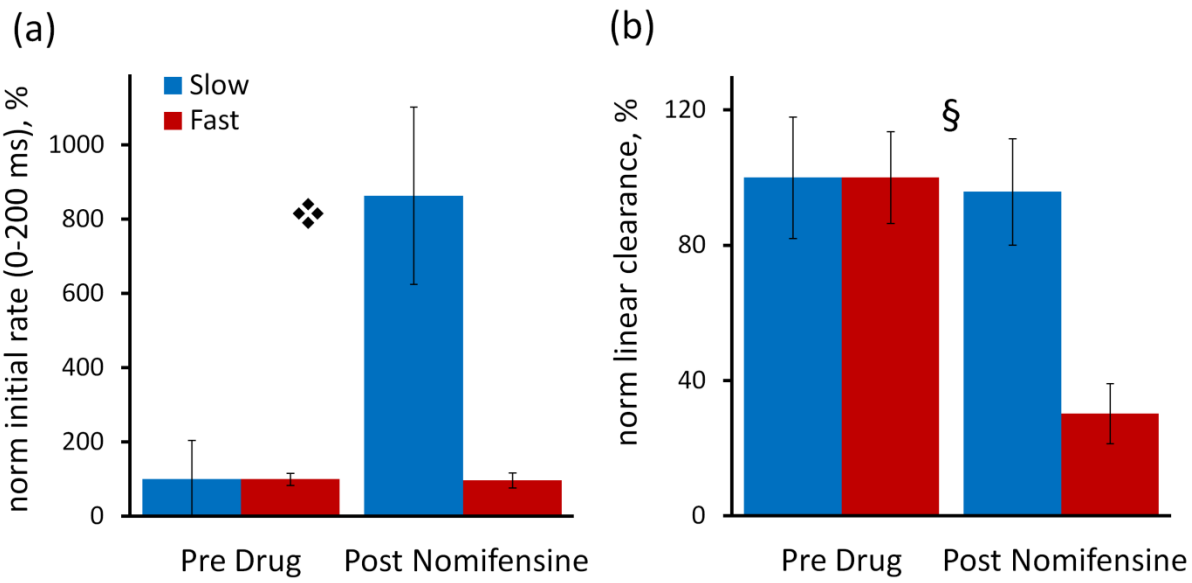


**Figure 2.5: Normalized domain dependent effects of nomifensine.**
The normalized effects of nomifensine are domain-dependent. The initial rates of overflow (Figure 2.5a) and linear clearance (Figure 2.5b) are normalized with respect to their pre-nomifensine values. Figure 2.5a) Nomifensine significantly increased the normalized initial rate of overflow in slow but not fast domains (❖, 2-way ANOVA with repeated measures: drug treatment (pre- and post-nomifensine) $F(1,12) = 14.517$, $p < 0.002$, interactions $F(1,12) = 14.771$, $p < 0.002$). Figure 2.5b) Nomifensine significantly decreased the rate of linear DA clearance in fast but not slow domains (§ 2-way ANOVA with repeated measures: treatment $F(1,12) = 79.332$, $p < 0.000002$, interactions $F(1,12) = 62.172$, $p < 0.000005$).

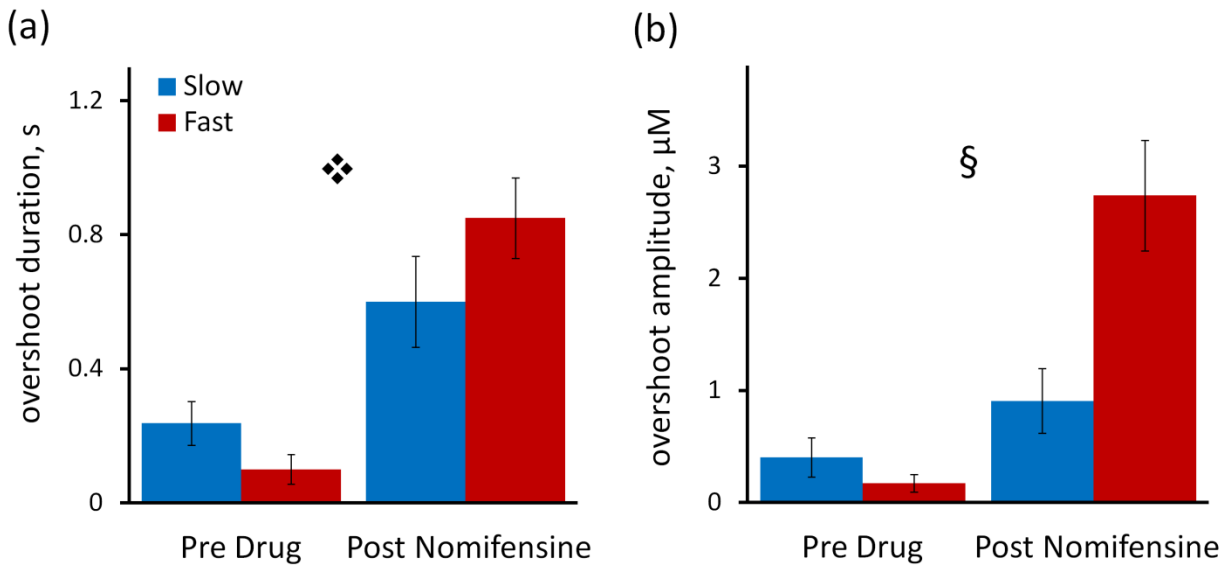


**Figure 2.6: Effect of nomifensine on DA overshoot.**
Nomifensine affects signal overshoot, a measure of the delay at the end of the stimulus (see Figure 2.4a for guidelines). Figure 2.6a) Nomifensine significantly increased the overshoot duration to 0.60 sec in the slow domains and to 0.85 sec in the fast domain (❖ 2-way ANOVA with repeated measures: treatment $F(1,12) = 64.152$, $p < 0.000005$, interactions $F(1,12) = 7.783$, $p < 0.02$). Figure 2.6 b) Nomifensine significantly increased the overshoot amplitude in fast but not slow domains (§ two way ANOVA with repeated measures: domains (fast and slow) $F(1,12) = 5.264$, $p < 0.05$, treatment $F(1,12) = 51.659$, $p < 0.000002$, interactions $F(1,12) = 23.166$, $p < 0.0005$).

significantly increased the overshoot amplitude ($p<0.00002$) but to a greater extent in fast domains (Figure 2.6b: 2-way ANOVA details are in the figure legend).

In both fast and slow domains, nomifensine slowed the rate of non-linear clearance, as expected given that nomifensine is a competitive DAT inhibitor (Wightman et al., 1988a, Wu et al., 2001b).

### 2.3.5: Electron Microscopy

Electron microscopy (Figure 2.7) exposes the ultrastructural details of the tissue architecture in the vicinity of the electrode track. This image was obtained, as previously described (Peters et al., 2004) by starting above the recording site where the track formed by the glass barrel of the electrode is obvious and following the track ventrally until it exhibits dimensions commensurate with the diameter of the carbon fiber. In this image, the track is visualized as an approximately round spot of red blood cells that apparently filled the void created when the electrode was explanted from the tissue. Because these red blood cells are outside vessels, they were not removed during the perfusion. The track has a well-defined boundary where the red blood cells meet the tissue. Numerous identifiable elements are present in close proximity to this boundary (see Figure 2.7 legend for details), including axon terminals forming symmetric or asymmetric synaptic junctions. Numerous synaptic junctions with normal morphology are present less than 1 µm from the track boundary.

## 2.4: DISCUSSION

This study reinforces the presence of distinct fast and slow DA kinetic domains in the rat dorsal striatum (Figure 2.1) and demonstrates that the actions of nomifensine on evoked DA responses are domain-dependent. Although several previous studies have examined nomifensine's actions on evoked DA (Jones et al., 1995b, Garris et al., 2003, Robinson and Wightman, 2004, Borland et al., 2005, Benoit-Marand et al., 2011), none addressed the domain-dependency. As discussed in detail below, the impact

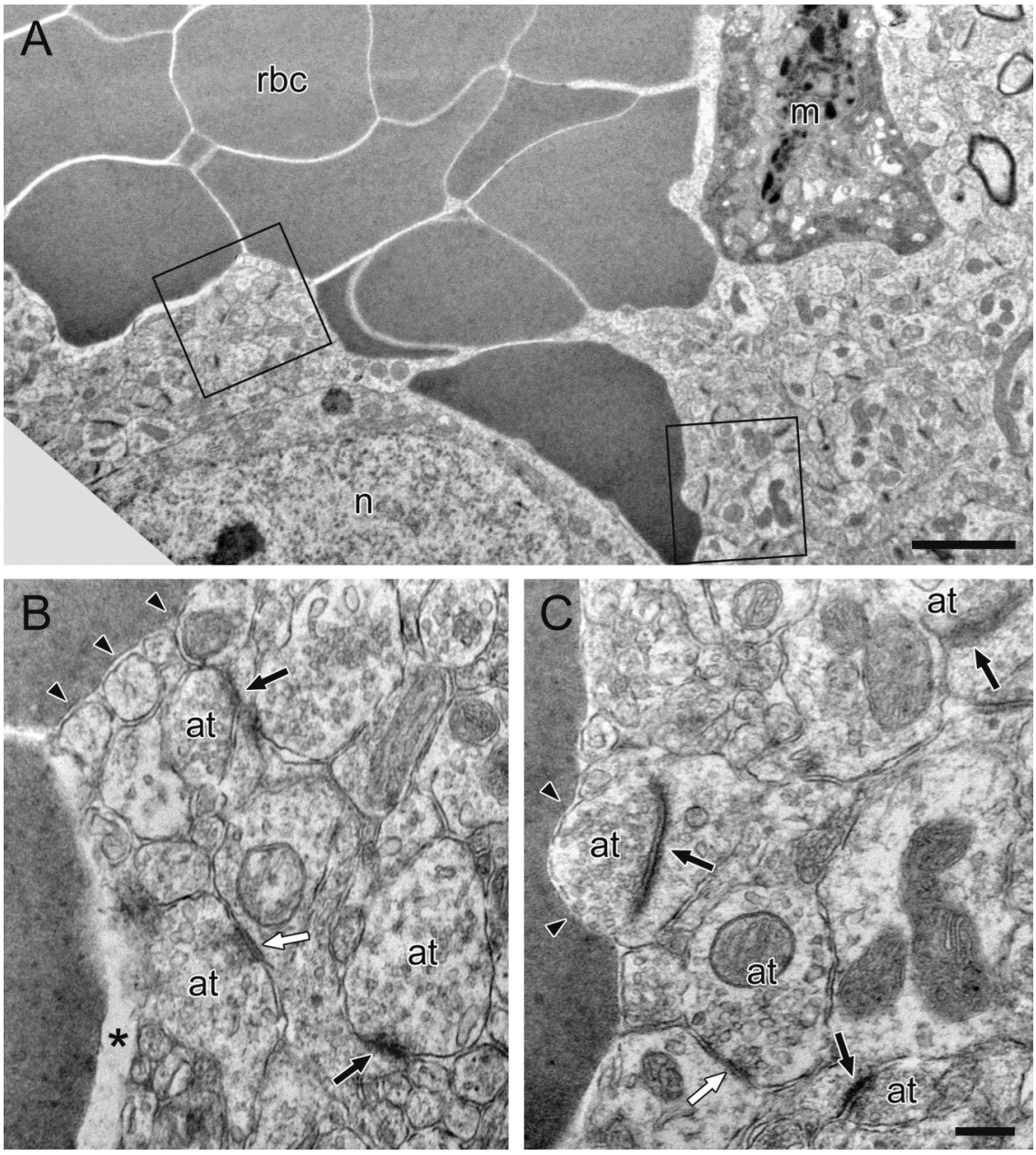


**Figure 2.7: Electron micrograph of the carbon fiber microelectrode track in the dorsal striatum.** Electron microscopic images of a carbon fiber track in the rat dorsal striatum. Figure 2.7A) At lower magnification, the track appears as an approximately round spot filled with red blood cells (rbc) that apparently fill the void formed when the electrode is explanted. Also visible are a single reactive monocyte (m) and the cell body of a neuron (n). The regions of interest outlined by boxes are shown at higher magnification in Figure 2.7B, Figure 2.7C. Blood cells are directly apposed to neuronal structures (arrowheads) or separated from them by a slightly larger space (asterisk in B). The morphological appearance of these neuronal structures is normal. Multiple axon terminals (at) form symmetric (white arrows) or asymmetric synapses (black arrows) onto dendritic shafts or spines, respectively. Scale bar in Figure 2.7A corresponds to 2 µm for Figure 2.7A and the scale bar in Figure 2.7C corresponds to 0.25 µm for Figure 2.7B and Figure 2.7C.

of nomifensine on evoked DA responses cannot be explained solely by its ability to increase the effective $K_M$ of DA uptake, which points to an additional action of nomifensine on DA. Based on the findings of this study, we propose that additional action involves an interaction with restricted DA diffusion processes in the extracellular space.

### 2.4.1: Detection of DA domains

In our experience, slow domains are found throughout the dorsal striatum (see Materials and Methods for coordinates) but it is necessary to optimize the electrode placement in order to identify fast domains. Optimization to find DA "hot spots" is a common procedure (May and Wightman, 1989a, Kawagoe et al., 1992, Garris et al., 1994, Garris et al., 2003, Venton et al., 2003), but relatively little attention has been devoted to the "cold spots", which have been viewed as non-DAergic sites (Venton et al., 2003). Our recent reports, however, demonstrated that the cold spots are slow DAergic domains wherein DA terminals are autoinhibited (Moquin and Michael, 2009, Wang et al., 2010). Although evoked DA release in the striatum is generally described as heterogeneous (Wightman et al., 1988a, May and Wightman, 1989b, Kawagoe et al., 1992, Zahniser et al., 1999, Venton et al., 2003), the fast and slow responses are reproducible across subjects (Figure 2.1).

Our findings provide some preliminary indication of the architecture of the domains. The schematic in Figure 2.8 depicts fast domains as "islands" on a slow background, with one microelectrode traversing a fast island and a second contained entirely within the slow "sea". The idea that fast domains are smaller than the length of the electrodes (200 µm) rests on the observation of hybrid responses, consisting of both fast and slow components, when the stimulus extends beyond 200 ms (Moquin and Michael 2009). The spacing between the fast domains appears to be more than the length of the electrode (200 µm), since many recording sites produce only the slow response.

**Equation 2.1**

$$\frac{\mathrm{d}[DA]}{\mathrm{d}t} = f \cdot [DA]_p - \frac{V_{max} \cdot [DA]}{[DA] + K_M}$$

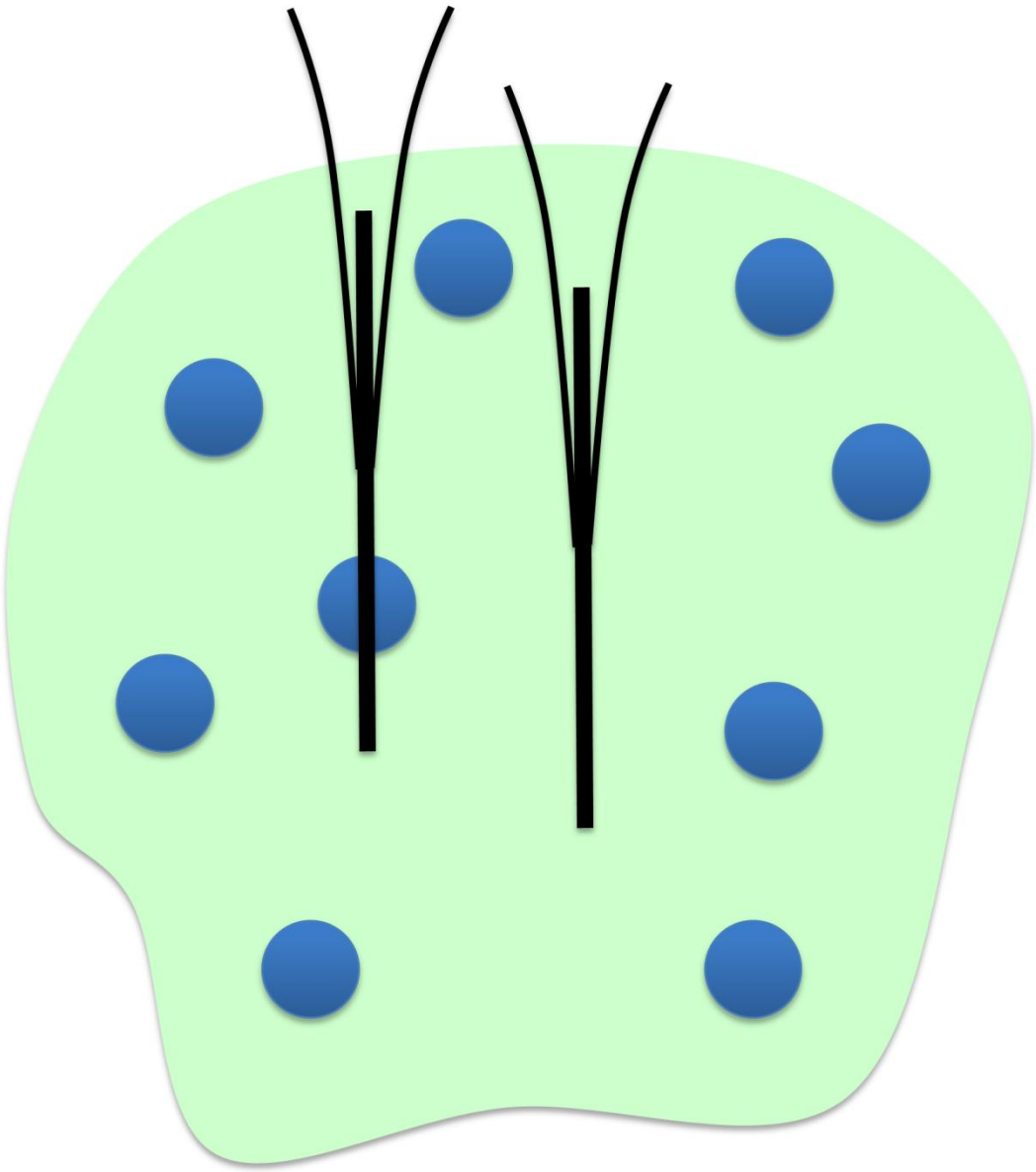

**Figure 2.8: Schematic representation of the proposed domain architecture.**
Schematic of the proposed domain architecture depicting island-like fast domains (blue circles) on a slow background (pale green). One electrode is depicted as traversing a fast island while a second electrode is depicted within the slow domain. Lowering the second electrode to deeper recording sites would not result in detection of a fast domain.

### 2.4.2: A model for evaluating evoked responses

Evoked DA responses are often evaluated with a model that combines the rates of DA release and clearance (May et al., 1988, Wightman et al., 1988a, Kennedy et al., 1992, Wu et al., 2001a, Michael et al., 2005): where [*DA*] is the extracellular DA concentration, *t* is time, *f* is the stimulus frequency, $[DA]_p$ is the concentration of DA released per stimulus pulse and $V_{max}$ and $K_M$ are the maximal rate and Michaelis constant, respectively, of DA uptake. So, $f \cdot [DA]_p$ is the rate of evoked DA release and $\frac{V_{max} \cdot [DA]}{[DA] + K_M}$ is the rate of DA uptake. Equation 2.1 was previously presented as Equation 1.5.

According to this model (see Supplementary Information), the difference between the rate of evoked release and DA uptake determines the rising phase of the evoked response, whereas uptake alone determines the descending phase of the response. If the DA concentration sufficiently exceeds $K_M$, then the descending phase of the response is predicted to exhibit an initial linear segment, reflecting the zero-order kinetics of saturated transporters ($V = V_{max}$), followed by a nonlinear segment when transporters are no longer saturated ($V \approx k[DA]$, where $k = V_{max}/K_M$) (Peters and Michael, 2000, Wu et al., 2001b).

Measured responses sometimes exhibit delays at the beginning and end of the stimulus. These delays are not described by Equation 2.1 and are usually attributed to diffusion across a gap between the electrode and DA terminals (Kristensen et al., 1987, Engstrom et al., 1988, Garris et al., 1994, Jones et al., 1995b). Such a gap might be caused by the use of a Nafion film or damage to the tissue adjacent to the electrode. The delays can be removed with a deconvolution algorithm. Once the responses are deconvoluted, the model can be used to determine "intrinsic" values $[DA]_p$, $V_{max}$, and $K_M$ (Engstrom et al., 1988, Wightman et al., 1988a, May and Wightman, 1989a, Kawagoe et al., 1992, Garris et al., 1994, Wu et al., 2001b, Venton et al., 2002, Garris et al., 2003). Without deconvolution, the slopes of the

responses can be used to estimate “apparent” kinetic values, which are likely to include diffusion contributions since diffusion acts on local DA concentrations (Rice and Cragg, 2008).

### 2.4.3: Evaluating slow responses

The rising phase of slow responses exhibits an obvious delay when the stimulus starts (the onset is delayed, begins slowly, and speeds up as the stimulus continues). But, rather than diffusion, this delay is due to autoinhibition: the delay is eliminated by the D2 antagonist, raclopride, and enhanced by the D2 agonist, quinpirole (Moquin and Michael, 2009). Because the delay is not due to diffusion, the deconvolution algorithm cannot be used, so we analyzed these responses for apparent kinetic parameters (we have not yet attempted to elaborate on Equation 2.1 to include autoinhibition: however, see (Montague et al., 2004)). Qualitatively, Equation 2.1 predicts that a competitive uptake inhibitor, which increases the effective $K_M$ (Miller and Tanner, 2008), is expected to a) increase the slope of the rising phase of the response, b) have no effect on the rate of the initial linear segment of the DA clearance profile, and c) increase the concentration at which the clearance kinetics transition from zero- to first-order (Peters and Michael, 2000, Wu et al., 2001b). Nomifensine produces all of these predicted effects in slow domains (Figure 2.2).

Two aspects of the post-nomifensine response in slow domains deserve further consideration. First, nomifensine eliminated the response delay at the start of the stimulus. This reinforces the conclusion that the delay is not diffusional because DA terminals must be present very near the electrode in order to detect DA release so quickly (100 ms) after the stimulus begins. Because nomifensine targets DAT, this observation also reveals the presence of functional DATs very near to the electrode, and in the dorsal striatum only DA terminals express this protein (Rocha et al., 1998). The detection by EM of axon terminals in close proximity to the electrode track (Figure 2.7) also supports this conclusion. An alternative possibility is that nomifensine eliminated the onset delay by triggering

the desensitization of autoreceptors (Katz et al., 2010): at present, we consider this mechanism unlikely because a) uptake inhibition is expected to increase the rate overflow and b) in our hands the D2 agonist quinpirole further suppressed evoked release, which is not the expected consequence of desensitization (Moquin and Michael, 2009). Second, even though nomifensine decreased the onset delay, it increased the response overshoot at the end of the stimulus (Figure 2.6). The asymmetry of nomifensine's impact on the response delays (i.e. decreasing the delay at the start of the stimulus and increasing the delay at the end of the stimulus) is very surprising and has not been commented on before in the literature. As mentioned above, delays are usually attributed to a diffusion gap, but a diffusion gap causes symmetrical delays, i.e. a larger gap will increase the delay at both the start and end of the stimulus (see Supplementary Information). As discussed below, the asymmetry of the delays observed in this study require careful consideration.

Analysis of the slope of the rising and descending phases of the slow responses yields a set of apparent DA kinetic parameters (Figure 2.2b and 2.2c). The uniformity of the slow domain responses implies an absence of concentration gradients during these measurements, so the apparent values are probably not greatly affected by diffusion. In that case, the apparent rate of DA clearance reflects the activity of transport, which primarily occurs via the DAT (Moron et al., 2002, Torres, 2006), with possible contributions from other transporters (Wu et al., 1998, Moron et al., 2002, Larsen et al., 2011). However, our experiments were not designed to resolve the contribution of individual transporters. The apparent rates must be viewed as semi-quantitative because EM analysis (Figure 2.7) shows that the electrodes are partially blocked, in this instance by a reactive monocyte (an immune cell) near the electrode track: such blockage of the electrode surface leads to underestimation of DA concentrations and rates. Assuming that the blockage is constant over the short duration of these experiments, proportional comparisons of the apparent clearance rates are justified (Figure 2.5).

### 2.4.4: Evaluating fast responses

In fast domains, the evoked responses (pre-nomifensine) exhibit no delay when the stimulus starts or stops. The responses exhibit all the main features predicted by Equation 2.1 (see Supplementary Information): a) the signal rises without delay when the stimulus begins, b) the signal slows down as the stimulus continues (because the rate of DA clearance increases as the DA concentration rises), and c) the DA clearance profile exhibits an initial linear segment (zero-order clearance) followed by a non-linear segment (the expected conversion to first-order clearance). This supports the view that the fast responses are affected by neither autoinhibition nor diffusion gaps.

Some features of the post-nomifensine fast responses are also consistent with the kinetic model (Equation 2.1). The most obvious is the overall decrease in the rate of DA clearance after the end of the stimulus (see Supplementary Information), since nomifensine is a DAT inhibitor. On the other hand, nomifensine had no effect on the initial rate of evoked release (Equation 2.1 predicts an increase) and dramatically increased the duration and amplitude of the overshoot (Equation 2.1 does not predict overshoot). Thus, as in slow domains, nomifensine has a highly asymmetric effect on the response delays not predicted by the kinetic model.

It is important to emphasize that we cannot use the deconvolution algorithm to remove the overshoot from the post-nomifensine fast responses. The delay in these responses is highly asymmetric, whereas the deconvolution was developed to correct symmetric delays arising from diffusion gaps (see Supplementary Information). In prior studies, diffusion gaps were attributed to Nafion films, which were not used in this study, or tissue damage. Although tissue damage is a concern when implanting devices into brain tissue (Jaquins-Gerstl and Michael, 2009, Jaquins-Gerstl et al., 2011), EM shows no evidence of damage-related diffusion gaps in our studies (Figure 2.7). Moreover, the pre-nomifensine response is not delayed, so there is no evidence for diffusion gaps in the fast recording sites.

It is necessary to consider whether the proposed island-like geometry of the fast domains (Figure 2.8) contributes to the overshoot. For example, it is often mentioned (Nicholson, 1995, Borland et al., 2005) that uptake inhibition provides DA with more time to diffuse further from its source. However, if molecules are produced within a small source, the rapid outward diffusion into an ever-expanding volume leads to rapid dilution at increasing distances from the source: this makes overshoots less likely, not more likely. For example, Rice and Cragg calculated the diffusion and uptake of DA after release from a single vesicle (Rice and Cragg, 2008). Their calculations show that even in the absence of uptake (see their Figure 2.1) DA in the striatum reaches its peak extracellular DA concentration within a few milliseconds of the quantal event, whereas the overshoot duration observed during our study reached as long as 850 ms (Figure 2.6).

It is also known that DAT inhibitors can activate DA release from intraneuronal storage pools (Ewing et al., 1983, Venton et al., 2006). It is possible that activation of storage pools could contribute to the post-nomifensine response observed during this study. However, additional release would not by itself lead to asymmetry of the response delays, which are the focus of the remainder of this discussion.

### 2.4.5: A role for restricted diffusion in the effects of nomifensine

As explained above, the existing model of DA kinetics (Equation 2.1), even when adjusted for a diffusion gap (Supplementary Information), cannot explain nomifensine's prominent impact on the asymmetry of the evoked responses. Thus, it appears that DA uptake is somehow coupled to extracellular DA diffusion in a manner not yet fully understood. We now present a new explanation that invokes restricted DA diffusion in the extracellular space.

The overshoot in the post-nomifensine fast response is remarkable in that its duration of 850 ms is 4-times longer than the stimulus itself (Figures 2.4 and 2.6). A similar overshoot occurs in slow domains when the stimulus is likewise limited to 200 ms (see Figure 2.3 and Figure 2.9). The overshoots

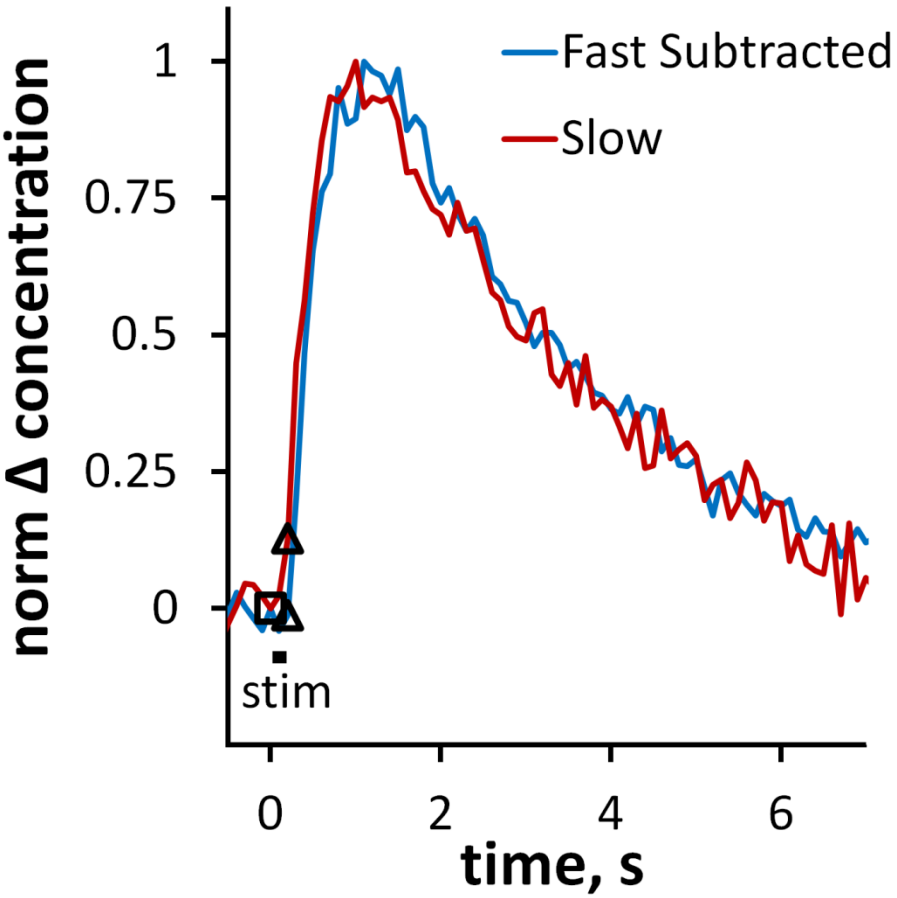


**Figure 2.9: Normalized fast and slow nomifensine induced overshoot kinetics.**
The "pure overshoots" observed in fast and slow domains post-nomifensine in response to a 200 ms stimulus. The two responses are normalized to their maximum amplitudes. The blue line was obtained from the fast domain by subtracting the pre-drug response from the post-nomifensine response. The red line is from Figure 2.3.

show that DAT inhibition allows DA to continue diffusing to the recording electrode long after DA terminals stop releasing DA. But, the large amplitude of the post-nomifensine responses shows that DA does not suffer substantial dilution during this process, so the diffusion occurs over a short distance. This combination, long diffusion time combined with little dilution, is highly suggestive of a restricted diffusion process.

In this restricted diffusion scenario, DA molecules are released near the electrode but are restricted from diffusing to the electrode and thus go undetected. There are several ways in which diffusion can be restricted but an obvious candidate in brain tissue is the tortuosity of the extracellular space (Nicholson, 1995, Nicholson and Sykova, 1998, Sykova and Nicholson, 2008). Because the extracellular space is tortuous, it is possible that some DA molecules are released into confined spaces connected to the surroundings by narrow passageways or bottlenecks. If diffusion through the bottlenecks is slow, DA could be taken up faster than it can diffuse to the surrounding. In this scenario a DAT inhibitor would promote the escape, and thus detection, of DA with the long-duration overshoot reflecting the rate of DA diffusion through the bottlenecks.

This restricted diffusion scenario explains the asymmetric impact of nomifensine on the response delays as not all DA molecules are restricted from diffusing to the electrode. The rapid onset of the fast response is presumably due to non-restricted molecules, whereas the overshoot is due to restricted molecules. The restricted diffusion concept also explains the asymmetry of nomifensine's actions on the slow responses. According to this new explanation of events, the decreased delay in the onset of the response is attributable, in the normal way, to a decreased rate of uptake (according to Equation 2.1, less uptake during the stimulus should increase the response rate), while the overshoot derives from overcoming restricted diffusion.

The literature offers precedent for this restricted diffusion concept. It was previously invoked by Floresco *et al.* (Floresco et al., 2003) to explain the effects of uptake inhibition on the detection of DA by

microdialysis. Floresco *et al.* suggested that DA molecules are restricted to synaptic clefts until the DAT is inhibited. This idea, however, is at odds with the concept that DA molecules escape rapidly from striatal synapses (Garris et al., 1994), given their nanometer dimensions (see, for example, Figure 2.7). Despite this caveat, it is interesting to note that the restricted diffusion model appears to be consistent with DA measurements by both voltammetry and microdialysis.

Other mechanisms of restricted diffusion are known. For example, diffusion can be restricted if molecules interact with stationary binding sites (see (Sykova and Nicholson 2008) and section 8.4 of (Crank, 1956)). In this case, molecules would not 'break through' to the electrode until the binding sites were completely occupied, which could be a consequence of uptake inhibition. Further investigation will be required to explain the precise mechanism by which DA diffusion is restricted but our results clearly suggest that DAT interacts with a complex diffusion process to maintain control of extracellular DA concentrations. Nomifensine's actions cannot be explained solely on the basis of an increase the $K_M$ of DA uptake.

## 2.5: CONCLUSION

This study reinforces the existence of distinct DA dynamical domains in the dorsal portion of the rat striatum and identifies the domain-dependent actions of nomifensine. The asymmetrical effects of nomifensine on the domain-selective responses suggest that DAT interacts with complex DA diffusion processes in the striatum. The restricted diffusion model is interesting in light of our previous reports that local differences in basal DA concentrations cause, via autoinhibition, the domain-dependent DA dynamics (Moquin and Michael, 2009, Wang et al., 2010). These local differences in DA concentration, while detected by voltammetry, are difficult to understand unless the local DA concentrations are

somehow prevented from freely mixing. Thus, the present study not only reinforces the existence of the domains but also contributes to explaining them.

## 2.6: SUPPLEMENTARY INFORMATION

### 2.6.1: The stability of evoked DA in the rat striatum

This study relies on comparisons of evoked DA responses in individual rats before and after the administration of nomifensine. This common practice relies on the well-known stability of evoked DA responses in the rat striatum (see references in main text). Prior studies have mainly focused on fast type responses recorded after optimization of the electrode placement. Figure S2.1 illustrates the stability of the slow responses by means of a representative example of multiple slow responses collected in an individual rat at 5, 15, and 45 minutes after an initial, baseline response. The delay in onset of the response and the rate of DA clearance after the end of the stimulus are both consistent.

### 2.6.2: Using Equation 1 to model competitive DAT inhibition

Equation 2.1 of the main text is a mathematical model used frequently to quantitatively evaluate evoked DA responses in terms of the intrinsic kinetic parameters $[DA]_p$, $V_{max}$, and $K_M$. A main theme of this study is that this standard model does not comprehensively fit the collection of evoked responses recorded in both the fast and slow domains, before and after the administration of nomifensine. This points to a major conclusion of our study, i.e. that nomifensine appears to do more than just increase $K_M$. In this Supplementary Information document, we present modeled evoked responses, with and without the effects of a diffusion gap, to examine the contrast between the modeled and measured results.

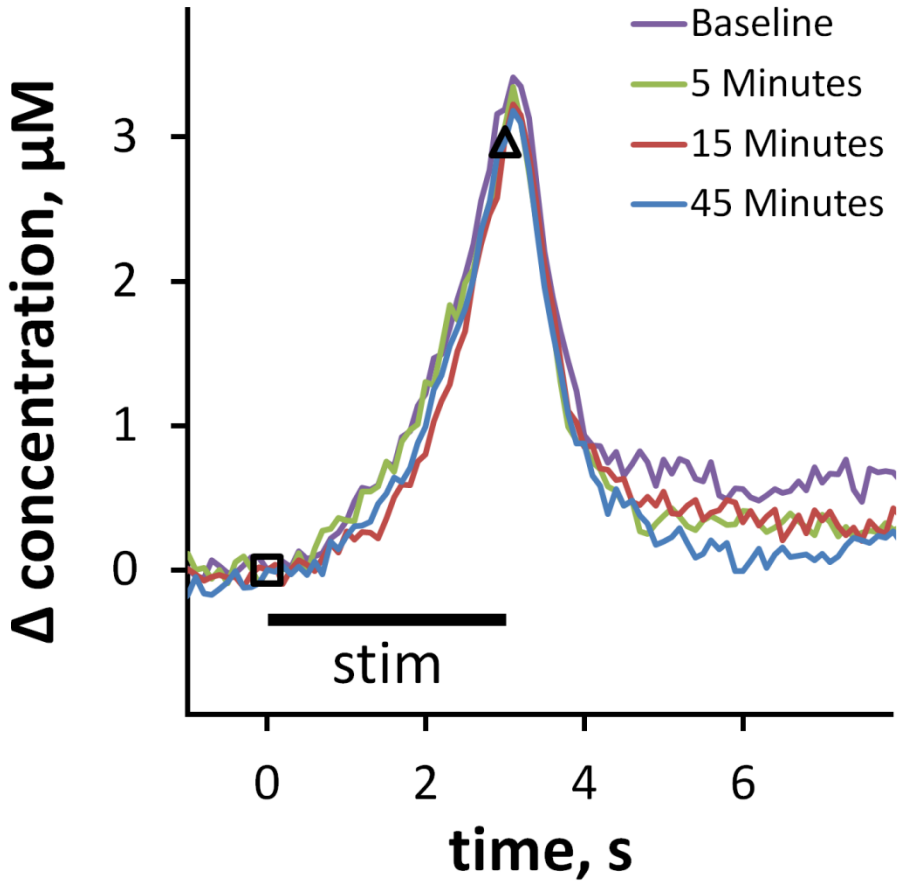


**Supplementary Figure S2.1: Reproducibility of stimulated release in the slow domain.**
The kinetic response of the slow domain is reproducible over time. Shown here are the evoked DA overflow responses to consecutive 3 sec, 60Hz stimulations in the slow domain of a single rat without altering the stimulation or working electrode positions or parameters. The initial response delay and linear clearance rate are consistent after 5, 15, and 45 minutes following collection of the baseline reading at t = 0.

Figure S2.2a shows evoked responses calculated with Equation 2.1 using some standard stimulus conditions (60 Hz, 1 s) and intrinsic kinetic parameters *($[DA]_p$* = 0.1 μM, $V_{max}$ = 5 μM/s, and $K_M$ = 0.2 μM and 0.8 μM: these two values of $K_M$ are typical pre-and post-nomifensine values). It is important to emphasize that these modeled responses are presented only to illustrate their essential features, not as a fit to any of the measured responses reported in the main text.

The rising phase of the modeled responses are always 'curved-downwards,' i.e. the response rate decreases as the stimulus proceeds. Mathematically, this occurs because the rate of evoked release, $f \cdot [DA]_p$, is constant while the rate of DA clearance, $\frac{V_{max} \cdot [DA]}{[DA] + K_M}$, increases as the DA concentration increases. Whereas the modeled responses are curved-downwards, the measured slow responses are 'curved-upwards,' i.e. they begin slowly but get faster as the stimulus proceeds. This contrast between the modeled and measured responses is the basis for the statement in the main text that model does not predict the measured slow responses.

Figure S2.2a compares responses modeled with two different values of $K_M$ to predict the actions of a competitive uptake inhibitor. A key point is that competitive uptake inhibition is not expected to substantially alter the initial slope of the clearance phase of the response. This is the basis for claiming, as we do in the main text, that the decrease in clearance slope of the fast responses caused by nomifensine is paradoxical. A slight decrease in initial slope might be expected if the pre-drug response did not reach sufficient concentrations to exceed $K_M$, but the fast responses well exceed the reported $K_M$.

In the case of fast responses, nomifensine did not alter the rising phase of the stimulus response during the 200 ms stimulus. This is another observation inconsistent with the model, which predicts that the slope of the response should increase when the rate of clearance decreases. In the case of Figure S2.2a, the signal is increased nearly 40% after the first 100 ms of the stimulus (see the first "data point" on the modeled responses).

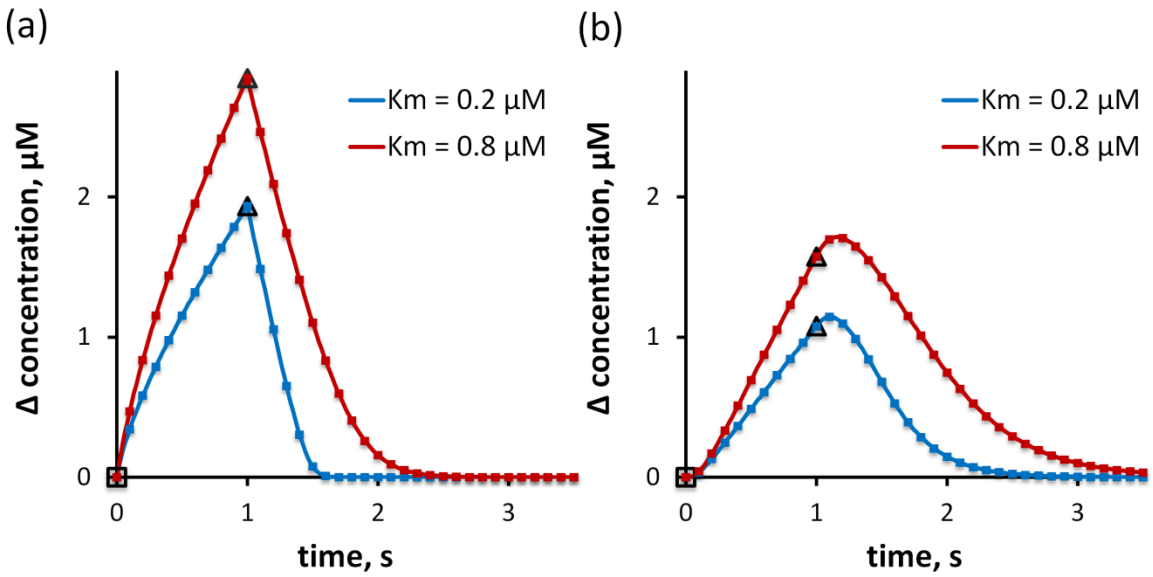


**Supplementary Figure S2.2: Simulated effect of increasing $K_M$ on evoked DA overflow.**
Simulations, according to equation 2.1, modeling the effect of increasing $K_M$ do not reproduce the observed effects of nomifensine in the fast domain. Figure S2.2a) The simulation modeling an increase in $K_M$ from 0.2 µM to 0.8 µM (representative of competitive DAT inhibition by nomifensine) in the absence of diffusion does not produce the overshoot and subsequent slowing of linear clearance observed in the fast domain. Figure S2.2b) Incorporation of a 10 µm diffusional gap into the model produces a small symmetrical distortion at the beginning and end of stimulation which also fails to mimic the large asymmetric overshoot observed in the fast domain after nomifensine.

Figure S2.2b repeats the calculation in Figure S2.2a but includes the effect of a 10 μm diffusion gap between the electrode and the site of DA release and uptake. A finite element simulation algorithm was used to calculate the diffusion effect. A diffusion gap in the in vivo experiments might arise from the use of Nafion films (which were not used in this study) or as consequence of penetration injury caused by the electrode. Figure S2.2b shows two important features of the response delays expected in the presence of a diffusion gap. First, the modeled delays when the stimulus starts and stops are symmetrical: in Figure S2.2b the delays are both about 200 ms. Second, the delay even from a diffusion gap as large as 10 μm should be relatively minor, i.e. only about 200 ms and far smaller than the 800 ms observed in fast domains after nomifensine. These features of the modeled response delays, i.e. that they are symmetrical and relatively minor, is the basis for claiming, in the main text, that the delays observed by voltammetry in the striatum do not conform to diffusion gap expectations. First, the delays are symmetrical and, especially in the fast domains post-nomifensine, are much longer than can be explained be even a large diffusion gap. The EM result (Figure 2.7 of the main text) shows that any diffusion gap due to penetration injury is much smaller than 10 μm.

## 3.0: RESTRICTED DIFFUSION OF DA IN THE RAT DORSAL STRIATUM

Adapted with revisions from Taylor et al. 2013. Reproduced with permission.

### 3.1: INTRODUCTION

Central dopamine (DA) systems participate in numerous aspects of brain function (Goto et al., 2007, Obeso et al., 2008) and their dysfunction contributes to a broad array of disorders and diseases including Parkinson's disease (Pavese et al., 2011), schizophrenia (Mizuno et al., 2012) and attention deficit hyperactivity disorder (Ludolph et al., 2008). Broadly speaking, the physiological function of the DA molecules themselves is to bind to post- and pre-synaptic receptors to modulate the activity of the postsynaptic targets (Korchounov et al., 2010) and to self-regulate DAergic activity (Starke et al., 1989), respectively. Consequently, numerous drugs act by modulating extracellular DA concentrations (e.g. L-DOPA, MAO inhibitors and inhibitors of the dopamine transporter (DAT) (Church et al., 1987, Brannan et al., 1995, Hornykiewicz, 2002, Schiffer et al., 2006)) or by modulating or mimicking the binding of DA to its receptors (DA agonists and antagonists) (Seeman et al., 1976, Kapur et al., 1999). Some of the drugs that target DA systems have important therapeutic applications (Gottwald and Aminoff, 2011, Guo et al., 2012) while others have high potential for illicit abuse (Sulzer et al., 1995, Phillips et al., 2003, Hollander and Carelli, 2007): some therapeutic drugs are also abused (White et al., 2006). Thus, it is significant to know the extracellular DA concentration per se, to know the kinetics of DA release and clearance that determine the concentration, and to know the actions of drugs that target DA systems.

Recently, we have demonstrated that the DA terminal field in the rat dorsal striatum contains a patchwork of kinetic spatial domains. The fast and slow domains were brought to light by recordings of

extracellular DA with fast-scan cyclic voltammetry (FSCV) at carbon fiber microelectrodes during electrical stimulation of the medial forebrain bundle (MFB). The extracellular concentration of DA, the kinetics of DA release and clearance, the short-term plasticity of DA release, and the actions of DA-targeting drugs are each domain-dependent (Moquin and Michael, 2009, Wang et al., 2010, Moquin and Michael, 2011, Taylor et al., 2012). The patchwork phenomenon brings a new perspective to the often mentioned heterogeneity of striatal DA (Wightman et al., 1988a, May and Wightman, 1989b, Kawagoe et al., 1992, Garris and Wightman, 1995, Moquin and Michael, 2009), because DA is notably homogeneous within the fast and slow domains (Taylor et al., 2012). Although the patchwork has only recently been described, there is precedence for the phenomenon as DA is known to function on multiple time courses (Schultz, 2007) and local differences in short-term plasticity of DA have been reported before (Cragg et al., 2002, Cragg, 2003, Montague et al., 2004, Kita et al., 2007, Chadchankar and Yavich, 2011).

Our prior findings indicate that the slow domains exist under a state of tonic autoinhibition derived from a tonic basal extracellular DA concentration sufficient to activate presynaptic D2 autoreceptors (Moquin and Michael, 2009, Wang et al., 2010). In contrast, such an autoinhibitory tone is absent in the fast domains (Moquin and Michael, 2009, Wang et al., 2010). This implies the presence of a persistent DA concentration gradient between the extracellular spaces of fast and slow domains. At present, however, it is unclear why DA extracellular diffusion (Engstrom et al., 1988, Nicholson, 1995, Peters and Michael, 2000, Rice and Cragg, 2008, Sykova and Nicholson, 2008) would not eliminate the concentration gradient, hence the domain-dependent autoinhibitory tone. Thus, the goal of the present study was to examine evoked DA responses in fast and slow domains of the dorsal striatum under a broader range of experimental conditions than used in our previous studies. The evoked responses reported herein support the novel conclusion that DA's ability to diffuse between the fast and slow domains is severely limited. We discuss this conclusion in the context of the restrictions on extracellular

diffusion as described by Nicholson and coworkers (Hrabetova et al., 2003, Hrabetova and Nicholson, 2004, Tao et al., 2005, Sykova and Nicholson, 2008).

## 3.2: MATERIALS AND METHODS

### 3.2.1: Carbon fiber electrodes

A single carbon fiber (7-µm diameter, T650; Cytec Carbon Fibers LLC, Piedmont, SC, USA) was threaded into a borosilicate capillary (0.4mm ID, 0.6mm OD; A-M systems Inc., Sequim, WA, USA) and pulled to a fine tip using a vertical puller (Narishige, Los Angeles, CA, USA). The tip was sealed with a low-viscosity epoxy (Spurr Embedding Kit; Polysciences Inc., Warrington, PA, USA) and the exposed fiber was trimmed to a length of 200 µm. A drop of mercury established the electrical connection between the fiber and a nichrome wire (Nichrome; Goodfellow, Oakdale, PA, USA). Electrodes were soaked for 30 minutes in isopropyl alcohol prior to use (Bath et al., 2000). Post-calibration was carried out using freshly prepared, nitrogen-purged dopamine HCl (Sigma Aldrich, St. Louis, MO, USA) standard solutions in artificial cerebrospinal fluid (144 mM $Na^+$, 1.2 mM $Ca^{2+}$, 2.7 mM $K^+$, 1.0 mM $Mg^{2+}$, 149.1 mM $Cl^-$ and 2.0 mM phosphate, pH 7.4). Concentrations *in vivo* were obtained using post calibration results.

### 3.2.2: Fast-scan cyclic voltammetry

Voltammetry was performed with an EI 400 potentiostat (Ensman Instruments; Bloomington, IN, USA) under software control (CV Tar Heels v4.3, courtesy of Dr. Michael Heien, University of Arizona, Tucson, AZ, USA). The voltammetric waveform consisted of 3 linear potential ramps starting at the rest potential of 0 V (vs. Ag/AgCl) first to +1.0 V, then to -0.5 V and back to 0 V at a scan rate of 400 V/s: the waveform was applied at a frequency of 10 Hz. DA was identified by inspection of background-subtracted

voltammograms and quantified with the oxidation current between +0.5 and +0.7 V on the initial ascending potential ramp.

### 3.2.3: Surgical and stimulation procedures

The University of Pittsburgh's Institutional Animal Care and Use Committee reviewed and approved all procedures involving animals. Male Sprague-Dawley rats (250 – 350 g; Hilltop, Scottsdale, PA, USA) were anesthetized with isoflurane (2.5% by volume $O_2$) and maintained at a body temperature of 37˚C (Harvard Apparatus; Holliston, MA, USA). Anesthetized rats were placed in a stereotaxic frame (David Kopf, Tujunga, CA, USA) with the incisor bar raised to 5 mm above the interaural line (Pellegrino et al., 1979). Dura mater was exposed by craniotomies and removed to allow insertion of the reference, working and stimulating electrodes. Contact between the brain surface and a Ag/AgCl reference electrode was established via a salt bridge. A carbon fiber electrode was implanted into the dorsal striatum (2.5 mm anterior to bregma, 2.5 mm lateral from bregma and 5-6 mm below the cortical surface). A stainless steel, twisted bi-polar stimulating electrode (MS303/a; Plastics One, Roanoke, VA, USA) was aimed at the medial forebrain bundle (MFB, 2.2 mm posterior to bregma, 1.6 mm lateral from bregma, and 7-9 mm below the cortical surface) and lowered until evoked DA release was observed in the striatum (Ewing et al., 1983, Kuhr et al., 1984, Stamford et al., 1988). The MFB stimulation was a biphasic, constant-current, square-wave waveform delivered by a pair of optical stimulus isolators (Neurolog 800, Digitimer; Letchworth Garden City, UK). The stimulus pulse width was held constant at 4 ms throughout this study.

### 3.2.4: Objective identification of fast and slow domains in the dorsal striatum

All experiments described herein began with an initial procedure to position the recording carbon fiber electrode in an objectively identified fast or slow domain. For this initial procedure, MFB stimulation

was performed with a frequency of 60 Hz and a current intensity of 250 μA. Fast and slow domains were identified according to our previously described classification criteria (Moquin and Michael, 2009, Moquin and Michael, 2011, Taylor et al., 2012): fast domains were identified by robust evoked DA release during the first 100 ms of the stimulus and subsequent short-term depression of evoked release, whereas slow domains were identified by an initial delay and subsequent short-term facilitation of evoked release. This classification scheme is objective because responses exhibiting short-term facilitation versus depression are easily discriminated. The recording electrode was lowered from its initial vertical coordinate (5 mm below dura) in small increments (50-100 μm) and the stimulus repeated until a fast domain was identified: to restrict these experiments to the dorsal striatum, lowering was stopped after 1 mm (6 mm below dura) if no fast domain was identified and responses from the slow domain were recorded.

**3.2.5: Experimental design**

Whereas our previous studies of the domain phenomenon were conducted with a single stimulus frequency and current intensity, herein we report evoked responses in objectively identified fast and slow domains (see previous paragraph) over a broader range of stimulus durations (12-180 pulses), frequencies (15-60 Hz) and current intensities (150-450 μA).

We also investigated the effects of raclopride and quinpirole on evoked responses in nomifensine-treated rats. First, recording carbon fiber electrodes were implanted in rats using the procedure, described above, for objective identification of fast and slow domains in dorsal striatum. An initial pre-drug stimulus response was recorded (200 ms, 60 Hz, 250 μA). Nomifensine (20 mg/kg i.p.) was administered and a second stimulus response was recorded 30 min later (the initial and post-nomifensine-only responses are not shown here: such responses are reported elsewhere (Taylor et al.,

2012)). Then, raclopride (2 mg/kg i.p.), quinpirole (1 mg/kg i.p.) or vehicle (PBS) was administered and a final stimulus response was recorded 30 min later (see Figure 3.4).

In a separate experiment in 4 additional rats (see Figure 3.5), we examined the effects of nomifensine on low-frequency stimulus responses (15 and 30 Hz, 180 stimulus pulses, 250 μA).

Davidson *et al.* (Davidson et al., 2000) reports that prolonged exposure to nomifensine decreases the sensitivity of carbon fiber electrodes to DA. However, in our hands, the impact of nomifensine on evoked responses is robust so any major effect of nomifensine on the electrode sensitivity seems unlikely. Moreover, in this study we compare the effects of raclopride and quinpirole under the same nomifensine pretreatment conditions, so we assume any effect of nomifensine would be equivalent and not affect the comparisons of major interest in this work.

### 3.2.6: Data analysis

Current vs. time graphs were generated using the peak oxidation potential for DA. Linear DA clearance rate was assessed by determining the slope of the descending phase of the response with an $r^2 > 0.96$. The overshoot duration is the time period from the end of stimulation that DA continues to increase in amplitude, and the overshoot amplitude is the concentration of DA increase during that duration. Statistical analyses were by one- and two-way ANOVA with a repeated measures design as well as post hoc pairwise comparison of main effects using a 95% confidence interval (IBM SPSS Statistics 20 software) and t-tests of independent (Figures 3.1, 3.3, and 3.4) or paired (Figure 3.5) samples.

## 3.3: RESULTS AND DISCUSSION

### 3.3.1: Domain-dependent effects of stimulus intensity: 60 Hz, 180 pulses

We recorded evoked DA release in objectively identified (see Methods) fast (Figure 3.1a, n=5) and slow (Figure 3.1b, n=8) domains of individual rats over a range of stimulus current intensities (150-450 μA, 180 pulses, 60 Hz: the solid lines in Figures 3.1a-b are the averages (error bars omitted for clarity) of responses recorded in different rats: error bars and statistics are reported in Figures 3.1c-e: see also Supplementary Figure S3.1). The responses recorded in fast and slow domains are different in both amplitude and temporal profile. The amplitudes at three time points were subjected to a 2-way ANOVA with repeated measures: the factors were the stimulus intensity and domain type (ANOVA details in the figure legend). The stimulus intensity was a significant factor at 60 (Figure 3.1c, $p<0.00002$), 120 (Figure 3.1d, $p < 0.00002$) and 180 stimulus pulses (Figure 3.1e, $p < 0.0001$). The domain type (fast and slow) was a significant factor at 60 and 120 stimulus pulses (Figure 3.1c, $p < 0.0005$; Figure 3.1d, $p < 0.005$) but not at 180 stimulus pulses (Figure 3.1e, $p>0.05$): this latter effect is due to the time course of the two profiles, as fast responses begin rapidly and slow down whereas slow responses begin slowly and speed up.

The responses in Figure 3.1 exhibit overshoot, i.e. the DA signal continues to increase after the end of the stimulus. The amplitude and duration of the overshoot depend on both the stimulus intensity and the type of domain (see Supplementary Figure S3.2). The overshoots observed here are more obvious than in our previous studies [20, 23] that involved shorter stimulus durations at a stimulus intensity of 240 or 270 μA. The less obvious overshoot associated with milder stimulus conditions is consistent with the dependence of the overshoot on the magnitude of evoked release observed here (Supplementary Figure S3.2).

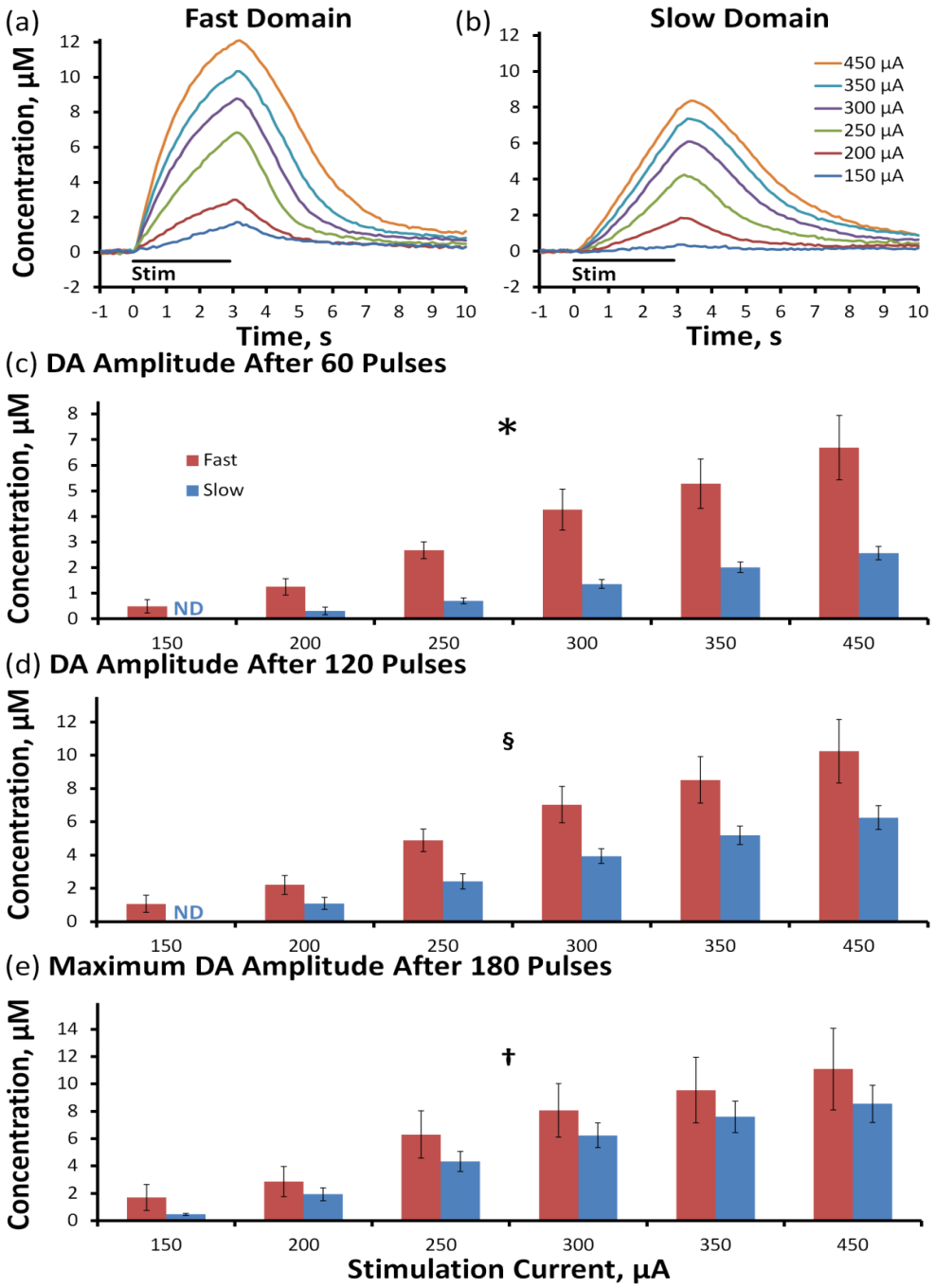


**Figure 3.1: Effect of stimulus intensity on fast and slow domains: 180 pulse stimulation.**
The intensity of a 180-pulse stimulation significantly affects the average evoked DA overflow in the fast (a) and slow (b) domains of n=5 and n=8 individual rats respectively. The average (± SEM) DA amplitude after 60 (c) and 120 (d) stimulus pulses is significantly different between fast and slow domains, but not at maximum amplitude (e). (2-way ANOVA with repeated measures: ❖ stimulation intensity $F(1.1,11.9) = 44.758$, $p < 0.00002$, domain (fast vs. slow) $F(1.1,11.9) = 28.818$, $p < 0.0005$, interactions $F(1,11) = 10.956$, $p < 0.02$; § stimulation intensity $F(1.1,12.5) = 43.122$, $p < 0.00002$, domain $F(1,11) = 15.267$, $p < 0.005$; † stimulation intensity $F(1.2,13.5) = 27.614$, $p < 0.0001$).

At stimulus intensities ≥250 μA the responses in both fast and slow domains exhibit a constant rate of linear DA clearance after the stimulus ends (Figure 3.1a,b), indicating that the extracellular DA concentration is sufficient to saturate the dopamine transporter (DAT). When the DAT is saturated, the slope of the linear clearance profile is the apparent $V_{max}$ of DA uptake (Wightman et al., 1988a, Wu et al. 2001b, Moquin and Michael, 2011) . The apparent $V_{max}$ in fast domains, 3.91 ± 0.40 μM/s, is significantly larger than in slow domains, 2.46 ± 0.14 μM/s (t-test of independent samples: $p < 0.0002$).

The results in Figure 3.1 (and Supplementary Figures S3.1 and S3.2) extend our prior studies, which were conducted at a single stimulus intensity (Moquin and Michael, 2009, Taylor et al., 2012), by demonstrating that objectively identified domains exhibit distinct rates of evoked DA release and clearance (apparent $V_{max}$) over a broad range of stimulus intensities. This confirms that domain-dependent responses are not restricted to a narrow set of stimulus parameters and (vide infra) establishes a starting point for a more detailed examination of the properties of the domains themselves.

### 3.3.2: Domain-dependent effects of stimulus intensity: 60 Hz, 12 pulses

Brief stimuli (12 pulses, 150-450 μA, 60 Hz) evoke robust DA responses in fast (Figure 3.2a) but not slow (Figure 3.2b) domains (the lines in Figure 3.2 are the average of responses recorded at the same sites used to obtain Figure 3.1, error bars are reported in Figure 3.2c). In fast domains the stimulus intensity significantly affects the response amplitude (Figure 3.2c: 1-way ANOVA with repeated measures, details provided in the figure legend). The expanded time scale of Figure 2 shows the details of DA release when the stimulus begins. In fast domains (Figure 3.2a) DA release is detected during the first FSCV scan performed 100 ms (6 stimulus pulses) after the stimulus begins. There is little or no delay in DA clearance at stimulus intensities ≤250 μA but a 100 ms delay appears at intensities ≥300 μA (the clearance delay is discussed in the section below entitled Response Overshoot). In slow domains (Figure

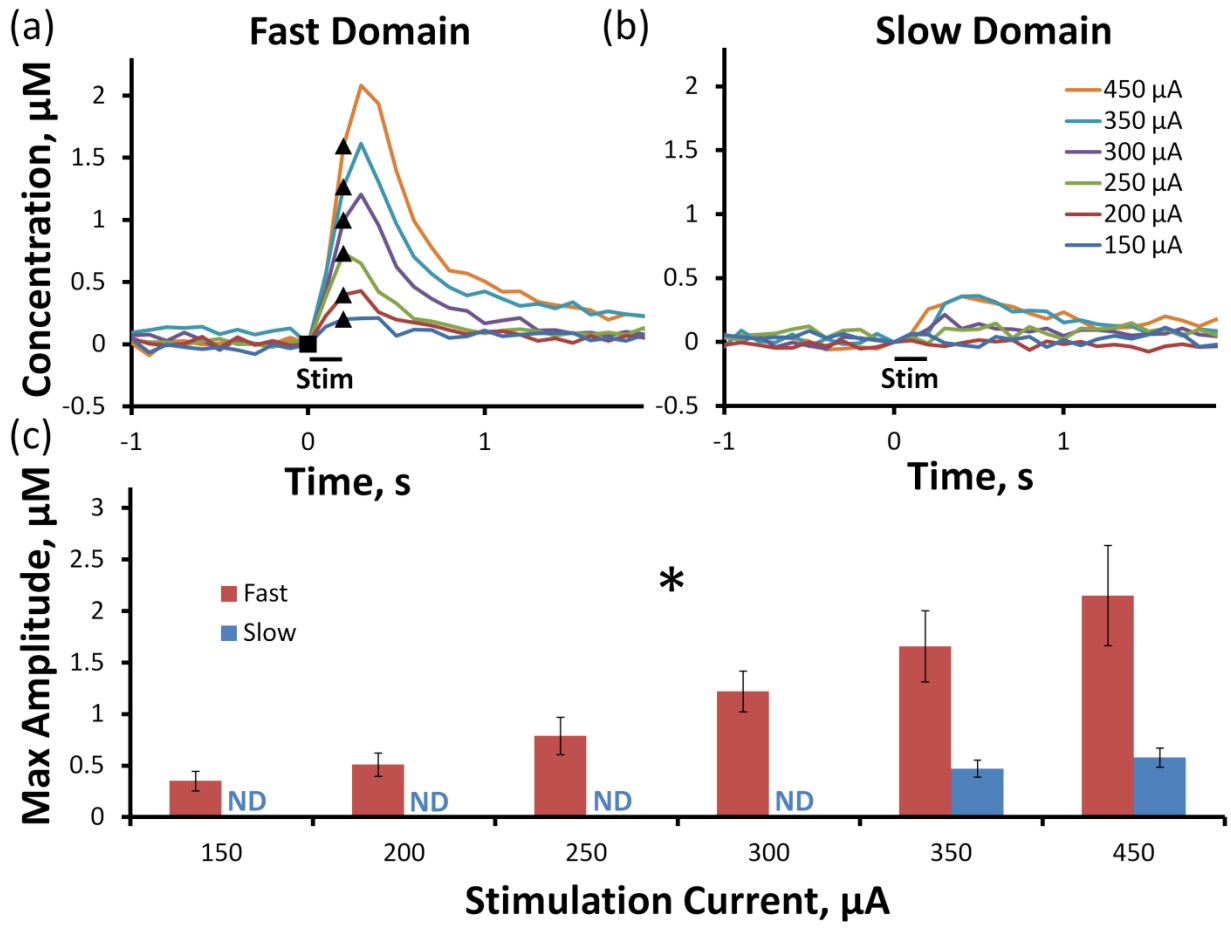


**Figure 3.2: Effect of stimulus intensity on fast and slow domains: 12 pulse stimulation.**
12-pulse stimulation reveals the difference between fast and slow domains. Evoked DA overflow is observed the fast domain (a) following each stimulus intensity ranging from 150-450 µA, whereas DA is only present in the slow domain (b) during 350 and 450 µA 12-pulse stimulations. The average (± SEM) maximum DA amplitude (c) is significantly increased by stimulus intensity in the fast domain. (1-way ANOVA with repeated measures: ❖ stimulation intensity $F(1.1,4.6) = 11.972$ , $p < 0.05$). The solid symbols mark the beginning (square) and ending (triangle) each stimulus.

3.2b) the brief stimuli evoked no quantifiable responses at intensities below 350 µA: higher intensities evoked delayed responses with small amplitudes. Under the conditions of this experiment, Figure 3.2 show that any contribution to the slow domain response derived from diffusion of DA from the fast domain is minimal.

### 3.3.3: Domain-dependent effects of stimulus frequency: 250 µA, 180 pulses

Varying the stimulus frequency (15-60 Hz, 180 stimulus pulses, 250 µA) has domain-dependent effects on evoked responses (the solid lines in Figures 3.3a-b are the average responses with error bars omitted for clarity: see also Supplementary Figure S3.3). Responses were non-detectable at 15 Hz. The stimulus frequency significantly affected the response amplitude (Figure 3.3c, $p < 0.000001$, 2-way ANOVA with repeated measures, details provided in the figure legend, 15 Hz data omitted from the ANOVA). Although the domain type was not a significant factor, both the 30 and 45 Hz stimuli evoked larger maximum amplitudes in the slow domains (the difference at 30 Hz was significant, t-test of independent samples, $p<0.05$). As far as we are aware, this amplitude reversal (i.e. sites exhibiting larger amplitude at 60 Hz exhibiting lower amplitudes at 45 and 30 Hz) has not been described before. Even so, the observed dependence of the amplitude on stimulus frequency is consistent with the difference in DA clearance from fast and slow domains (Moquin and Michael, 2011, Taylor et al., 2012) (see discussion of the apparent $V_{max}$ values in Figure 3.1, above). Lower stimulus frequencies provide more time between the stimulus pulses for DA clearance, so the response amplitude decreases with frequency. However, the amplitude decreases more rapidly in the fast domain because DA clearance is faster there. So, this is the first report showing that the amplitudes of fast and slow responses exhibit a differential dependence on stimulus frequency.

The responses recorded at 30 and 45 Hz show no sign of DA diffusing from fast to slow domains. First, the responses show that DA is more rapidly cleared from the fast domains (see previous

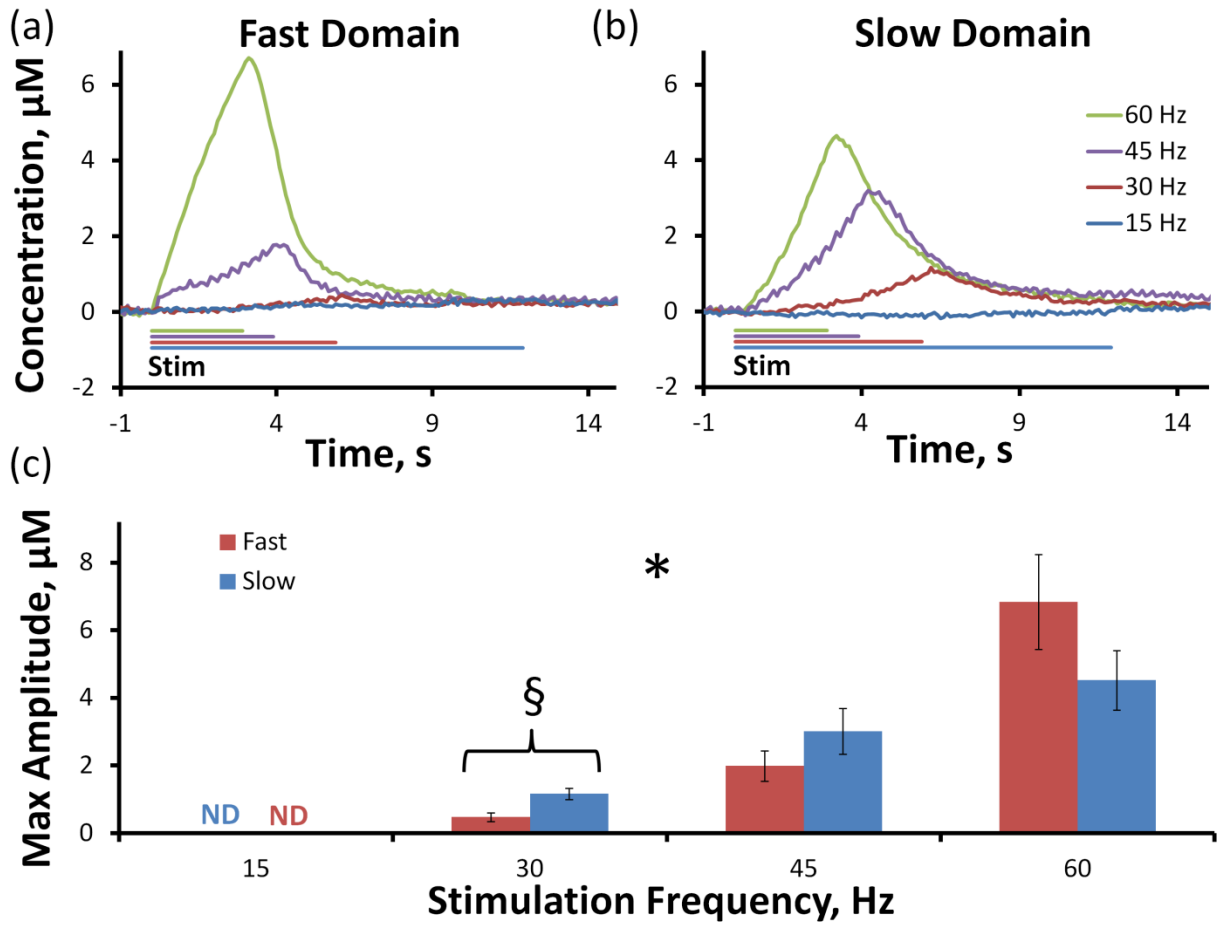


**Figure 3.3: Effect of stimulus frequency on fast and slow domains: 180 pulse stimulation.**
Fast (a) and slow (b) domains are significantly altered by the frequency of the stimulus (2-way ANOVA with repeated measures: ❖ stimulation frequency $F(1.4,15.3) = 38.022$ , $p < 0.000001$). 180-pulse stimulation lasts for 12 s at 15 Hz, 6 s at 30 Hz, 4 s at 45 Hz and 3 s at 60 Hz. 30 Hz stimulation produces significantly higher maximum evoked DA overflow (c) in the slow domain (t-test of independent samples: § $p < 0.05$).

paragraph), in which case it is not available to diffuse to the slow domains. Second, since the evoked concentration is higher in the slow domains (see also Supplementary Figure S3.3 for a direct comparison), there is no concentration gradient to drive diffusion from fast to slow domains. So, under the conditions of this experiment, diffusion of DA from fast to slow domains is not evident.

### 3.3.4: Diffusion after uptake inhibition

Uptake inhibition prolongs DA's lifetime in the extracellular space (Church et al., 1987, Floresco et al., 2003, Cragg and Rice, 2004, Taylor et al., 2012). Thus, an important question is whether or not uptake inhibition also increases DA's diffusion distance. Without uptake inhibition, evoked DA in slow domains is barely detectable during 200 ms stimuli (Figure 3.2b). However, robust responses are detected in fast and slow domains after rats are treated with nomifensine, a DA uptake inhibitor (Taylor et al., 2012). Nevertheless, our previous results did not indicate diffusion between the fast and slow domains. The temporal profiles of the fast and slow responses after nomifensine administration were identical (see Figure 2.9 in chapter 2.0 of this document). If the slow domain response were due to diffusion, then it should have risen slower, peaked later and lasted longer than the fast domain response: these features were not observed. Thus, we are interested now to investigate further whether uptake inhibition promotes diffusion of DA between fast and slow domains.

We have extended this line of investigation by modulating evoked DA release with a D2 receptor antagonist, raclopride (2 mg/kg i.p.) and a D2 receptor agonist, quinpirole (1 mg/kg i.p.) (Moquin and Michael, 2009, Wang et al., 2010), in nomifensine-treated rats. In fast domains (Figure 3.4a), raclopride significantly ($p < 0.05$) increased (Figure 3.4c), while quinpirole significantly ($p < 0.005$) decreased (Figure 3.4c), the response amplitude (ANOVA details provided in the figure legend). In slow domains (Figure 3.4b), evoked DA responses were barely detectable after vehicle (PBS) or quinpirole administration (the post-nomifensine responses in Figure 3.4 are smaller than in Figure 2.9 of chapter 2.0 of this document

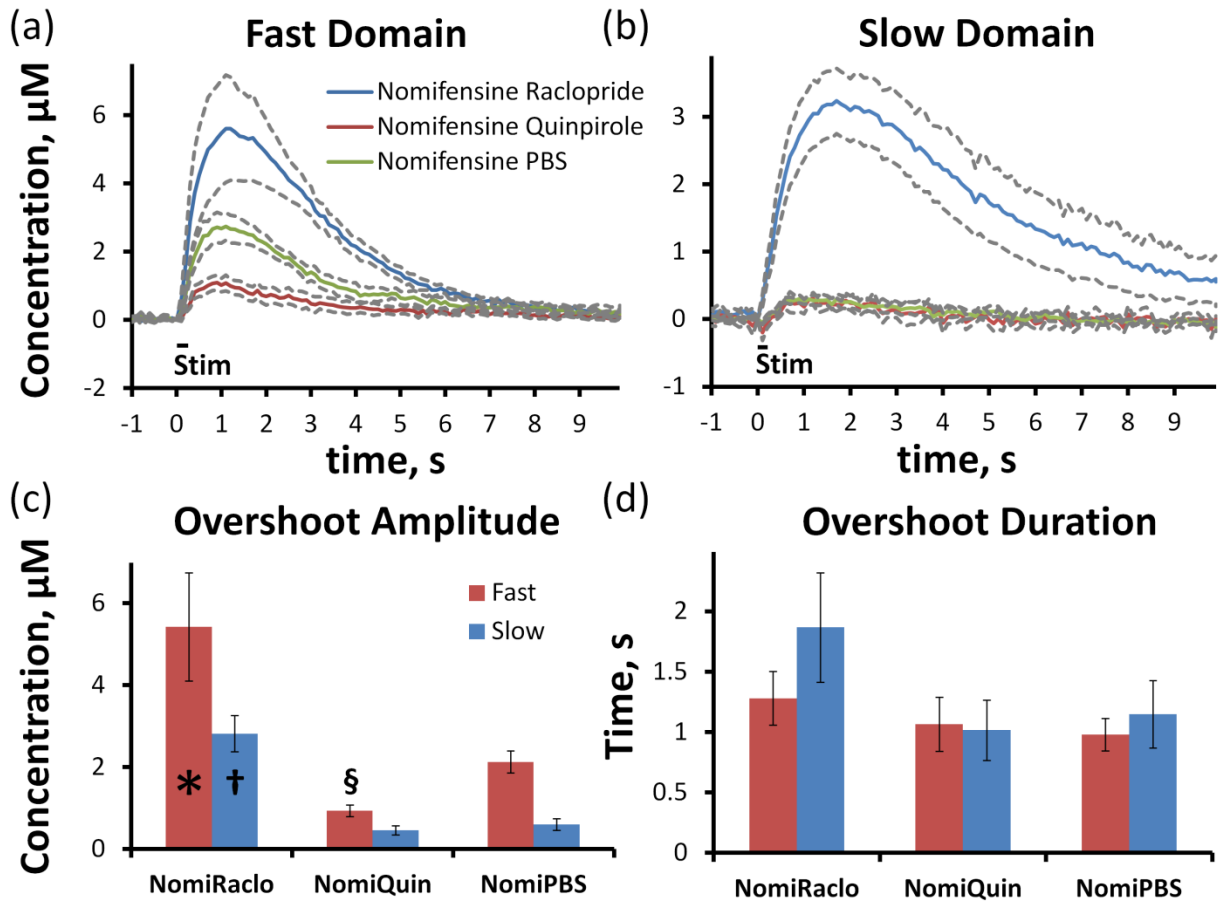


**Figure 3.4: Effect of D2 targeting drugs during competitive DAT inhibition.**
D2 targeting drugs alter the average amplitude of the nomifensine induced DA overshoot in fast (a) and slow (b) domains. In the fast domain, raclopride (n = 5) significantly increases the amplitude of DA overshoot (c), and quinpirole (n = 6) significantly decreases the amplitude of DA overshoot compared to PBS (n = 5) control. In the slow domain, raclopride (n =6) significantly increases the overshoot duration, while quinpirole (n = 6) has no significant effect compared to PBS (n = 6) control. The D2 induced changes in DA amplitude do not significantly alter the duration (d) of the nomifensine induced overshoot. (t-test of independent samples: ❖ $p < 0.05$, § $p < 0.005$, † $p < 0.0005$).

due to the extra 30 min interval after the vehicle injection). Even though DA in the fast domains was elevated for ~6-7 s (Figure 3.4a, red and green), diffusion of DA to the slow domains was not detected (Figure 3.4b, red and green). Raclopride significantly ($p < 0.0005$) increased the response amplitude in the slow domain without an initial delay (Figure 3.4b, blue), confirming the presence of autoinhibited DA terminals in slow domains. Figure 3.4 confirms that even after uptake inhibition voltammetry records the DA concentration in the immediate proximity of the recording electrode but does not "pick up" DA diffusing between domains.

### 3.3.5: Response overshoot

The responses in Figures 3.1-4 exhibit overshoot, i.e. the DA signal continues to increase after the stimulus ends (see also Supplementary Figures 3.1-3). Overshoot is usually attributed to a diffusion gap between the recording electrode and DA terminals but our results show that this cannot be so. The amplitude and duration of overshoot is highly sensitive to the magnitude of DA overflow, i.e. the net rate of DA release and clearance. There is a systematic increase in overshoot duration and amplitude, in both domains, with increasing stimulus intensity (Supplementary Figure S3.2). Likewise, overshoot increases with stimulus frequency (Figure 3.3 and Supplementary Figure S3.3) and after uptake inhibition (Figure 3.4 and chapter 2.0 of this document), both of which increase DA overflow. Finally, our results show that all recording sites exhibit overshoot if overflow is high enough. If overshoot were due to a physical diffusion gap, then over flow would be a permanent feature of the responses recorded at any given site: it would not be sensitive to the stimulus or pharmacological conditions.

Inspection of our results shows that overshoot is strongly impacted by DAT kinetics. Overshoot is smaller in fast domains compared to slow domains (Supplementary Figure S3.2), which coincides with the larger apparent $V_{max}$ of clearance in the fast domains (above) and is largest after uptake inhibition

(Figure 3.4). Thus, we report here for the first time that overshoot is a function of DAT kinetics rather than a diffusion gap.

### 3.3.6: DA diffusion after uptake inhibition: low frequency stimulation

In slow domains, evoked DA release is non- or barely detectable at stimulus frequencies of 15 or 30 Hz, respectively (250 μA, 180 stimulus pulses, Figure 3.5a,b). This might be because uptake prevents DA from reaching the electrode. However, there is an obvious problem with this explanation because the intervals between the 15 and 30 Hz stimulus pulses (67 and 33 ms, respectively) are substantially less than the time needed for DA clearance. For example, under mild stimulus conditions, pseudo-first order DA clearance from slow domains requires several seconds (e.g. Figure 3.1b, 200-300 μA). In that case, complete DA clearance in 67 ms should not be possible. So, there is a timing mismatch between these observations.

Nomifensine (20 mg/kg i.p.) dramatically increased the response amplitude in slow domains at 15 and 30 Hz (Figure 3.5a,b: solid lines are the averages from n=4 rats and dashed lines are the confidence intervals based on the SEM). The first 1.5 s of the responses are displayed on an expanded scale in Figures 3.5c and 3.5d to emphasize that nomifensine did not abolish the initial delay in evoked release. At 15 Hz, the DA signal increased significantly 1.3 s after the stimulus began (t-test of paired samples, $p < 0.05$ compared to pre drug response), i.e. after 19 stimulus pulses. At 30 Hz, the DA signal reached significance 600 ms after the stimulus began (t-test of paired samples, $p < 0.05$ compared to pre drug response), i.e. after 18 stimulus pulses. Thus, regardless of the stimulus frequency, the same number of stimulus pulses, i.e. the same amount of DA release, was required before the DA signal appeared at the electrode.

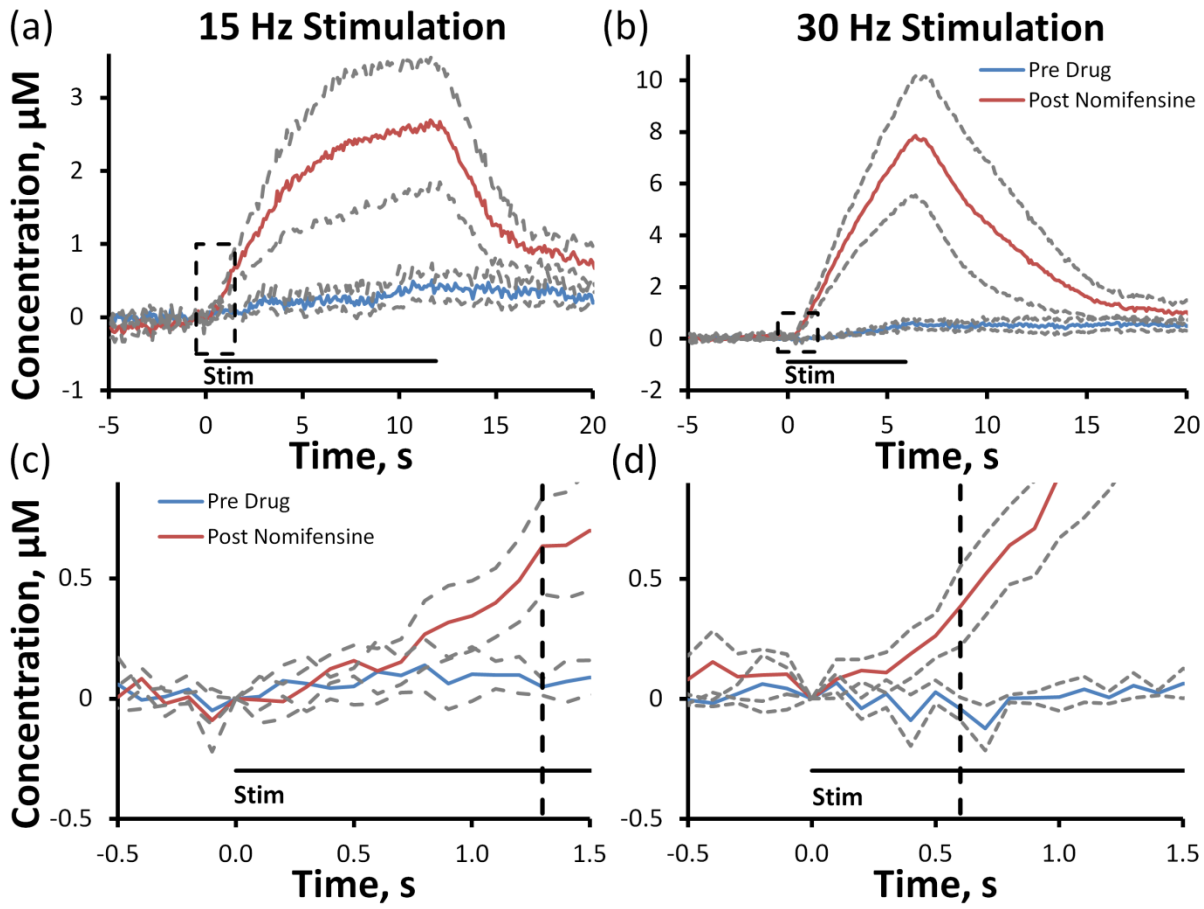


**Figure 3.5: Effect of nomifensine during low frequency stimulation.**
Nomifensine increases the average (± SEM) evoked DA overflow in the slow domain in response to low frequency 15 (a) and 30 Hz (b) stimulations in n = 4 rats. After treatment with nomifensine, DA arrives after 1.3 s of 15 Hz (c, enlargement of the dashed box in (a)) stimulation (vertical dashed line, 19 stimulus pulses) and after 0.6 s of 30 Hz (d, enlargement of the dashed box in (b)) stimulation (vertical dashed line, 18 stimulus pulses).

### 3.3.7: Restricted diffusion of DA in the extracellular space of the rat striatum

In a previous report (Taylor et al., 2012), we suggested that Nicholson's model of restricted diffusion (Hrabetova et al., 2003, Hrabetova and Nicholson, 2004, Tao et al., 2005, Sykova and Nicholson, 2008) explained several unexpected features of evoked DA responses in the dorsal striatum. This same mechanism explains the new findings of the present study. A major new finding is that DA's ability to diffuse between fast and slow domains is severely limited. Obviously, DA diffuses between DA terminals and the recording electrode in both domains: DA would not be detected otherwise. But, we find no clear evidence that DA makes its way from the fast domains to the slow domains under any conditions we have examined. The simplest explanation for this observation is that pathways through the extracellular space are obstructed, as described by Nicholson and coworkers(Hrabetova et al., 2003, Hrabetova and Nicholson, 2004, Tao et al., 2005, Sykova and Nicholson, 2008).

A second new finding is the dependence of DA overshoot on the magnitude of evoked overflow. Our working hypothesis is that restricted diffusion causes DA to be "held up" in the extracellular space and then either make its way to the electrode or return to DA terminals according to the balance between the rate of release and clearance. Thus, there is less overshoot if release is small (mild stimulation conditions) or if uptake is more efficient (DA is cleared faster in the fast domain than from the slow domain (Moquin and Michael, 2011)). There is more overshoot if uptake cannot efficiently remove DA from the extracellular space, allowing more DA to "leak" over to the electrode. This happens when release is large (longer, more intense, or higher frequency stimulation) or when uptake is slowed (observed in the slow domain or following uptake inhibition).

A third major finding is in regards to the response to low frequency stimulation (15 Hz, Figure 3.5). The absence of a detectable response highlights the timing mismatch issue explained above. Again, our working hypothesis is that DA is "held up" in the extracellular space but in this case, because the stimulus frequency is so low, there is not enough DA to overcome the capacity of the restrictions

upon diffusion and DA is cleared by DAT without "leaking" over to the electrode. Thus, restricted diffusion accounts for the timing mismatch in these low-frequency responses.

## 3.4: CONCLUSIONS

Numerous investigators, ourselves included, have long adopted a by-now conventional model to describe DA's diffusion in the extracellular space. In the conventional model, the diffusion coefficient is affected by tissue tortuosity and the DA's lifetime for diffusion is constrained by DA uptake. While the conventional model aptly describes some evoked responses, it does not capture the several new features of the domain-dependent responses recorded from the dorsal striatum. A central conclusion stemming from this finding is that restricted diffusion, the subject of in-depth investigations by Nicholson and coworkers (Hrabetova et al., 2003, Hrabetova and Nicholson, 2004, Tao et al., 2005, Sykova and Nicholson, 2008), plays a dominant role in determining DA's spatiotemporal dynamics in the extracellular space. Thus, we conclude that restricted diffusion enables DA terminal field to maintain a domain-dependent autoinhibitory tone, a demonstrated feature of the dorsal striatum's domain patchwork.

## 3.5: SUPPLEMENTARY INFORMATION

Supplementary Figure S3.1 contains the same data as Figure 3.1 of the main text presented in a different format to aide comparison of the domain-dependent evoked responses at each current intensity (150-450 μA, 60 Hz, 3 s). The solid lines are the average of multiple responses recorded in multiple rats in objectively identified fast (red, n=5) and slow (blue, n=8) domains: the dashed lines are confidence intervals based on standard errors: the solid symbols mark the beginning (square) and ending (triangle)

each stimulus. The previously-identified (Moquin and Michael, 2009, Moquin and Michael, 2011, Taylor et al., 2012) hallmark features of responses recorded in fast domains include (i) immediate DA release when the stimulus begins, (ii) short-term depression with the rate of evoked response decreasing as the stimulus proceeds (except at the lowest stimulus intensity, 150 μA) and (iii) rapid DA clearance compared to the slow domains (based on the apparent $V_{max}$, see main text). Responses in slow domains exhibit (i) an initial delay in the onset of DA release when the stimulus begins, (ii) short term facilitation with the rate of evoked response increasing as the stimulus proceeds and (iii) slow DA clearance compared to the fast domains.

Supplementary Figure S3.2 summarizes the duration (a) and amplitude (b) (mean ± SEM) of the overshoots observed at the end of 3-s stimuli over a range of stimulus intensities (the responses themselves are contained in Figure 3.1 of the main text and Supplementary Fig. S3.1). Both the duration and amplitude of the response overshoots increase significantly with stimulation intensity (2-way ANOVA with repeated measures: ❖ stimulation intensity $F(1,4) = 6.640$, $p < 0.0005$; **§** stimulation intensity $F(1,4) = 5.842$, $p < 0.0002$). At the higher stimulation intensities of 350 and 450 μA, the overshoot duration is significantly larger in the slow domains compared to the fast domains (**†** post hoc tukey test comparison, $p < 0.05$). Responses reported in our previous studies of fast and slow domains contain relatively little evidence of overshoot, except after uptake inhibition. However, those studies mainly involved shorter stimulus durations at a stimulus intensity of 240 or 270 μA: such stimulus conditions keep DA overflow at a relatively low magnitude, which explains why overshoot was less apparent.

Supplementary Figure S3.3 contains the same data as Figure 3.3 of the main text but in a different format designed to aid comparison of the responses recorded in fast and slow domains at 30 (a) and 45 Hz (b). The response in slow domains at 30 Hz is highly asymmetric, exhibiting an initial delay of 2-3 s but a much shorter delay with the stimulus ends. The conventional model of evoked responses

does not predict these asymmetric delays when the stimulus begins and ends (Taylor et al., 2012). Likewise, the conventional model does not predict that the delays should be affected by the stimulus conditions.

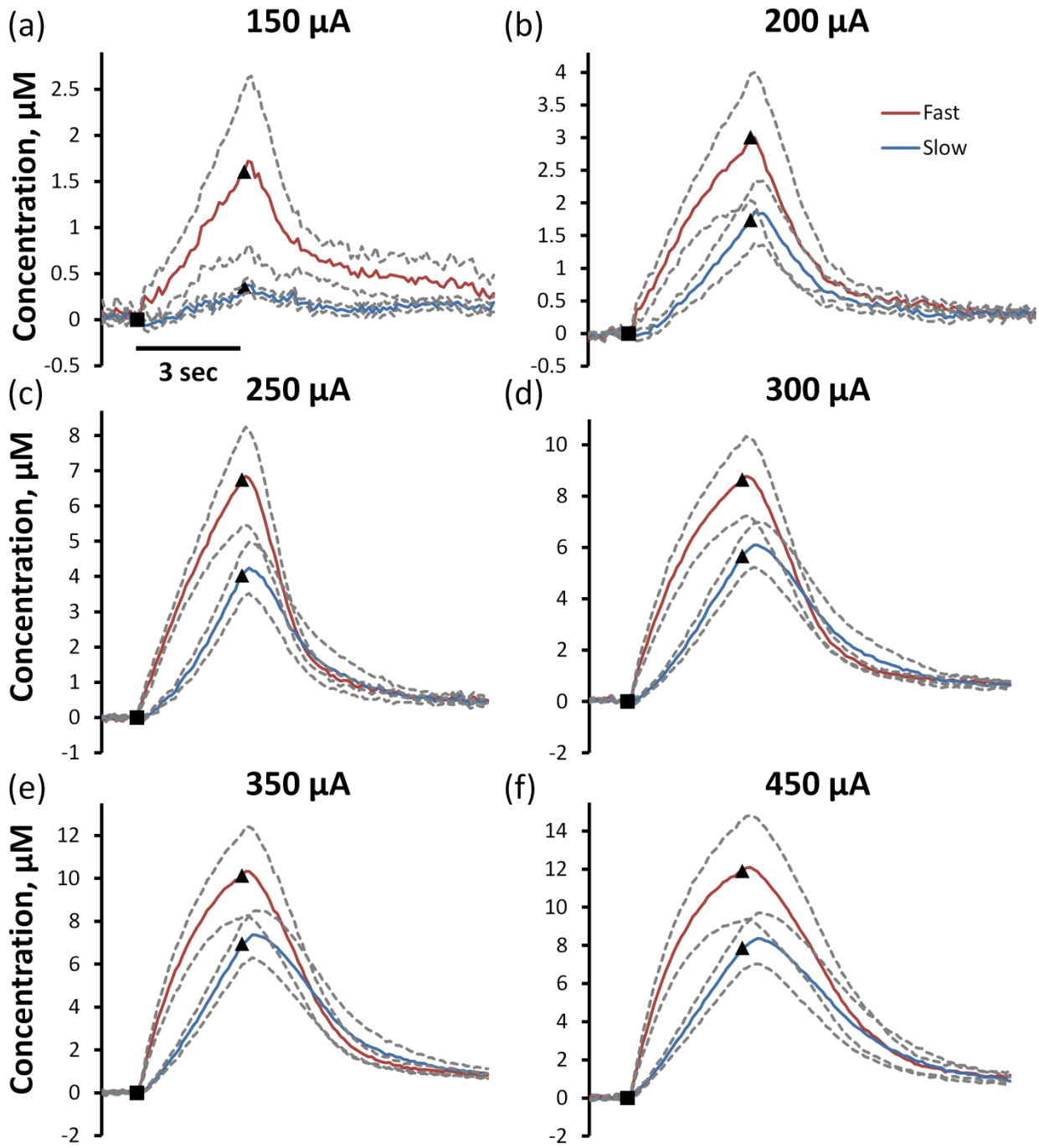


**Supplementary Figure S3.1: Comparative effects of stimulus intensity on fast and slow domains.** This rerepresentation of Figure 3.1 comparatively shows that average (±SEM) fast (red) and slow (blue) domains exhibit domain dependent responses to 3 second MFB stimulations of varying current intensity. The beginning of stimulation is denoted by the square and the end of stimulation is denoted by the triangle.

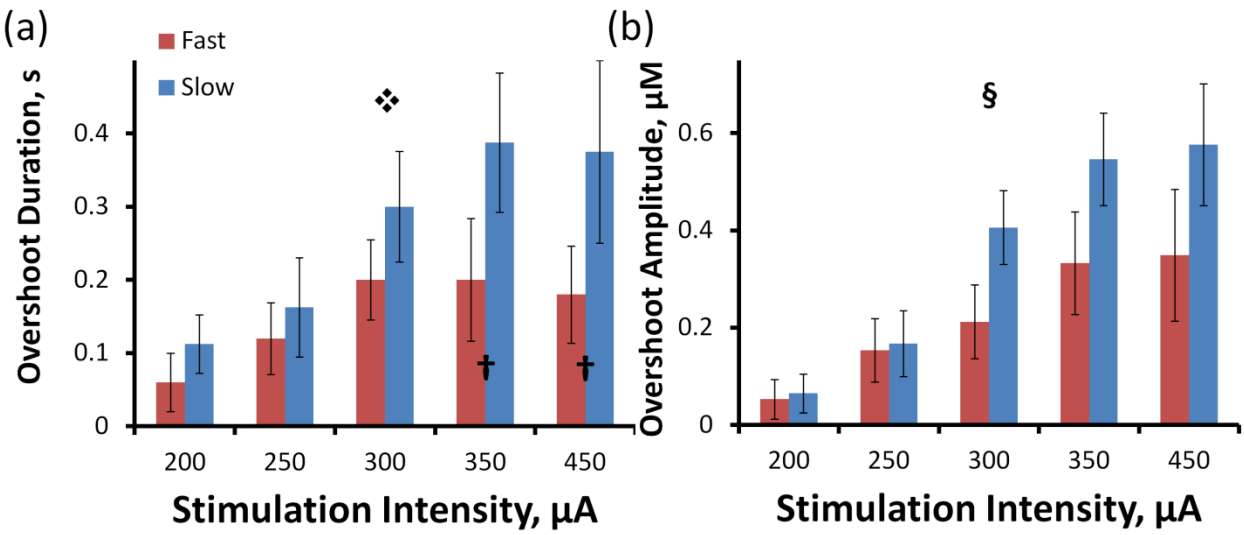


**Supplementary Figure S3.2: Effect of stimulus intensity of DA overshoot.**
Both the duration and amplitude of the response overshoots observed in Figure 3.1 of the main text increase significantly with stimulation intensity (2-way ANOVA with repeated measures: ❖ stimulation intensity $F(1,4) = 6.640$, $p < 0.0005$; **§** stimulation intensity $F(1,4) = 5.842$, $p < 0.0002$). At the higher stimulation intensities of 350 and 450 µA, the overshoot duration is significantly larger in the slow domains compared to the fast domains (**†** post hoc tukey test comparison, $p < 0.05$).

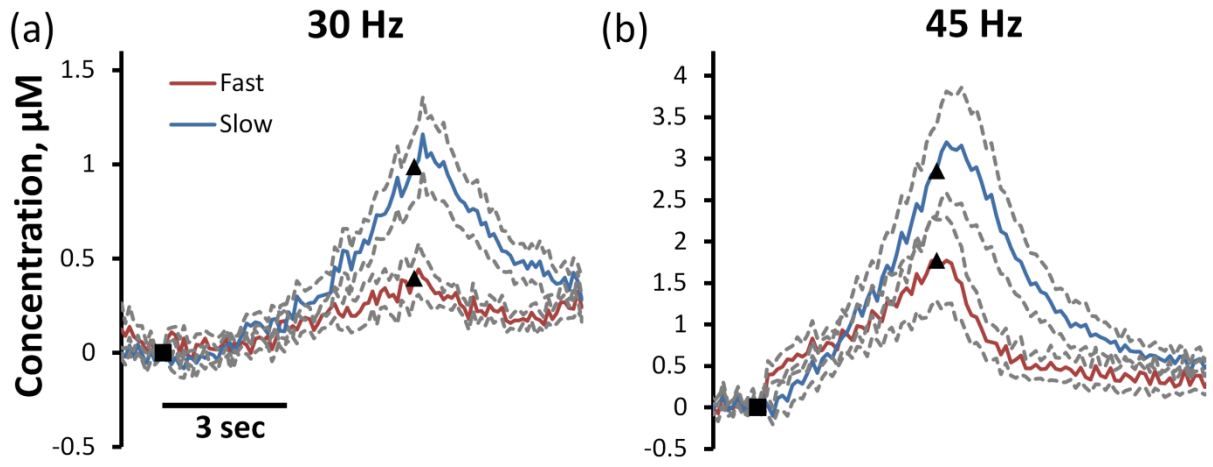


**Supplementary Figure S3.3: Comparative effect of stimulus frequency on fast and slow domains.** This rerepresentation of Figure 3.3 comparatively shows that average (±SEM) fast (red) and slow (blue) domains exhibit domain dependent responses to 3 second MFB stimulations of varying stimulation frequency. In both the 30 and 45 Hz stimulations, the slow domain produces a higher amplitude of evoked DA overflow than the fast domain. The beginning of stimulation is denoted by the square and the end of stimulation is denoted by the triangle.

# 4.0: FIVE DA DOMAINS IN THE DORSAL STRIATUM: INSIGHT ON DA CLEARANCE

## 4.1: INTRODUCTION

Dopamine (DA) is an important neurotransmitter involved in the signaling pathway for a variety of physiological functionality including motor control, sexual arousal and reward (Hull et al., 1999, Brooks, 2001, Urban et al., 2012). Its dysfunction is associated with numerous devastating disorders, such as Parkinson's disease, Alzheimer's, and schizophrenia (Pappata et al., 2008, de la Fuente-Fernandez et al., 2011, Kim et al., 2011). Furthermore, it has been shown that DA signaling on multiple time scales is responsible for this varied functionality (Grace, 1991, Schultz, 2007). Because of this time dependence, it is important to understand the rapid kinetics of DA signaling *in vivo*. Fast scan cyclic voltammetry (FSCV) at carbon fiber microelectrodes (CFE) paired with medial forebrain bundle (MFB) stimulated DA release affords the high spatial and temporal resolution necessary to study DA kinetics (Michael and Wightman, 1999).

Previous studies have revealed the existence of two spatially discrete DA domains in the rat dorsal striatum, termed the fast and slow domains (Moquin and Michael, 2009, Wang et al., 2010, Moquin and Michael, 2011, Taylor et al., 2012, Taylor et al., 2013). The fast domain was identified as a location where the ascending phase of the evoked DA signal begins to rise immediately upon the onset of MFB stimulation and the response exhibited short term depression upon further stimulation. The slow domain was described as a location where initial DA release inhibited upon the start of MFB stimulation and the profile exhibits short term facilitation upon continued stimulation. It was believed

that the evoked DA response from the fast domain was short lived (< 500 ms) due to the short term inhibition caused by the onset of autoinhibition in the fast domain (Moquin and Michael, 2009). Furthermore, prolonged stimulation allows for the co-detection of neighboring slow domains, yielding a hybrid response (Wang et al., 2010). Because of this, many studies comparing fast and slow domains restrict the stimulus duration (200 ms, 60 Hz) in order to exclude the slow domain contribution (Moquin and Michael, 2009, Moquin and Michael, 2011, Taylor et al., 2012). While this may be the case in certain instances, further examination of the effect of prolonged stimulation on the fast domain show the existence of four kinetically discrete sub-domains in the dorsal striatum.

## 4.2: MATERIALS AND METHODS

### 4.2.1: Carbon fiber microelectrodes

A single carbon fiber (7-µm diameter, T650; Cytec Carbon Fibers LLC., Piedmont, SC, USA) was aspirated through a borosilicate capillary (0.4 mm ID, 0.6 mm OD; A-M systems Inc., Sequim, WA, USA) and then pulled to a fine tip using vertical puller (Narishige, Los Angeles, CA, USA). The carbon fiber was immobilized by sealing the tip with low viscosity epoxy (Spurr Epoxy; Polysciences Inc., Warrington, PA, USA), and the exposed portion of the fiber was trimmed to a final length of 200 µm. Electrical connection was made using a drop of mercury and a nichrome hookup wire (annealed nichrome wire; Goodfellow, Oakdale, PA, USA). Electrodes were bathed in isopropyl alcohol for at least 15 minutes prior to use (Bath et al., 2000).

### 4.2.2: Fast scan cyclic voltammetry

Fast scan cyclic voltammetry was performed using either an EI-400 (Ensman Instruments, Bloomington, IN) or a custom-built potentiostat (Electronics Shop, Department of Chemistry, University of Pittsburgh)

and a Keithly 428 current amplifier (Keithley Instruments, Cleveland, OH, USA) controlled by 'CV Tar Heels v4.3' software (courtesy of Dr. Michael Heien, University of Arizona, Tucson, AZ, USA). The reference electrode was Ag/AgCl. The applied potential waveform linearly swept at 400 V/s from a resting potential of 0 V vs. Ag/AgCl to +1.0 V, then to -0.5 V and then back to 0 V at a frequency of 10 Hz. DA was identified via inspection of background-subtracted cyclic voltammograms and was quantified using the oxidation currents recorded between 0.5 and 0.7 V on the initial ramp.

#### 4.2.3: Electrode calibration

Electrodes were calibrated in a flow cell using freshly prepared, nitrogen-purged, dopamine HCl (Sigma Aldrich, St. Louis, MO, USA) standard solutions dissolved in artificial cerebrospinal fluid (144 mM $Na^+$, 1.2 mM $Ca^{2+}$, 2.7 mM $K^+$, 1.0 mM $Mg^{2+}$, 149.1 mM $Cl^-$, and 2.0 mM phosphate, pH 7.4). In vivo DA concentrations were determined by post calibration results.

#### 4.2.4: Animals

All work involving the use and care of animals was approved by the University of Pittsburgh Institutional Animal Care and Use Committee. Male Sragues-Dawley rats (250-350 g, Hilltop Labs, Scottsdale, PA, USA) were intubated and anesthetized with isoflurane (2.5% by volume) prior to being placed in a stereotaxic frame with the incisor bar raised to 5 mm above the interaural line (Pellegrino et al., 1979). Internal body temperature was maintained at 37˚C using a heating blanket (Harvard Apparatus, Holliston, MA, USA). After removing the scalp, three holes were drilled into the skull for the purpose of electrode implantation. The CFE was implanted in the dorsal striatum (2.5 mm anterior to bregma, 2.5 mm lateral from bregma and 5 mm below the cortical surface: the final vertical placement was optimized so that the electrode was positioned in either the fast or the slow domain (Moquin and Michael, 2009, Moquin and Michael, 2011, Taylor et al., 2012, Taylor et al., 2013)). Electrical contact

between brain tissue and a reference electrode was via a salt bridge. The stimulating electrode (bipolar stainless steel, MS303/a; Plastics One, Roanoke, VA, USA) was positioned over the MFB (2.2 mm posterior to bregma, 1.6 mm lateral from bregma and 7-8.5 mm below the cortical surface: the final vertical placement was optimized to evoke maximal DA release in the ipsilateral striatum (Ewing et al., 1983, Kuhr et al., 1984, Stamford et al., 1988)). The MFB was stimulated for 3 seconds using an optically isolated stimulus waveform (Neurolog 800, Digitimer, Letchworth Garden City, U.K.) of a biphasic, constant-current, square wave (4 ms per pulse, 250 µA pulse height and 60Hz frequency).

**4.2.5: Data analysis**

The kinetic profiles of each response were assessed by comparing the amplitude of the evoked DA overflow every 500 ms during the 3 second stimulation. Linear clearance rates were measured as the slope of the descending phase of the response where at least five data points produce an $r^2>0.99$. Statistical analysis within and between groups were completed using either one-way ANOVA or two-way ANOVA with a repeated measures design (SPSS software). Average color plots were produced using MATLAB. The false color distribution was optimized for each trace to provide detailed information of any small amplitude changes. Clearance profiles were modeled using a model of first order clearance adjusted with the addition of a constant efflux term as well as with Michaelis-Menten uptake kinetics (Wightman et al., 1988a, Wu et al., 2001b) using a fixed $K_M$ value of 0.2 µM (Near et al., 1988, Wu et al., 2001b) and $V_{max}$ values determined by the individual curves.

## 4.3: RESULTS

### 4.3.1: Identification of fast and slow domains

Fast and slow domains were initially identified using the well documented procedure of optimizing the CFE position through incremental 50-100 µm dorsal-ventral (DV) adjustments (Moquin and Michael, 2009, Moquin and Michael, 2011, Taylor et al., 2012, Taylor et al., 2013). Once either a fast or slow domain was obtained, the response to a 3 second 60 Hz stimulation was collected. The carbon fiber was lowered along a single DV track located at the coordinates described in the methods section. To ensure that the recording location remained within the dorsal striatum, DV lowering was limited to no more than 1 mm. Multiple penetrations were not conducted.

### 4.3.2: Four kinetic sub domains of the fast domain in the dorsal striatum

The fast domain of the dorsal striatum is composed of four unique kinetic sub domains, termed Fast Types 1-4 (average traces ± SEM displayed in Figure 4.1). Each sub domain is objectively identified based on fixed criteria describing the kinetic profile of the ascending portion of the evoked DA overflow curve. Type 1 responses are defined as those where the rising edge is linear during the entire duration of a 3 second stimulation. They are objectively identified as locations where the slope of the rising edge exhibits an $r^2>0.99$. Type 2 responses are linear for the majority of a 3 second stimulation, but exhibit short term depression during the latter portion of the stimulus. These are objectively identified as responses where the slope of the rising edge exhibits an $r^2<0.99$ and the evoked DA overflow increases for the entire duration of the stimulation. Type 3 responses are defined as those that initially rise upon the onset of stimulation, but quickly exhibit short term depression to such an extent that the evoked DA overflow response begins to descend before the end of stimulation. These are objectively identified as responses where the slope of the rising edge exhibits an $r^2<0.99$ and the evoked DA overflow descends

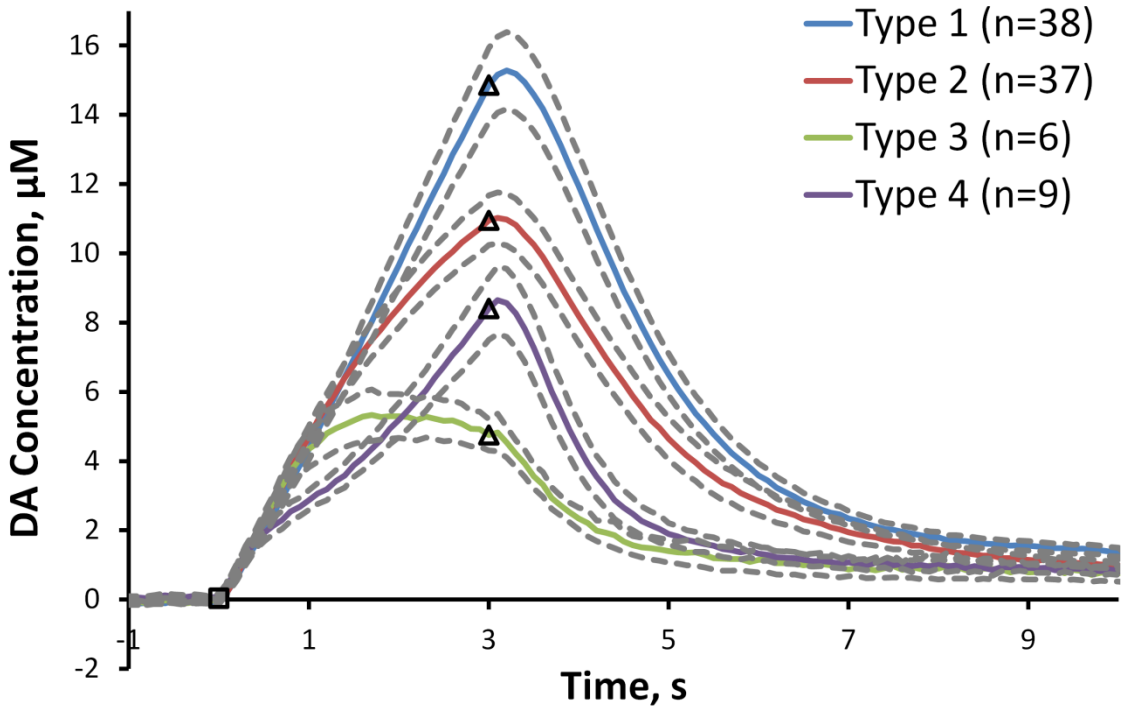


**Figure 4.1: Four discrete sub domains of the fast domain in the dorsal striatum.**
There are four discrete fast sub domains in the rat dorsal striatum. In n=90 individual animals, 38 were Type 1 (blue), 37 were Type 2 (red), 6 were Type 3 (green) and 9 were Type 4 (purple). The average (±SEM) response from each sub domain to a 3 second, 60 Hz stimulation is shown above. For this and all subsequent evoked DA overflow curves, the start of stimulation is denoted by the open square and the end of stimulation is marked by the open triangle.

prior to the end of stimulation. Type 4 responses were previously termed “hybrid sites” (Moquin and Michael, 2009) and are defined as a response where DA increases upon the start of stimulation, immediately exhibits short term depression and further stimulation promotes short term facilitation. Type 4 profiles are objectively identified as responses where the slope of the rising edge exhibits an $r^2<0.99$ and the first derivative of the rising edge of the evoked DA overflow response switches from negative to positive as the stimulation proceeds.

Figure 4.1 displays the average kinetic profiles for Types 1-4 collected from 90 individual animals. This large sample group provides insight to the relative distribution of each sub domain in the dorsal striatum. Type 1 responses were observed in 38/90 animals, Type 2 responses were found in 37/90 animals, Type 3 in 6/90 and Type 4 in 9/90. This corresponds to a percent composition of 42% Type 1, 41% Type 2, 7% Type 3 and 10% Type 4 in the dorsal striatum.

As shown in previous studies, comparison of maximum amplitude alone may preclude the identification of discrete kinetic domains (Stamford et al., 1986, May and Wightman, 1989b, Kawagoe et al., 1992, Taylor et al., 2013). Instead, careful consideration must be paid to kinetic profile of the evoked DA overflow responses, which manifest as changes in DA concentration over time. A convenient way to statistically compare kinetic domains is to plot their respective DA concentrations at various time points during stimulation (Taylor et al., 2013). Figure 4.2 represents the average responses shown in Figure 4.1 by displaying the average DA concentrations (± SEM) every 500 ms over the duration of the 3 second stimulation. According to two-way ANOVA with repeated measures design, Types 1-4 are significantly different ($p<0.005$) over the duration of the stimulation. One-way ANOVA between site types at each time point reveal that Types 1-4 do not significantly deviate from each other until after the first second of stimulation. In fact, the average (± SEM) DA concentration of all four fast sub domains entirely overlap 500 ms after the start of stimulation.

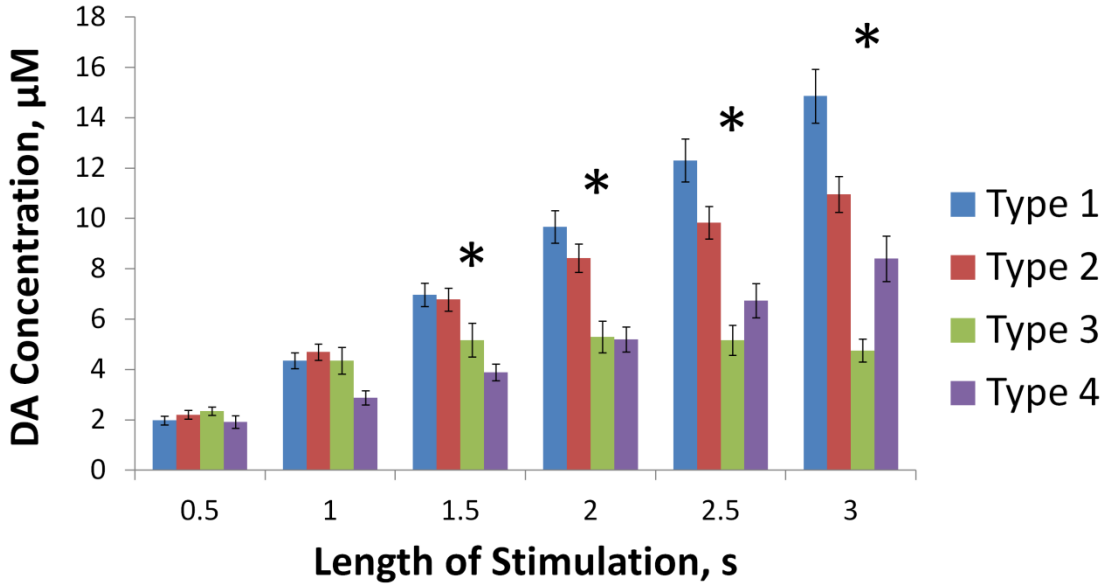


**Figure 4.2: Sub domains exhibit significantly different kinetic profiles.**
The average DA concentrations (± SEM) of the evoked DA overflow curves shown in Figure 4.1 plotted every 500 ms over the duration of the 3 second stimulation reveals that the four fast sub domains are significantly different (Two-way ANOVA with repeated reassures $p<0.005$). The four sub domains significantly differ after one second of stimulation (One-way ANOVA $p<0.02$).

### 4.3.3: Sub domain dependent linear clearance rates

Maximum linear clearance rate is sub domain dependent. One-way ANOVA comparison of average (± SEM) linear clearance rates from Types 1-4 (displayed in Figure 4.3) show that clearance rates significantly ($p<0.05$) depend on site type. Type 1 exhibits a linear clearance rate of 6.94 ± 0.64 µM/s, Type 2 clears DA at 5.27 ± 0.35 µM/s, Type 3 has a rate of 3.90 ± 0.86 µM/s and Type 4 has a rate of 6.57 ± 0.81 µM/s. This reduces to three distinct clearance rates. Type 1 and Type 4 exhibit similar fast clearance kinetics, followed by slower clearance typical of Type 2 and then again by the slowest clearance from Type 3 sites.

Comparison of average linear clearance rates (Figure 4.3) with average maximum DA amplitude (Figure 4.2, 3sec) reveals that linear clearance rate scales with maximum amplitude (with the exception of Type 4 sites). In fact, Figure 4.4 shows that the comparison of linear clearance rate to maximum concentration for each of the 90 responses in this study produces a statistical linear correlation (Pearson's correlation coefficient 0.760, 2-tailed t-test $p<0.00002$). Each sub domain is displayed in Figure 4.4 as a different symbol. Type 1 animals are shown as blue diamonds, Type 2 are red squares, Type 3 are green triangles, and Type 4 are displayed as purple X's. The symbols for Types 1-3 appear to be equally distributed around the linear regression fit, whereas the Type 4 animals lie primarily above the regression fit.

### 4.3.4: Selective detection of DA hang-up

Evoked DA overflow curves do not return to baseline for at least 8 seconds following the end of stimulation. Figure 4.5 is a re representation of the data displayed in Figure 4.1 with the SEM traces removed for clarity. Figure 4.5 also includes the average response from the slow domain of 78 individual animals in response to 3 second MFB stimulation. Slow domains do not appear to be composed of any discernible sub domains, thus Figure 4.5 represents a total of five discrete kinetic DA

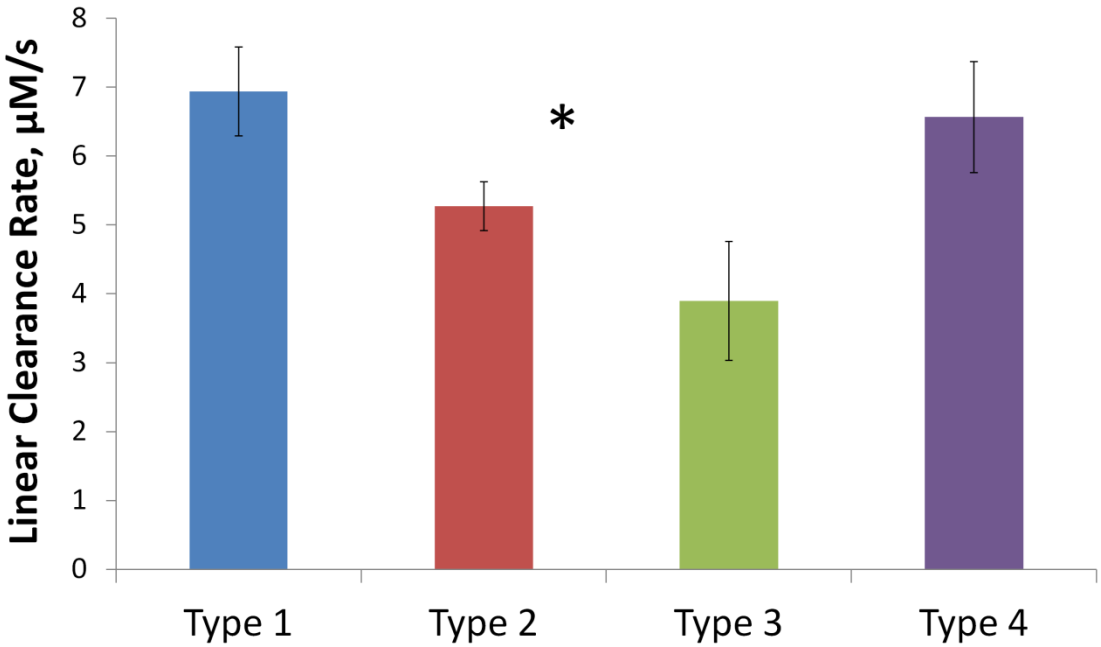


**Figure 4.3: Sub domains exhibit significantly different linear clearance rates.**
Maximum linear clearance rate is sub domain dependent. The average (± SEM) linear clearance rates of the evoked DA overflow responses shown in Figure 4.1 are significantly different by sub domain type (One-way ANOVA $p<0.05$).

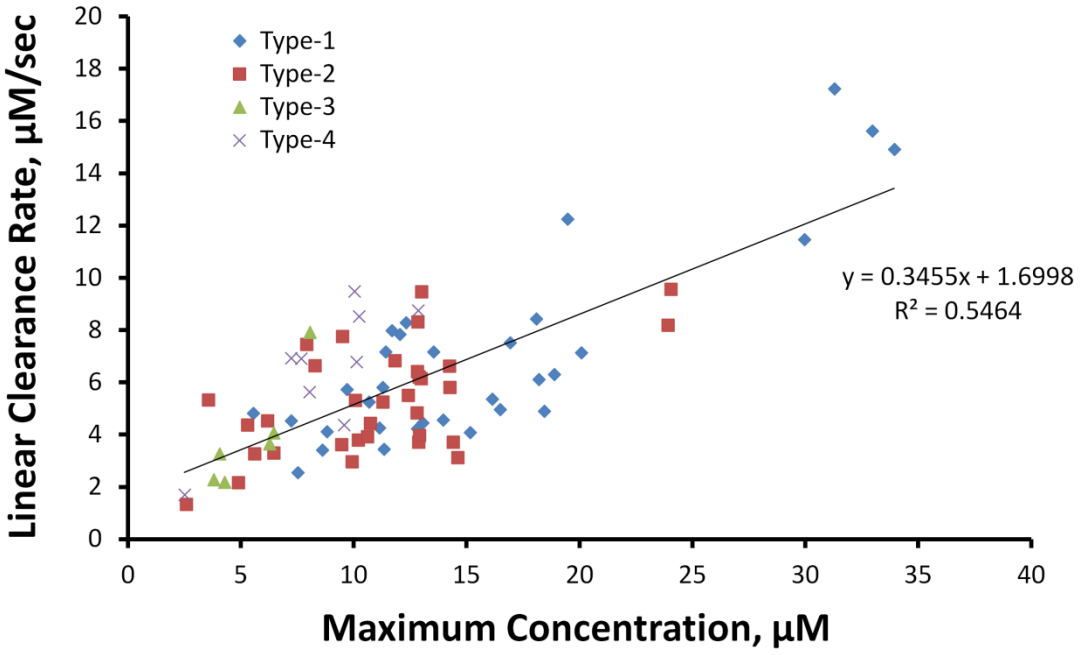


**Figure 4.4: Linear correlation of between maximum amplitude and linear clearance rate.**
Maximum linear clearance rate scales linearly with the maximum total amplitude of evoked DA overflow. In a plot representing all 90 animals represented in Figure 4.1 the linear clearance rate is significantly correlated with maximum concentration (Pearson's correlation coefficient 0.760, 2-tailed t-test $p<0.00002$). Type 1 animals are shown as blue diamonds, Type 2 are red squares, Type 3 are green triangles and Type 4 are displayed as purple X's.

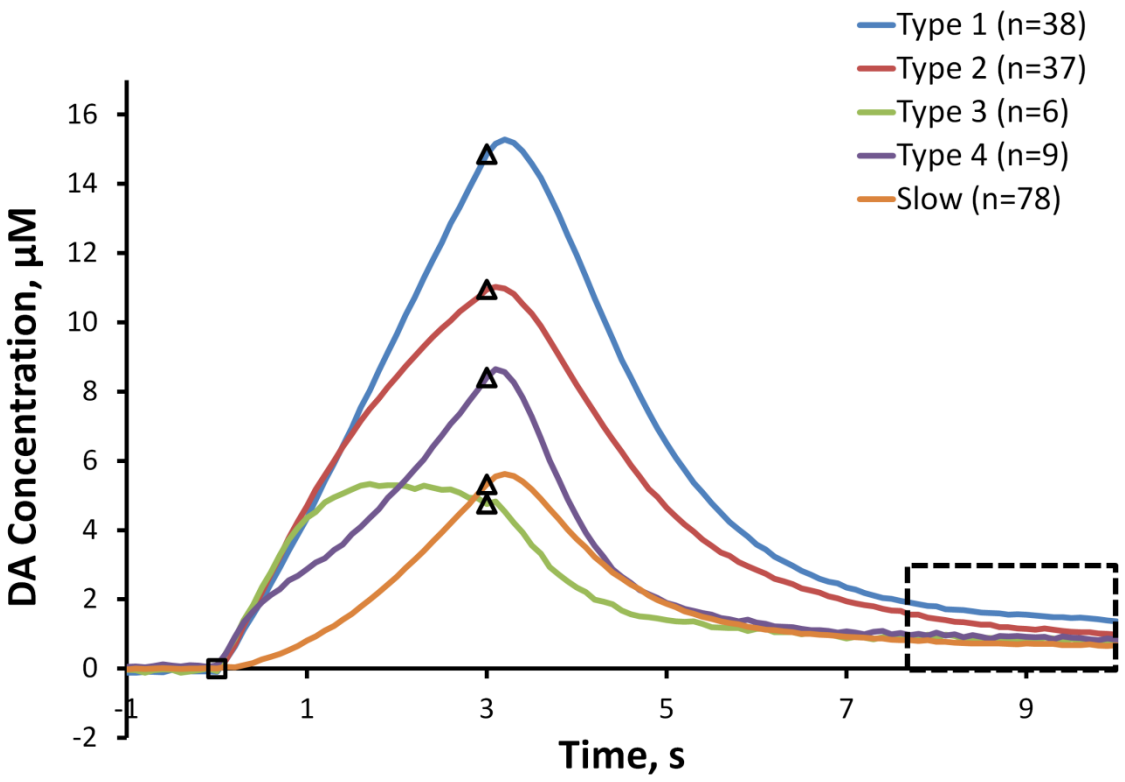


**Figure 4.5: Five kinetic domains in the dorsal striatum: existence of a hang up feature.**
All five DA domains in the dorsal striatum return to an elevated steady state DA tone following the end of stimulation (shown by the portion of the curves enclosed in the dashed box). Above is a rerepresentation of the average responses shown in Figure 4.1 (±SEM removed for clarity) with the addition of the average response to an identical stimulation from the slow domain (orange) of 78 individual animals. All five domains fail to return to baseline DA concentration established prior to the start of stimulation.

domains that exist in the dorsal striatum. Detailed examination of the responses from approximately 7.5-10 seconds (highlighted by the dashed box in Figure 4.5) show that all five domains reach a steady state condition where DA levels are elevated compared to the pre-stimulus baseline. This lasting elevation will be termed the "DA hang-up".

The DA hang-up feature is confirmed to be solely DA in nature by examination of average false color plots. Figure 4.6a represents the average false color plot for Type 1 responses (largest amplitude DA hang-up) and Figure 4.6b represents the average false color plot from the slow domain responses (smallest amplitude DA hang-up). Both Figures 4.6a and b are oriented with time on the x-axis, applied potential on the y-axis and DA concentration in false color. Evoked DA overflow traces, like those shown in Figure 4.1, are obtained by plotting the concentration vs time at the potential of maximum DA oxidation (denoted by the white dashed lines). DA concentration values can only be assigned to the DA oxidation peak, which initially appears in green and tapers off to red at approximately +0.7 V. The characteristic DA reduction peak is shown in blue at approximately -0.2 V. Stimulation begins at 0 seconds and continues for 3 seconds. In both Type 1 and slow responses, both the DA oxidation and reduction peaks continue out to 10 seconds. This serves as a characteristic fingerprint for DA and confirms that the DA hang-up is the result of elevated DA.

Further analysis of the average color plots show that there is an initial current fluxuation around +0.2 V (blue band) as well as a series of fluxuations appearing following the switching potentials (red band around +0.9 V and blue band around +0.3 V above the DA reduction peak). Due to the unique positioning of each of these current contributions, DA quantification can be carried out without unwanted interference from outside current contaminants.

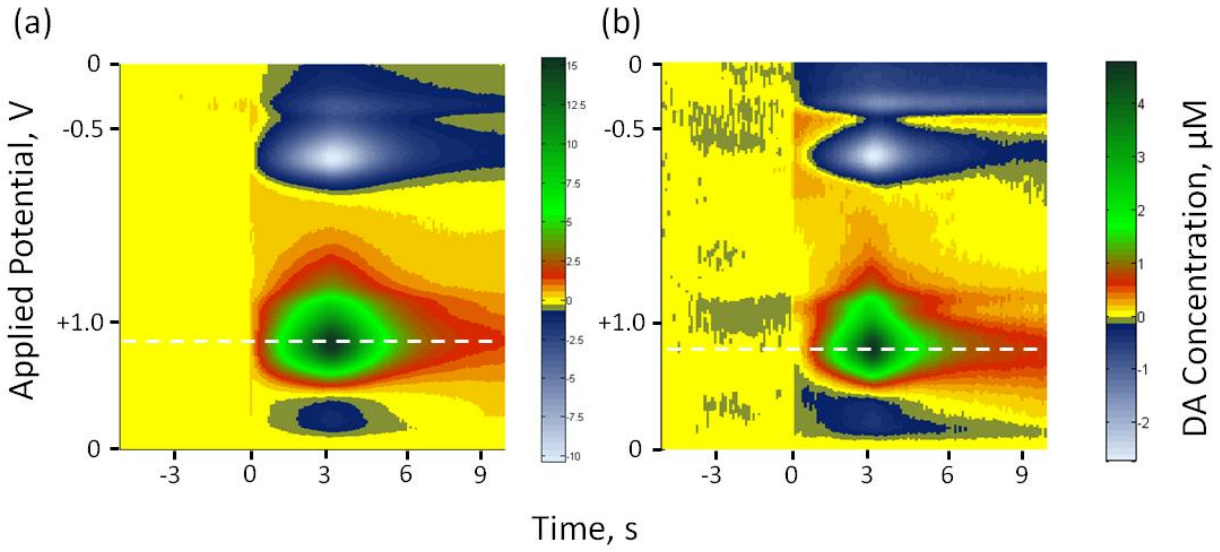


**Figure 4.6: False color plots selectively confirm the hang up feature is DA in origin.**
Average false color plots for Type 1 (a, n = 30) and slow (b, n = 30) domain responses to 3 second 60 Hz stimulation. Stimulation occurs from 0-3 seconds. Time is displayed on the x-axis, applied potential on the y-axis and DA concentration is in false color. The white dashed line corresponds with the peak DA oxidation potential and is used for generating evoked DA overflow traces. The DA concentration scale is only used to quantify DA oxidation features (green tapering to red). Both plots exhibit the characteristic fingerprint of DA out to 10 seconds.

### 4.3.5: Modeling of clearance profiles

The average DA clearance profiles from all five domains were modeled using a first order clearance relationship scaled with a constant efflux term as well as with the conventional Michaelis-Menten uptake model (Wightman et al., 1988a, Wu et al., 2001b). In each case the fit was set to begin at the point where the first derivative of the descending phase reaches its maximum to remove any effects of mass transport due to DA overshoot phenomena. Figures 4.7a and b each display the average responses from all five domains (shown previously in Figure 4.5) in dot representation. The solid red lines in Figure 4.7a show the scaled first order fit for each curve created using the following relationship, d[DA]/dt = [DA](1-U)*dt + S*dt. In each case, the newly proposed fit modeled the latter portion of the clearance profile, including the DA hang-up feature. The U and S terms for each domain are displayed in Table 4.1. Figure 4.7b shows the Michaelis-Menten fit of the average responses, using a fixed $K_M$ value of 0.2 µM (Near et al., 1988, Wu et al., 2001b) and $V_{max}$ values determined by the maximum linear clearance rate for each average curve. The Michaelis-Menten fit does not account for the DA hang-up feature and thus does not adequately fit the data.

## 4.4: DISCUSSION

This study serves as an extension of previous work from our laboratory concerning the existence of discrete fast and slow kinetic domains in the dorsal striatum (Moquin and Michael, 2009, Wang et al., 2010, Moquin and Michael, 2011, Taylor et al., 2012, Taylor et al., 2013). We have shown that these spatially distributed domains are unique entities that exhibit domain dependent responses to pharmacological treatment. Until recently, studies in the fast domain were limited to brief MFB stimulations (200 ms, 60 Hz stimuli) due to the belief that contribution from fast domains was limited due to the rapid onset of autoinhibition (Benoit-Marand et al., 2001, Moquin and Michael, 2009). This

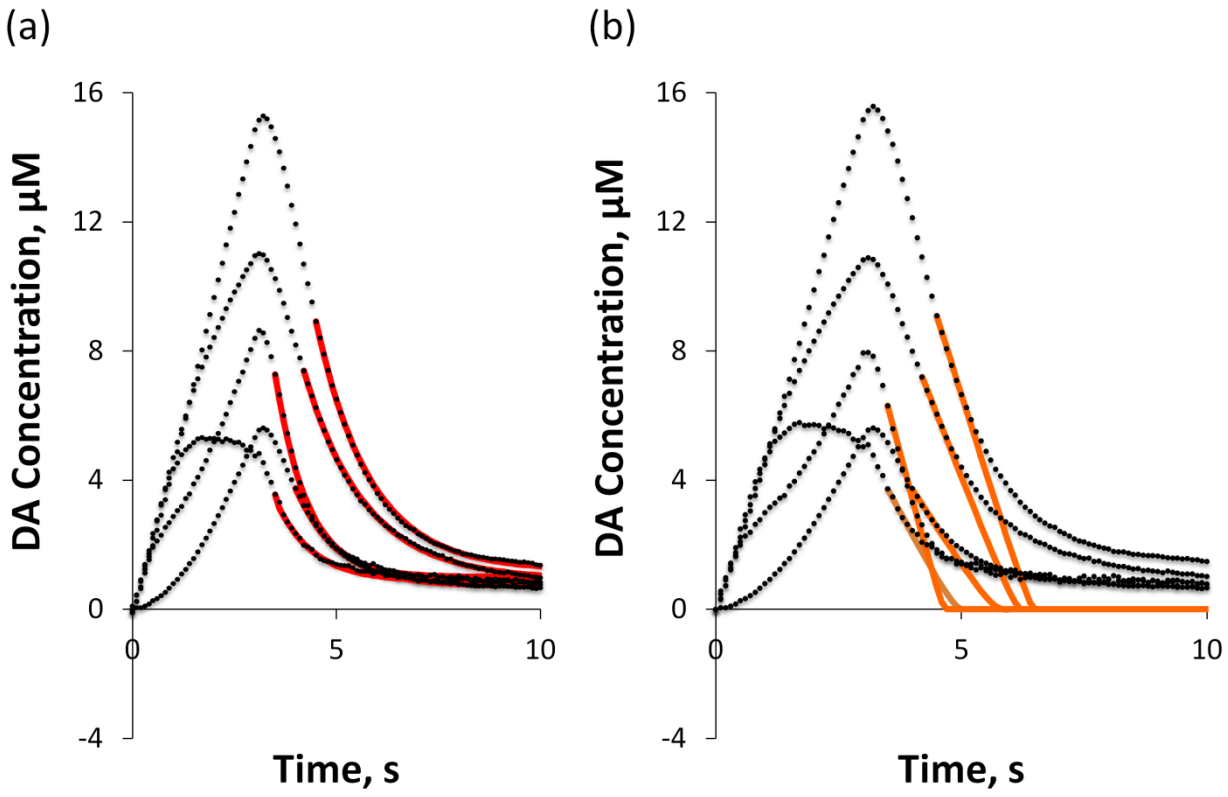


**Figure 4.7: Modeling of DA clearance profiles.**
Mathematical modeling of the average evoked DA overflow curves (black dots) for all five domains are displayed in Figure 4.5 using a scaled first order clearance model (a, red traces) and the traditional Michaelis-Menten uptake model (b, orange traces) with a fixed $K_m$ of 0.2 µM. The parameters for each fit are displayed in Table 4.1.

**Table 4.1: Modeling parameters used for the fits in shown in Figure 4.7.**
Parameters for the mathematical models of each average evoked DA overflow response displayed in Figure 4.7. The U and S terms correspond to the scaled first order fit in Figure 4.7a and the $V_{max}$ and $K_M$ terms were used for the Michaelis-Menten model shown in Figure 4.7b. $K_M$ was fixed to 0.2 μM in accordance to the literature (Near et al., 1988, Wu et al., 2001b).

| | **U ($s^{-1}$)** | **S ($s^{-1}$)** | **$V_{max}$ (μM/s)** | **$K_M$ (μM)** |
|---|---|---|---|---|
| **Type 1** | 0.73 | 0.089 | 5 | 0.2 |
| **Type 2** | 0.65 | 0.06 | 4 | 0.2 |
| **Type 3** | 1.05 | 0.092 | 3 | 0.2 |
| **Type 4** | 1.2 | 0.12 | 6 | 0.2 |
| **Slow** | 0.91 | 0.065 | 2.5 | 0.2 |

study shows that while that may be the case in some instances (e.g. Type 4 response), the majority of fast domain exhibits a robust response to continued stimulation.

### 4.4.1: Evaluating discrete DA kinetic domains

The dorsal striatum is composed of five discrete DA kinetic domains (shown in Figure 4.5): the previously described slow domain (Moquin and Michael, 2009) and the newly discovered four sub domains of the fast domain (Types 1-4). The four fast sub domains do not significantly deviate from each other until the duration of a 60 Hz stimulation exceeds one second. This explains the omission of the Type 1-4 sub domains in previous studies where the stimulation duration in the fast domain was limited to 200 ms. While we acknowledge that the 3 second 60 Hz MFB stimulations needed to reveal the differences between these sub domains is super-physiological, the information provided by such stimulations is quite relevant.

The large sample group used in this study allows us to draw conclusions as to the relative distribution of the Type 1-4 domains. Domains Type 1 and 2 are by far the most common of the fast sub domains, combining together to compose 83% of the total responses. This is not surprising, due to the prevalence of Type 1 and Type 2 responses in the literature (Stamford et al., 1986, Wightman et al., 1988a, May and Wightman, 1989a, Kawagoe et al., 1992, Wu et al., 2001b, Wu et al., 2002, Greco et al., 2006, Taylor et al., 2013). They are followed by 10% Type 4 and 7% Type 3. While these lesser observed responses have appeared in the literature (Kawagoe et al., 1992, Garris and Wightman, 1995, Garris et al., 1997, Venton et al., 2006, Moquin and Michael, 2009), they are far outnumbered by the previous two. This is likely due to CFE optimization via repositioning (Kawagoe et al., 1992, Jones et al., 1995a, Greco and Garris, 2003, Venton et al., 2003). Optimization is a commonly practiced procedure that takes into account that DA kinetic domains are spatially discrete regions (Taylor et al., 2013) to position the CFE in a location yielding maximum DA amplitude. This practice was first introduced because of the

belief that any feature inconsistent with a Type 1 or 2 responses was the result of a diffusional distortion caused by a physical gap between the DA release terminals and the CFE detector (Kawagoe et al., 1992, Venton et al., 2003). As a result of this belief, many of the published evoked DA overflow responses have been subjected to a mathematical deconvolution algorithm to account for those unwanted features of the data (Kawagoe et al., 1992, Jones et al., 1995a, Wu et al., 2001b). Our laboratory has shown in this and in previous studies that those features are in fact physiological (Moquin and Michael, 2009, Wang et al., 2010, Moquin and Michael, 2011, Taylor et al., 2012, Taylor et al., 2013) in origin and should not be subjected to any mathematical manipulation. Due to CFE optimization and deconvolution, previous studies have unknowingly extensively optimized for Type 1 and 2 domains, thus describing only a portion of the entire DA terminal field.

The existence of five discrete DA domains is not surprising based on the multiple functionality of DA (Hull et al., 1999, Brooks, 2001, Obeso et al., 2008, Urban et al., 2012) and the known multiple time courses of DA signaling (Schultz, 2007). Although we have yet to conduct any behavioral studies concerning DA domains, we hypothesize that such a varied functionality could require several mechanisms of DA signaling.

### 4.4.2: Multiple linear clearance rates

Linear clearance rate is sub domain dependent. Classic DA modeling describes evoked DA overflow in a specific brain region as a balance of release and Michaelis-Menten governed uptake described by single $K_M$ and $V_{max}$ values (Wightman et al., 1988a, Wu et al., 2001b). $V_{max}$ is described as the maximum linear rate of DA uptake into the dopamine transporter (DAT). Furthermore, the apparent $V_{max}$ value measured by electrochemical sensors depends on the DAT density surrounding the probe (Stamford et al., 1986, Wightman et al., 1988a). The domain dependence of linear clearance rate is in direct conflict with the idea of a single $V_{max}$ value governing the dorsal striatum. In addition, the statistical correlation

of linear clearance rate to maximum DA amplitude suggests that DA clearance is better described using a first order relationship instead of Michaelis-Menten kinetics. This correlation between linear clearance rate and maximum DA amplitude was previously shown by Stamford et al. (1986) to support the idea of a single $V_{max}$ value. In that study, Stamford suggested that the reasoning underlying the relationship was due to a mutual increase in DA releasing sites and DAT, thus increasing both terms in a fixed proportion. While this may be the case, further consideration of other possible clearance mechanisms is still justified.

### 4.4.3: Benefits afforded from signal averaging: Selective DA detection

Effective analytical detection is dependent on the sensitivity, selectivity and limits of detection of the detector (Harris, 2003). In vivo electrochemical detection of DA at CFEs exhibit high spatial and temporal resolution, high sensitivity and a LOD of approximately 200 nM. An issue that commonly arises with electrochemical detection methods is analyte selectivity. Chronoamperometry provides unparalleled temporal resolution, but is unable to discern between analytes. FSCV provides a moderately higher selectivity, but is still unable to separate any analytes exhibiting the same redox potentials. Therefore, it is of utmost importance to account for any possible interferences during the analysis of electrochemical detection (Michael and Wightman, 1999). Many recent studies have been published describing the use of Principle Component Analysis (PCA) to extract the contributions of individual analytes, such as pH and $O_2$, from an in vivo FSCV recording (Phillips et al., 2003, Heien et al., 2004, Heien et al., 2005). While much work has been published justifying PCA data manipulation, great care must still be made to not unintentionally remove chemically relevant features. Detailed analysis of electrochemical data can be complicated by a poor signal to noise ratio. In this study, we make us of the fact that signal and noise are uncorrelated. Signal strength is constant during repeated measurements, whereas noise is random. Therefore signal averaging will decrease the random noise, thus increasing

the affective signal to noise ratio of the measurement. This allows for detailed data interpretation of small amplitude phenomena typically masked by noise interferents.

The average false color plots of Type 1 and slow domain responses (Figure 4.6) show the selectivity of our detection for DA. Neither Figure 4.6a or b show any feature attributable to pH or any other interferent presenting at the potential of DA oxidation. The only non-DAergic current fluxuations observed in the color plots appear initially at approximately +0.2 V and following the switching potentials, features typical of a capacitive change (Takmakov et al., 2010). These fluxuations are triggered by the onset of MFB stimulation, suggesting that they are action potential mediated. While many factors can affect the double layer leading to a change in capacitive current, it is likely that the action potential mediated cation flux (e.g. $Ca^{2+}$, $K^{+}$, $Na^{+}$) leads to the current fluxuation. Regardless of the source of the non-DAergic fluxuation, the important factor is that the current does not appear at the maximum potential of DA oxidation used for DA quantification. Therefore, our detection method is highly selective for DA and requires no PCA data manipulation. Any PCA manipulation would only risk distorting the DA signal.

#### 4.4.4: Long term DA hang-up

The lowered affective LOD afforded by the color plot averaging allows for the definitive detection of the low amplitude DA hang-up. DA levels remain elevated for at least 8 seconds following the end of MFB stimulation. In both the Type 1 and slow domain, DA assumes an elevated steady state level exhibiting a clear characteristic DA CV fingerprint. This >8 second elevation far exceeds any contribution of DA adsorption/desorption to the CFE surface in both duration and concentration (Bath et al., 2000). This indicates that the DA hang-up observed in all five kinetic domains is physiologically relevant. An elevated DA tone could play a role in synaptic plasticity. Synaptic plasticity can manifest as short or long term facilitation or short or long term depression and has been shown to play a role in a learning and

memory (Hamilton et al., 2010). Neurochemically, fast and slow DA domains have been shown to exhibit differences in short term plasticity upon repeated MFB stimulation (Cragg, 2003, Montague et al., 2004, Kita et al., 2007, Moquin and Michael, 2009, Chadchankar and Yavich, 2011, Shu et al., 2013).

#### 4.4.5: Rethinking the model of DA clearance

This study has revealed the existence of multiple linear clearance rates dependant on anatomical location, concentration dependent linear clearance rates and a long term DA hang-up feature. These findings are in direct contradiction of the current description of Michaelis-Menten governed DAT mediated uptake (Wightman et al., 1988a, Wu et al., 2001b). In fact, the current Michaelis-Menten model of DA clearance is unable to model the DA hang-up feature of the evoked DA overflow response (Figure 4.7b). This requires a reassessment of the current model of DA clearance. Our newly proposed model of DA uptake is no more complicated than Michaelis-Menten uptake, having the same number of adjustable parameters. The new model incorporates first order DA clearance (Sabeti et al., 2002) and is capable of making excellent fits to the descending portion of all five DA kinetic domains within the dorsal striatum, including the DA hang-up feature (Figure 4.7a). The presence of overshoots in our data are indicative of continuing mass transport effects after the end of stimulus and so we have chosen to fit only the back portion of the evoked DA response curves to our new uptake model, in an effort to minimize interference of any mass transport effects with uptake. At this time, we do not assert any specific mechanism for the U or S terms. The insight of this work is that the data is unable to be fit by the existing Michaelis-Menten model and are easily fit by first order uptake coupled with a constant efflux term.

## 4.5: CONCLUSIONS

The DA terminal field in the dorsal striatum is composed of five discrete kinetic domains, including the slow domain and the four sub domains of the fast domain (Type 1-4). Each exhibits a significantly different kinetic profile. Due to the complicated nature of DA signaling, extreme care and attention must be paid during analysis. DA levels are elevated at concentrations at or near the LOD of FSCV detection methods for at least 8 seconds following MFB stimulation. Therefore, any mathematical adjustment could possibly remove a DAergic feature, thus making the use of PCA data manipulation of great concern. Our selective detection of DA does not require a deconvolution algorithm nor PCA adjustment and allows for the unbiased analysis of evoked DA overflow kinetics. From this we were able to identify the DA hang-up feature and suggest a new first order model of DA clearance that provides an excellent fit to all five kinetic domains.

## 5.0: CONCLUSIONS

This dissertation details numerous discoveries that have the potential to greatly impact the understanding of DA transmission. Using *in vivo* fast scan cyclic voltammetry at carbon fiber microelectrodes, we first discovered that the effects of the competitive DAT inhibitor, nomifensine, are domain dependent (Taylor et al., 2012). Moreover, the domain dependent effects of nomifensine led to the restricted diffusion model of DA transmission in the dorsal striatum. This model suggests that DA transmission throughout the extracellular space does not occur through free radial diffusion, as was suggested by previous models (Cragg et al., 2001, Cragg and Rice, 2004). Instead, DA is subjected to a highly efficient restriction mechanism that limits the distance of DA diffusion (Sykova and Nicholson, 2008). In this case, evoked DA overflow is considered to be a tightly controlled balance between vesicular release, DAT mediated uptake and restricted diffusion. The effects of restricted DA diffusion are only observed after DAT mediated uptake is inhibited by nomifensine.

We went on to test the efficiency of restricted diffusion to control DA crosstalk between fast and slow domains. We discovered that DA is unable to diffuse between fast and slow domains, even in the presence of nomifensine (where conditions for DA diffusion are optimal) (Taylor et al., 2013). Furthermore, we discovered that the restriction mechanisms allow for varying concentration gradients between fast and slow domains. Fast domains produced larger evoked DA overflow responses during high frequency stimulations (60 Hz), whereas low frequency stimulation (30 and 45 Hz) elicit higher evoked DA overflow in slow domains. This interconversion in concentration gradients confirms that the fast and slow domains are completely isolated from each other and that a standing concentration gradient between the two domains does not exist over all conditions. This supports the finding that the

slow domain is caused by the presence of a 2 μM resting basal DA concentration (Borland and Michael, 2004, Wang et al., 2010). If DA were allowed to freely diffuse between the fast and slow domains, the domain dependent difference in basal DA concentration could not exist.

Our continued work led to the discovery of four significantly different sub domains of the fast domain. All four sub domains respond identically through the first 500 ms of a 3 second, 60 Hz MFB stimulation, but exhibit varying extents of regulation when stimulation exceeds one second. When considered along with the slow domain, this confirms the existence of five discrete DA domains in the dorsal striatum. All five domains exhibit a DA hang-up following MFB stimulation. This confirms that DA establishes a long lasting steady state elevation following release. While the mechanism underlying this DA elevation is unknown, a first order DA clearance model adjusted with a constant efflux term provides a remarkably close fit to the data. Further work must be done to characterize any possible physiological relevance to the constant efflux source.

This work has the potential to be highly influential to the understanding of DA transmission. In fact, the major findings of this dissertation have already served as the intellectual base for numerous studies in our laboratory. The restricted diffusion model of DA transmission has been incorporated into a novel mathematical model of evoked DA overflow responses (Walters et al. *submitted*). This model is no more complicated than the existing model based on Equations 1.5 and 2.1 of this dissertation, but is able to provide high correlation fits to previously unexplained features of the data. The restricted diffusion model was also used to describe the effects of nomifensine on the fast and slow DA domains in the Nucleus Accumbens core region of brain (Shu et al., *submitted*).

The discovery of the domain dependent effects of the competitive DAT inhibitor, nomifensine, could be of great significance to the understanding and possible treatment of ADHD. Approximately 11% of children ages 4-17 (6.4 million) in the United States are being diagnosed with ADHD (CDC 2011).

This manifests an enormous economical burden on not only the families involved, but also the nation as a whole. ADHD is believed to be the result of increased DA signaling in the brain (Gonon, 2009). The current treatment for ADHD is the competitive DAT inhibitor, methylphenidate (Ritalin) (Schlochtermeier et al., 2011). This choice of treatment is paradoxical being that competitive DAT inhibitors are classically known in increase the resting DA concentration in the brain (Church et al., 1987), which would subsequently cause additional postsynaptic receptor signaling, only adding to the problem. The finding that the competitive DAT inhibitor, nomifensine, acts in a domain dependent manner may provide some meaningful insight to this issue. If Ritalin is acting through a similar domain dependent effect, one might be able to pinpoint the DA domain responsible for the symptomatology of ADHD and more selectively suppress it.

While the physiological relevance underlying the existence of the five kinetic domains and the DA hang-up are unknown, there are a few possibilities that merit further testing. First being the multiple functionalities of the DA system. As previously described, DA is involved in a myriad of neurological tasks, such as motor control, sexual arousal, reward, reinforcement and addiction (Horn et al., 1979, Hull et al., 1999, Brooks, 2001, Urban et al., 2012). It would make sense that these unique physiological functionalities would require specific modes of DA signaling, possibly afforded by different DA domains. Furthermore, it serves to reason that DA transmission would be tightly regulated in space via restricted diffusion. One could imagine the negative ramifications that could arise from eliciting a motor response from DA released for the intended purpose of signaling reward or sexual arousal. This hypothesis could be tested by monitoring DA signaling in each of the five domains in the behaving rat.

Schizophrenia is a devastating mental disorder with symptomatology including delusions and paranoia. The existence of the DA hang-up could play a role in better understanding schizophrenia though the effects of synaptic plasticity or long term DA signaling. DA signaling is known to occur on

multiple time scales (Schultz, 2007), most notably as the result of tonic and phasic firing rates (Grace, 1991). Tonic firing is described as a slow pacemaker neuron firing that maintains the basal DA concentration in the extracellular space. Phasic firing consists of short bursts of high frequency action potentials that result in a transient DA elevation. Tonic and phasic firing patterns have garnered interest since they were found to be relevant to the pathophysiology of schizophrenia. Schizophrenia is believed to be characterized by decreased tonic signaling. Decreased tonic signaling results in a lower baseline DA concentration. This low basal DA tone leads to an up regulation of DA receptors and an increased amplitude of DA released during phasic firing. This elevated phasic DA signaling is believed to be the cause of the positive symptoms associated with Schizophrenia (delusions) (Grace, 1991). The newly discovered preference of the slow domain for low frequency stimulation (Taylor et al., 2013), along with the DA hang-up feature could play a significant role in baseline receptor saturation and subsequent phasic firing. From this, I hypothesize that the slow domain is responsible for tonic firing. Furthermore, because of that, I hypothesize that Schizophrenia is a disorder of the slow domain. Testing this hypothesis would first require determining the currently unknown physiological or anatomical cause of the slow domain.

In closing, the discoveries detailed in this dissertation raise interesting questions and provide a new prospective for studying the brain. Many of the well characterized DAergic phenomena must be reexamined taking into account the newly discovered DA domains as well as the domain dependent effects of DA targeting drugs. In doing so, it will be possible to gain further insight into the complex regulation of the DA system in route to the discovery of the cause and novel treatment techniques for various neurological disorders.

## 6.0: REFERENCES


Bard AJ, Faulkner LR (2001) Electrochemical Methods: Fundamentals and Applications. Hoboken, NJ: John Wiley & Sons, Inc.

Barger G, Ewins AJ (1910) CCXXXVII. - Some Phenolic Derivatives of β-Phenylethylamine. J Chem Soc, Trans 97:2253-2261.

Bath BD, Michael DJ, Trafton BJ, Joseph JD, Runnels PL, Wightman RM (2000) Subsecond adsorption and desorption of dopamine at carbon-fiber microelectrodes. Anal Chem 72:5994-6002.

Benoit-Marand M, Ballion B, Borrelli E, Boraud T, Gonon F (2011) Inhibition of dopamine uptake by D(2) antagonists: an in vivo study. J Neurochem 116:449-458.

Benoit-Marand M, Borrelli E, Gonon F (2001) Inhibition of Dopamine Release Via Presynaptic D2 Receptors: Time Course and Functional Characteristics In Vivo. The Journal of Neuroscience 21:9134-9141.

Benoit-Marand M, Jaber M, Gonon F (2000) Release and elimination of dopamine in vivo in mice lacking the dopamine transporter: functional consequences. European Journal of Neuroscience 12:2985-2992.

Borland LM, Michael AC (2004) Voltammetric study of the control of striatal dopamine release by glutamate. J Neurochem 91:220-229.

Borland LM, Shi GY, Yang H, Michael AC (2005) Voltammetric study of extracellular dopamine near microdialysis probes acutely implanted in the striatum of the anesthetized rat. J Neurosci Methods 146:149-158.

Brannan T, Prikhojan A, MartinezTica J, Yahr MD (1995) In vivo comparison of the effects of inhibition of MAO-A versus MAO-B on striatal L-DOPA and dopamine metabolism. Journal of Neural Transmission-Parkinsons Disease and Dementia Section 10:79-89.

Brooks DJ (2001) Functional imaging studies on dopamine and motor control. J Neural Transm 108:1283-1298.

Carlsson A, Lindqvist M, Magnusson T, Waldeck B (1958) On the Presence of 3-Hydroxytyramine in Brain. Science 127:471-471.

Ceccarelli B, Hurlbut WP (1980) Vesicle Hypothesis of the Release of Quanta of Acetylcholine. Physiol Rev 60:396-441.

Chadchankar H, Yavich L (2011) Sub-regional differences and mechanisms of the short-term plasticity of dopamine overflow in striatum in mice lacking alpha-synuclein. Brain Res 1423:67-76.

Church WH, Justice JB, Byrd LD (1987) Extracellular dopamine in rat striatum following uptake inhibition by cocaine, nomifensine and benztropine. Eur J Pharmacol 139:345-348.

Cragg SJ (2003) Variable dopamine release probability and short-term plasticity between functional domains of the primate striatum. J Neurosci 23:4378-4385.

Cragg SJ, Hille CJ, Greenfield SA (2002) Functional domains in dorsal striatum of the nonhuman primate are defined by the dynamic behavior of dopamine. J Neurosci 22:5705-5712.

Cragg SJ, Nicholson C, Kume-Kick J, Tao L, Rice ME (2001) Dopamine-mediated volume transmission in midbrain is regulated by distinct extracellular geometry and uptake. J Neurophysiol 85:1761-1771.

Cragg SJ, Rice ME (2004) DAncing past the DAT at a DA synapse. Trends Neurosci 27:270-277.

Crank J (1956) The mathematics of diffusion. Oxford,: Clarendon Press.

Davidson C, Ellinwood EH, Douglas SB, Lee TH (2000) Effect of cocaine, nomifensine, GBR 12909 and WIN 35428 on carbon fiber microelectrode sensitivity for voltammetric recording of dopamine. J Neurosci Methods 101:75-83.

de la Fuente-Fernandez R, Schulzer M, Kuramoto L, Cragg J, Ramachandiran N, Au WL, Mak E, McKenzie J, McCormick S, Sossi V, Ruth TJ, Lee CS, Calne DB, Stoessl AJ (2011) Age-Specific Progression of Nigrostriatal Dysfunction in Parkinson's Disease. Ann Neurol 69:803-810.

Deakin MR, Wightman RM (1986) The Kinetics of Some Substituted Catechol/*o*-Quinone Couples at a Carbon Paste Electrode. J Electroanal Chem 206:167-177.

del Castillo J, Katz B (1956) Biophysical aspects of Neuro-Muscular Transmission. Prog Biophys Mol Biol 6:122-&.

Doucet G, Descarries L, Garcia S (1986) Quantification of the Dopamine Innervation in Adult Rat Neostriatum. Neuroscience 19:427-&.

DuVall SH, McCreery RL (1999) Control of catechol and hydroquinone electron-transfer kinetics on native and modified glassy carbon electrodes. Anal Chem 71:4594-4602.

DuVall SH, McCreery RL (2000) Self-catalysis by catechols and quinones during heterogeneous electron transfer at carbon electrodes. J Am Chem Soc 122:6759-6764.

Eiden LE, Schafer MKH, Weihe E, Schutz B (2004) The vesicular amine transporter family (SLC18): amine/proton antiporters required for vesicular accumulation and regulated exocytotic

secretion of monoamines and acetylcholine. Pflugers Archiv-European Journal of Physiology 447:636-640.

Elsworth JD, Roth RH (1997) Dopamine synthesis, uptake, metabolism, and receptors: Relevance to gene therapy of Parkinson's disease. Exp Neurol 144:4-9.

Engstrom RC, Wightman RM, Kristensen EW (1988) Diffusional distortion in the monitoring of dynamic events. Anal Chem 60:652-656.

Ewing AG, Bigelow JC, Wightman RM (1983) Direct in vivo monitoring of dopamine released from two striatal compartments in the rat. Science 221:169-171.

Feng JX, Brazell M, Renner K, Kasser R, Adams RN (1987) Electrochemical pretreatment of carbon fibers for in vivo electrochemistry: Effects on sensitivity and response time. Anal Chem 59:1863-1867.

Floresco SB, West AR, Ash B, Moore H, Grace AA (2003) Afferent modulation of dopamine neuron firing differentially regulates tonic and phasic dopamine transmission. Nat Neurosci 6:968-973.

Fon EA, Pothos EN, Sun BC, Killeen N, Sulzer D, Edwards RH (1997) Vesicular transport regulates monoamine storage and release but is not essential for amphetamine action. Neuron 19:1271-1283.

Garris PA, Budygin EA, Phillips PEM, Venton BJ, Robinson DL, Bergstrom BP, Rebec GV, Wightman RM (2003) A role for presynaptic mechanisms in the actions of nomifensine and haloperidol. Neuroscience 118:819-829.

Garris PA, Christensen JRC, Rebec GV, Wightman RM (1997) Real-time measurement of electrically evoked extracellular dopamine in the striatum of freely moving rats. J Neurochem 68:152-161.

Garris PA, Ciolkowski EL, Pastore P, Wightman RM (1994) Efflux of dopamine from the synaptic cleft in the nucleus accumbens of the rat brain. J Neurosci 14:6084-6093.

Garris PA, Wightman RM (1995) Distinct pharmacological regulation of evoked dopamine efflux in the amygdala and striatum of the rat in vivo. Synapse 20:269-279.

Giros B, Jaber M, Jones SR, Wightman RM, Caron MG (1996) Hyperlocomotion and indifference to cocaine and amphetamine in mice lacking the dopamine transporter. Nature 379:606-612.

Gonon F (2009) The dopaminergic hypothesis of attention-deficit/hyperactivity disorder needs re-examining. Trends Neurosci 32:2-8.

Gonon F, Cespuglio R, Ponchon JL, Buda M, Jouvet M, Adams RN, Pujol JF (1978) *In Vivo* Electrochemical Determination of Dopamine Release in Rat Neostriatum. Comptes Rendus Hebdomadaires Des Seances De L Academie Des Sciences Serie D 286:1203-1206.

Goto Y, Otani S, Grace AA (2007) The Yin and Yang of dopamine release: a new perspective. Neuropharmacology 53:583-587.

Gottwald MD, Aminoff MJ (2011) Therapies for dopaminergic-induced dyskinesias in parkinson disease. Ann Neurol 69:919-927.

Grace AA (1991) Phasic versus tonic dopamine release and the modulation of dopamine system responsivity: A hypothesis for the etiology of schizophrenia. Neuroscience 41:1-24.

Greco PG, Garris PA (2003) In vivo interaction of cocaine with the dopamine transporter as measured by voltammetry. Eur J Pharmacol 479:117-125.

Greco PG, Meisel RL, Heidenreich BA, Garris PA (2006) Voltammetric measurement of electrically evoked dopamine levels in the striatum of the anesthetized Syrian hamster. J Neurosci Methods 152:55-64.

Greengard P, Valtorta F, Czernik AJ, Benfenati F (1993) Synaptic Vesicle Phosphoproteins and Regulation of Synaptic Function. Science 259:780-785.

Guillot TS, Miller GW (2009) Protective Actions of the Vesicular Monoamine Transporter 2 (VMAT2) in Monoaminergic Neurons. Molecular Neurobiology 39:149-170.

Gulley JM, Zahniser NR (2003) Rapid regulation of dopamine transporter function by substrates, blockers and presynaptic receptor ligands. Eur J Pharmacol 479:139-152.

Guo XF, Zhang ZC, Zhai JG, Fang MS, Hu MR, Wu RR, Liu ZN, Zhao JP, Early-Stage Schizophrenia O (2012) Effects of antipsychotic medications on quality of life and psychosocial functioning in patients with early-stage schizophrenia: 1-year follow-up naturalistic study. Compr Psychiatry 53:1006-1012.

Hamilton TJ, Wheatley BM, Sinclair DB, Bachmann M, Larkum ME, Colmers WF (2010) Dopamine modulates synaptic plasticity in dendrites of rat and human dentate granule cells. Proceedings of the National Academy of Sciences 107:18185-18190.

Harris DC (2003) Quantitative chemical analysis. New York: W.H. Freeman and Co.

Hawley MD, Tatawawa.Sv, Piekarsk.S, Adams RN (1967) Electrochemical Studies of Oxidation Pathways of Catecholamines. J Am Chem Soc 89:447-&.

Heien M, Johnson MA, Wightman RM (2004) Resolving neurotransmitters detected by fast-scan cyclic voltammetry. Anal Chem 76:5697-5704.

Heien MLAV, Khan AS, Ariansen JL, Cheer JF, Phillips PEM, Wassum KM, Wightman RM (2005) Real-time measurement of dopamine fluctuations after cocaine in the brain of behaving rats. Proc Natl Acad Sci U S A 102:10023-10028.

Hollander JA, Carelli RM (2007) Cocaine-associated stimuli increase cocaine seeking and activate accumbens core neurons after abstinence. J Neurosci 27:3535-3539.

Horn AS, Korf J, Westerink BHC (1979) The Neurobiology of dopamine. London ; New York: Academic Press.

Hornykiewicz O (2002) L-DOPA: From a biologically inactive amino acid to a successful therapeutic agent. Amino Acids 23:65-70.

Hrabetova S, Hrabe J, Nicholson C (2003) Dead-space microdomains hinder extracellular diffusion in rat neocortex during ischemia. J Neurosci 23:8351-8359.

Hrabetova S, Nicholson C (2004) Contribution of dead-space microdomains to tortuosity of brain extracellular space. Neurochem Int 45:467-477.

Hull EM, Lorrain DS, Du J, Matuszewich L, Lumley LA, Putnam SK, Moses J (1999) Hormone-neurotransmitter interactions in the control of sexual behavior. Behav Brain Res 105:105-116.

Hunt P, Kannengi.Mh, Raynaud JP (1974) Nomifensine: a new potent inhibitor of dopamine uptake into synaptosomes from rat-brain corpus striatum. J Pharm Pharmacol 26:370-371.

Jaquins-Gerstl A, Michael AC (2009) Comparison of the brain penetration injury associated with microdialysis and voltammetry. J Neurosci Methods 183:127-135.

Jaquins-Gerstl A, Shu Z, Zhang J, Liu YS, Weber SG, Michael AC (2011) Effect of Dexamethasone on Gliosis, Ischemia, and Dopamine Extraction during Microdialysis Sampling in Brain Tissue. Anal Chem 83:7662-7667.

Jones SR, Gainetdinov RR, Jaber M, Giros B, Wightman RM, Caron MG (1998) Profound neuronal plasticity in response to inactivation of the dopamine transporter. Proc Natl Acad Sci U S A 95:4029-4034.

Jones SR, Garris PA, Kilts CD, Wightman RM (1995a) Comparison of Dopamine Uptake in the Basolateral Amygdaloid Nucleus, Caudate-Putamen, and Nucleus Accumbens of the Rat. J Neurochem 64:2581-2589.

Jones SR, Garris PA, Wightman RM (1995b) Different effects of cocaine and nomifensine on dopamine uptake in the caudate-putamen and nucleus accumbens. J Pharmacol Exp Ther 274:396-403.

Kahlig KM, Binda F, Khoshbouei H, Blakely RD, McMahon DG, Javitch JA, Galli A (2005) Amphetamine induces dopamine efflux through a dopamine transporter channel. Proc Natl Acad Sci U S A 102:3495-3500.

Kapur S, Zipursky RB, Remington G (1999) Clinical and theoretical implications of 5-HT(2) and D(2) receptor occupancy of clozapine, risperidone, and olanzapine in schizophrenia. Am J Psychiatry 156:286-293.

Katz NS, Guiard BP, El Mansari M, Blier P (2010) Effects of acute and sustained administration of the catecholamine reuptake inhibitor nomifensine on the firing activity of monoaminergic neurons. J Psychopharm 24:1223-1235.

Kawagoe KT, Garris PA, Wiedemann DJ, Wightman RM (1992) Regulation of transient dopamine concentration gradients in the microenvironment surrounding nerve terminals in the rat striatum. Neuroscience 51:55-64.

Kennedy RT, Jones SR, Wightman RM (1992) Dynamic observation of dopamine autoreceptor effects in rat striatal slices. J Neurochem 59:449-455.

Kim J-H, Son Y-D, Kim H-K, Lee S-Y, Cho S-E, Kim Y-B, Cho Z-H (2011) Antipsychotic-Associated Mental Side Effects and Their Relationship to Dopamine D(2) Receptor Occupancy in Striatal Subdivisions A High-Resolution PET Study With (11)C Raclopride. J Clin Psychopharmacol 31:507-511.

Kissinger PT, Hart JB, Adams RN (1973) Voltammetry in Brain Tissue - New Neurophysiological Measurement. Brain Res 55:209-213.

Kita JM, Parker LE, Phillips PEM, Garris PA, Wightman RM (2007) Paradoxical modulation of short-term facilitation of dopamine release by dopamine autoreceptors. J Neurochem 102:1115-1124.

Korchounov A, Meyer MF, Krasnianski M (2010) Postsynaptic nigrostriatal dopamine receptors and their role in movement regulation. J Neural Transm 117:1359-1369.

Kristensen EW, Kuhr WG, Wightman RM (1987) Temporal Characterization of Perfluorinated Ion Exchange Coated Microvoltammetric Electrodes for in vivo Use. Anal Chem 59:1752-1757.

Kuhr WG, Ewing AG, Caudill WL, Wightman RM (1984) Monitoring the stimulated release of dopamine with in vivo voltammetry. I: Characterization of the response observed in the caudate nucleus of the rat. J Neurochem 43:560-569.

Kulagina NV, Zigmond MJ, Michael AC (2001) Glutamate regulates the spontaneous and evoked release of dopamine in the rat striatum. Neuroscience 102:121-128.

Larsen MB, Sonders MS, Mortensen OV, Larson GA, Zahniser NR, Amara SG (2011) Dopamine Transport by the Serotonin Transporter: A Mechanistically Distinct Mode of Substrate Translocation. J Neurosci 31:6605-6615.

Laviron E (1984) Electrochemical Reactions With Protonations at Equilibrium: Part X. The Kinetics of the *p*-Benzoquinone/Hydroquinone Couple on a Platinum Electrode. J Electroanal Chem 164:213-227.

Ludolph AG, Kassubek J, Schmeck K, Glaser C, Wunderlich A, Buck AK, Reske SN, Fegert JM, Mottaghy FM (2008) Dopaminergic dysfunction in attention deficit hyperactivity disorder (ADHD), differences between pharmacologically treated and never treated young adults: A 3,4-dihdroxy-6- F-18 fluorophenyl-L-alanine PET study. NeuroImage 41:718-727.

Makos MA, Han K-A, Heien ML, Ewing AG (2010) Using in Vivo Electrochemistry To Study the Physiological Effects of Cocaine and Other Stimulants on the Drosophila melanogaster Dopamine Transporter. ACS Chem Neurosci 1:74-83.

Mannich C, Jacobsohn W (1910) Über Oxyphenyl-alkylamine und Dioxyphenyl-alkylamine. Berichte der deutschen chemischen Gesellschaft 43:189-197.

Martel P, Leo D, Fulton S, Berard M, Trudeau LE (2011) Role of Kv1 Potassium Channels in Regulating Dopamine Release and Presynaptic D2 Receptor Function. PLoS One 6.

May LJ, Kuhr WG, Wightman RM (1988) Differentiation of dopamine overflow and uptake processes in the extracellular fluid of the rat caudate nucleus with fast-scan in vivo voltammetry. J Neurochem 51:1060-1069.

May LJ, Wightman RM (1989a) Effects of D2 antagonists on frequency dependent stimulated dopamine overflow in nucleus accumbens and caudate putamen. J Neurochem 53:898-906.

May LJ, Wightman RM (1989b) Heterogeneity of stimulated dopamine overflow within rat striatum as observed with in vivo voltammetry. Brain Res 487:311-320.

Michael AC, Borland LM (2007) Electrochemical methods for neuroscience. Boca Raton: CRC Press/Taylor & Francis.

Michael AC, Borland LM, Mitala JJ, Willoughby BM, Motzko CM (2005) Theory for the impact of basal turnover on dopamine clearance kinetics in the rat striatum after medial forebrain bundle stimulation and pressure ejection. J Neurochem 94:1202-1211.

Michael AC, Ikeda M, Justice JB (1987a) Dynamics of the recovery of releasable dopamine following electrical stimulation of the medial forebrain bundle. Neurosci Lett 76:81-86.

Michael AC, Ikeda M, Justice JB (1987b) Mechanisms contributing to the recovery of striatal releasable dopamine following MFB stimulation. Brain Res 421:325-335.

Michael DJ, Wightman RM (1999) Electrochemical monitoring of biogenic amine neurotransmission in real time. J Pharm Biomed Anal 19:33-46.

Millar J, Stamford JA, Kruk ZL, Wightman RM (1985) Electrochemical, pharmacological and electrophysiological evidence of rapid dopamine release and removal in the rat caudate nucleus following electrical stimulation of the median forebrain bundle. Eur J Pharmacol 109:341-348.

Miller A, Tanner J (2008) Essentials of Chemical Biology: Structure and Dynamics of Biological Macromolecules. Chichester, West Sussex, UK: John Wiley & Sons Ltd.

Missale C, Nash SR, Robinson SW, Jaber M, Caron MG (1998) Dopamine receptors: From structure to function. Physiol Rev 78:189-225.

Mizuno Y, Bies RR, Remington G, Mamo DC, Suzuki T, Pollock BG, Tsuboi T, Watanabe K, Mimura M, Uchida H (2012) Dopamine D2 receptor occupancy with risperidone or olanzapine during maintenance treatment of schizophrenia: A cross-sectional study. Prog Neuropsychopharmacol Biol Psychiatry 37:182-187.

Montague PR, McClure SM, Baldwin PR, Phillips PEM, Budygin EA, Stuber GD, Kilpatrick MR, Wightman RM (2004) Dynamic gain control of dopamine delivery in freely moving animals. J Neurosci 24:1754-1759.

Moquin KF, Michael AC (2009) Tonic autoinhibition contributes to the heterogeneity of evoked dopamine release in the rat striatum. J Neurochem 110:1491-1501.

Moquin KF, Michael AC (2011) An inverse correlation between the apparent rate of dopamine clearance and tonic autoinhibition in subdomains of the rat striatum: a possible role of transporter-mediated dopamine efflux. J Neurochem 117:133-142.

Moron JA, Brockington A, Wise RA, Rocha BA, Hope BT (2002) Dopamine uptake through the norepinephrine transporter in brain regions with low levels of the dopamine transporter: Evidence from knock-out mouse lines. J Neurosci 22:389-395.

Nakachi N, Kiuchi Y, Inagaki M, Inazu M, Yamazaki Y, Oguchi K (1995) Effects of various dopamine uptake inhibitors on striatal extracellular dopamine levels and behaviours in rats. Eur J Pharmacol 281:195-203.

Near JA, Bigelow JC, Wightman RM (1988) Comparison of uptake of dopamine in rat striatal chopped tissue and synaptosomes. J Pharmacol Exp Ther 245:921-927.

Nicholson C (1995) Interaction between diffusion and Michaelis-Menten uptake of dopamine after iontophoresis in striatum. Biophys J 68:1699-1715.

Nicholson C, Sykova E (1998) Extracellular space structure revealed by diffusion analysis. Trends Neurosci 21:207-215.

Obeso JA, Rodriguez-Oroz MC, Benitez-Temino B, Blesa FJ, Guridi J, Marin C, Rodriguez M (2008) Functional organization of the basal ganglia: Therapeutic implications for Parkinson's disease. Mov Disord 23:S548-S559.

Okada M, Nakao R, Hosoi R, Zhang M-R, Fukumura T, Suzuki K, Inoue O (2011) Microdialysis with radiometric monitoring of L- beta-(11)C DOPA to assess dopaminergic metabolism: effect of inhibitors of L-amino acid decarboxylase, monoamine oxidase, and catechol-O-methyltransferase on rat striatal dialysate. J Cereb Blood Flow Metab 31:124-131.

Onali P, Olianas MC, Gessa GL (1985) Characterization of Dopamine Receptors Mediating Inhibition of Adenylate Cyclase Activity in Rat Striatum. Mol Pharmacol 28:138-145.

Palermo-Neto J (1997) Dopaminergic systems - Dopamine receptors. Psychiatr Clin North Am 20:705-+.

Pappata S, Salvatore E, Postiglione A (2008) In vivo imaging of neurotransmission and brain receptors in dementia. J Neuroimaging 18:111-124.

Pavese N, Rivero-Bosch M, Lewis SJ, Whone AL, Brooks DJ (2011) Progression of monoaminergic dysfunction in Parkinson's disease: A longitudinal (18)F-dopa PET study. NeuroImage 56:1463-1468.

Pellegrino LJ, Pellegrino AS, Cushman AJ (1979) A Stereotaxic Atlas of the Rat Brain. New York, NY: Plenum Press.

Peters JL, Michael AC (2000) Changes in the kinetics of dopamine release and uptake have differential effects on the spatial distribution of extracellular dopamine concentration in rat striatum. J Neurochem 74:1563-1573.

Peters JL, Miner LH, Michael AC, Sesack SR (2004) Ultrastructure at carbon fiber microelectrode implantation sites after acute voltammetric measurements in the striatum of anesthetized rats. J Neurosci Methods 137:9-23.

Phillips PEM, Stuber GD, Heien M, Wightman RM, Carelli RM (2003) Subsecond dopamine release promotes cocaine seeking. Nature 422:614-618.

Ramsson ES, Covey DP, Daberkow DP, Litherland MT, Juliano SA, Garris PA (2011) Amphetamine augments action potential-dependent dopaminergic signaling in the striatum in vivo. J Neurochem 117:937-948.

Rice ME, Cragg SJ (2008) Dopamine spillover after quantal release: Rethinking dopamine transmission in the nigrostriatal pathway. Brain Res Rev 58:303-313.

Robinson DL, Wightman RM (2004) Nomifensine amplifies subsecond dopamine signals in the ventral striatum of freely-moving rats. J Neurochem 90:894-903.

Rocha BA, Fumagalli F, Gainetdinov RR, Jones SR, Ator R, Giros B, Miller GW, Caron MG (1998) Cocaine self-administration in dopamine-transporter knockout mice. Nat Neurosci 1:132-137.

Roitman MF, Stuber GD, Phillips PEM, Wightman RM, Carelli RM (2004) Dopamine operates as a subsecond modulator of food seeking. J Neurosci 24:1265-1271.

Sabeti J, Adams CE, Burmeister J, Gerhardt GA, Zahniser NR (2002) Kinetic analysis of striatal clearance of exogenous dopamine recorded by chronoamperometry in freely-moving rats. J Neurosci Methods 121:41-52.

Salahpour A, Ramsey AJ, Medvedev IO, Kile B, Sotnikova TD, Holmstrand E, Ghisi V, Nicholls PJ, Wong L, Murphy K, Sesack SR, Wightman RM, Gainetdinov RR, Caron MG (2008) Increased amphetamine-induced hyperactivity and reward in mice overexpressing the dopamine transporter. Proc Natl Acad Sci U S A 105:4405-4410.

Schiffer WK, Volkow ND, Fowler JS, Alexoff DL, Logan J, Dewey SL (2006) Therapeutic doses of amphetamine or methylphenidate differentially increase synaptic and extracellular dopamine. Synapse 59:243-251.

Schlochtermeier L, Stoy M, Schlagenhauf F, Wrase J, Park SQ, Friedel E, Huss M, Lehmkuhl U, Heinz A, Ströhle A (2011) Childhood methylphenidate treatment of ADHD and response to affective stimuli. Eur Neuropsychopharmacol 21:646–654.

Schmitt KC, Reith MEA (2010) Regulation of the dopamine transporter Aspects relevant to psychostimulant drugs of abuse. Addiction Reviews 2 1187:316-340.

Schultz W (2007) Multiple dopamine functions at different time courses. Annu Rev Neurosci 30:259-288.

Seeman P, Lee T, Chauwong M, Wong K (1976) Antipsychotic drug doses and neuroleptic dopamine receptors. Nature 261:717-719.

Shu Z, Taylor IM, Michael AC (2013) The dopamine patchwork of the rat nucleus accumbens core. Eur J Neurosci 38:3221-3229.

Smith AD, Bolam JP (1990) The Neural Network of the Basal Ganglia as Revealed by the Study of Synaptic Connections of Identified Neurons. Trends Neurosci 13:259-265.

Spyraki C, Fibiger HC (1981) Intravenous self-administration of nomifensine in rats: Implications for abuse potential in humans. Science 212:1167-1168.

Stamford JA, Kruk ZL, Millar J (1986) In vivo voltammetric characterization of low affinity striatal dopamine uptake: Drug inhibition profile and relation to dopaminergic innervation density. Brain Res 373:85-91.

Stamford JA, Kruk ZL, Millar J (1988) Stimulated limbic and striatal dopamine release measured by fast cyclic voltammetry: anatomical, electrochemical and pharmacological characterisation. Brain Res 454:282-288.

Starke K, Gothert M, Kilbinger H (1989) Modulation of neurotransmitter release by presynaptic autoreceptors. Physiol Rev 69:864-989.

Suaud-Chagny MF, Dugast C, Chergui K, Msghina M, Gonon F (1995) Uptake of dopamine released by impulse flow in the rat mesolimbic and striatal systems in vivo. J Neurochem 65:2603-2611.

Sulzer D, Chen TK, Lau YY, Kristensen H, Rayport S, Ewing A (1995) Amphetamine redistributes dopamine from synaptic vesicles to the cytosol and promotes reverse transport. J Neurosci 15:4102-4108.

Sulzer D, Maidment NT, Rayport S (1993) Amphetamine and Other Weak Bases Act to Promote Reverse Transport of Dopamine in Ventral Midbrain Neurons. J Neurochem 60:527-535.

Sykova E, Nicholson C (2008) Diffusion in brain extracellular space. Physiol Rev 88:1277-1340.

Takmakov P, Zachek MK, Keithley RB, Bucher ES, McCarty GS, Wightman RM (2010) Characterization of Local pH Changes in Brain Using Fast-Scan Cyclic Voltammetry with Carbon Microelectrodes. Anal Chem 82:9892-9900.

Tao A, Tao L, Nicholson C (2005) Cell cavities increase tortuosity in brain extracellular space. J Theor Biol 234:525-536.

Taylor IM, Ilitchev AI, Michael AC (2013) Restricted Diffusion of Dopamine in the Rat Dorsal Striatum. ACS Chem Neurosci 4:870-878.

Taylor IM, Jaquins-Gerstl A, Sesack SR, Michael AC (2012) Domain-dependent effects of DAT inhibition in the rat dorsal striatum. J Neurochem 122:283-294.

Torres GE (2006) The dopamine transporter proteome. J Neurochem 97:3-10.

Torres GE, Amara SG (2007) Glutamate and monoamine transporters: new visions of form and function. Curr Opin Neurobiol 17:304-312.

Tse DCS, McCreery RL, Adams RN (1976) Potential Oxidative Pathways of Brain Catecholamines. J Med Chem 19:37-40.

Urban NL, Slifstein M, Meda S, Xu X, Ayoub R, Medina O, Pearlson G, Krystal J, Abi-Dargham A (2012) Imaging human reward processing with positron emission tomography and functional magnetic resonance imaging. Psychopharmacology (Berl) 221:67-77.

Valenti O, Cifelli P, Gill KM, Grace AA (2011) Antipsychotic Drugs Rapidly Induce Dopamine Neuron Depolarization Block in a Developmental Rat Model of Schizophrenia. J Neurosci 31:12330-12338.

Venton BJ, Seipel AT, Phillips PEM, Wetsel WC, Gitler D, Greengard P, Augustine GJ, Wightman RM (2006) Cocaine increases dopamine release by mobilization of a synapsin-dependent reserve pool. J Neurosci 26:3206-3209.

Venton BJ, Troyer KP, Wightman RM (2002) Response times of carbon fiber microelectrodes to dynamic changes in catecholamine concentration. Anal Chem 74:539-546.

Venton BJ, Zhang H, Garris PA, Phillips PEM, Sulzer D, Wightman RM (2003) Real-time decoding of dopamine concentration changes in the caudate-putamen during tonic and phasic firing. J Neurochem 87:1284-1295.

Waldmeier PC, Delinistula A, Maitre L (1976) Preferential Deamination of Dopamine by an A Type Monoamine-Oxidase in Rat Brain. Naunyn Schmiedebergs Arch Pharmacol 292:9-14.

Wang YX, Moquin KF, Michael AC (2010) Evidence for coupling between steady-state and dynamic extracellular dopamine concentrations in the rat striatum. J Neurochem 114:150-159.

White BP, Becker-Blease KA, Grace-Bishor K (2006) Stimulant medication use, misuse, and abuse in an undergraduate and graduate student sample. J Am Coll Health 54:261-268.

Wightman RM, Amatore C, Engstrom RC, Hale PD, Kristensen EW, Kuhr WG, May LJ (1988a) Real-time characterization of dopamine overflow and uptake in the rat striatum. Neuroscience 25:513-523.

Wightman RM, May LJ, Michael AC (1988b) Detection of Dopamine Dynamics in the Brain. Anal Chem 60:A769-&.

Winn P (2001) Dictionary of biological psychology. New York: Routledge.

Wipf DO, Kristensen EW, Deakin MR, Wightman RM (1988) Fast-Scan Cyclic Voltammetry as a Method To Measure Rapid, Heterogeneous Electron-Transfer Kinetics. Anal Chem 60:306-310.

Wu Q, Reith MEA, Kuhar MJ, Carroll FI, Garris PA (2001a) Preferential increases in nucleus accumbens dopamine after systemic cocaine administration are caused by unique characteristics of dopamine neurotransmission. J Neurosci 21:6338-6347.

Wu Q, Reith MEA, Walker QD, Kuhn CM, Carroll FI, Garris PA (2002) Concurrent autoreceptor-mediated control of dopamine release and uptake during neurotransmission: An in vivo voltammetric study. J Neurosci 22:6272-6281.

Wu Q, Reith MEA, Wightman RM, Kawagoe KT, Garris PA (2001b) Determination of release and uptake parameters from electrically evoked dopamine dynamics measured by real-time voltammetry. J Neurosci Methods 112:119-133.

Wu X, Kekuda R, Huang W, Fei YJ, Leibach FH, Chen JW, Conway SJ, Ganapathy V (1998) Identity of the organic cation transporter OCT3 as the extraneuronal monoamine transporter (uptake(2)) and evidence for the expression of the transporter in the brain. J Biol Chem 273:32776-32786.

Zahniser NR, Larson GA, Gerhardt GA (1999) In vivo dopamine clearance rate in rat striatum: Regulation by extracellular dopamine concentration and dopamine transporter inhibitors. J Pharmacol Exp Ther 289:266-277.